

# Encapsulation of flax oil by complex coacervation

A Thesis Submitted to the College of

Graduate Studies and Research

in Partial Fulfillment of the Requirements

for the Degree of Master of Science

in the Department of Food and Bioproduct Sciences

University of Saskatchewan

Saskatoon, Saskatchewan, Canada

By

Shuanghui Liu

© Copyright Shuanghui Liu, September 2009. All rights reserved.

## **PERMISSION TO USE**

In presenting this thesis/dissertation in partial fulfillment of the requirements for a Postgraduate degree from the University of Saskatchewan, I agree that the Libraries of this University may make it freely available for inspection. I further agree that permission for copying of this thesis/dissertation in any manner, in whole or in part, for scholarly purposes may be granted by the professor or professors who supervised my thesis work or, in their absence, by the Head of the Department or the Dean of the College in which my thesis work was done. It is understood that any copying or publication or use of this thesis/dissertation or parts thereof for financial gain shall not be allowed without my written permission. It is also understood that due recognition shall be given to me and to the University of Saskatchewan in any scholarly use which may be made of any material in my thesis/dissertation.

Requests for permission to copy or to make other uses of materials in this thesis in whole or part should be addressed to:

Head of the Department of Food and Bioproduct Sciences  
University of Saskatchewan  
Saskatoon, Saskatchewan S7N 5A8  
Canada

## ABSTRACT

The focus of this research was to develop a plant-based microcapsule for flax oil by complex coacervation. Complex coacervation involves the electrostatic attraction between two polymers of opposing charges. Specifically, the research aimed to: a) identify the ideal biopolymer and solvent conditions required for complex coacervation involving pea protein isolate (PPI) and gum Arabic (GA); b) understand the functional behaviour of PPI-GA complexes as food and biomaterial ingredients; and c) develop methodologies for encapsulating flax oil within PPI-polysaccharide capsules. Complex coacervation between PPI-GA was found to be optimized at a biopolymer weight mixing ratio of 2:1 in the absence of salt. The functional behaviours of the optimized biopolymer mixture were then investigated as a function of pH (4.30-2.40) within a region dominated by complex coacervation. Emulsion stability was found to be greater for PPI-GA mixture systems relative to PPI alone at pH values between 3.10 and 4.00; emulsions produced under one-step emulsification exhibited higher stability compared to those of two-step emulsification at all pH values. Foam expansion was independent of both biopolymer content and pH, whereas foam stability improved for the mixed system between pH 3.10 and 4.00. The solubility minimum was broadened relative to PPI at more acidic pH values. These findings suggested that the admixture of PPI and GA under complexing conditions could represent a new food and/or biomaterial ingredient, and has potential as an encapsulating agent. Two encapsulation processes were employed in this research: high speed mixing (two-step emulsification) and low speed mixing (one-step emulsification). Flax oil capsules formed using the gelatin-GA mixture (as control) under high speed mixing exhibited low moisture content, water activity and surface oil, and afforded adequate protection against oxidation relative to free oil over a 25 d storage period. The PPI-GA mixture failed to produce acceptable capsules using either high or low speed mixing. In contrast, PPI-alginate capsules were produced and exhibited similar chemical properties as gelatin-GA capsules, except with lower

encapsulated flax oil content (30% vs. 50% w/w). However, oxidative stability may adversely affected by the low speed mixing condition during encapsulation.

## ACKNOWLEDGEMENTS

I would like to express my sincerest gratitude to my supervisors, Drs. Michael T. Nickerson and Nicholas H. Low for their guidance, support and constant encouragement throughout my studies and research. I appreciate the advice and guidance given from members of my advisory committee, Drs. Brain Bandy, Rick Green, and from my graduate chair Drs. Takuji Tanaka and Phyllis Shand. I gratefully acknowledge Drs. Darren R. Korber, Martin Reaney, and Robert T. Tyler for their expertise. Catherine Elmer, Yuanlong Cao, Bonnie Li, and Heather Silcox are greatly appreciated for their technical assistance and support. I would also like to thank Dr. Dèrick Rousseau, Dr. Supratim Ghosh and Muhammad Ali, at Ryerson University, for their expertise and technical assistance. I would like to thank Dr. Udaya Wanasundara and all my colleagues at POS Pilot Plant Corporation for their kind encouragement and support. I appreciate the help, support and friendship from my colleagues, Kornsulee Ratanapariyanuch, Darlene Klassen, Kimberly Wood, Tahereh Haji, Kelly Konecsni, Karla Klemmer, Alison Ozog, and Nina Castillo. I would also like to thank Tanya Napper, Brenda Rebeyka and Ann Harley for their administrative assistance. Other thanks go to all other staff members and graduate students for their kind help during my studies. I thank to my families and friends for their lofty love, patience, support and encouragement.

Financial support for this study was provided by the Advanced Foods and Materials Network, and Saskatchewan Ministry of Agriculture. Flax oil and pea flour were kindly donated for this work by Bioriginal Food and Science Corporation (Saskatoon, SK) and Parrheim Foods (Saskatoon, SK), respectively.

## TABLE OF CONTENTS

	<b>Page</b>
PERMISSION TO USE.....	i
ABSTRACT.....	ii
ACKNOWLEDGMENTS.....	iv
TABLE OF CONTENTS.....	v
LIST OF TABLES.....	ix
LIST OF FIGURES.....	x
LIST OF ABBREVIATIONS .....	xiii
<b>1. INTRODUCTION</b>	
1.1 Summary.....	1
1.2 Objectives.....	2
1.3 Hypotheses.....	2
<b>2. LITERAURE REVIEW</b>	
2.1 Encapsulation technology.....	3
2.2 Encapsulation by coacervation.....	3
2.2.1 Simple coacervation .....	5
2.2.2 Complex coacervation.....	6
2.2.2.1 Formation of complex coacervate.....	7
2.2.2.2 Structure-function relationship of complex coacervate .....	12
2.2.2.3 Encapsulation by complex coacervation.....	16
2.3 Choice of wall materials.....	18
2.4 Flax oil as core ingredient.....	21

### **3. EFFECT OF PH, SALT AND BIOPOLYMER RATIO ON THE FORMATION OF PEA PROTEIN ISOLATE - GUM ARABIC COMPLEXES**

3.1 Abstract .....	23
3.2 Introduction.....	24
3.3 Materials and Methods.....	26
3.3.1 Materials.....	26
3.3.2 Turbidimetric analysis during an acid titration.....	27
3.3.3 Electrophoretic mobility.....	28
3.3.4 Statistical analysis.....	28
3.4 Results and Discussion.....	29
3.4.1 Associative phase behaviour as a function of NaCl.....	29
3.4.2 Associative phase behaviour as a function of biopolymer mixing ratio.....	31
3.5 Conclusion.....	37
3.6 Transition to the next study.....	37

### **4. EFFECT OF PH ON THE FUNCTIONAL BEHAVIOUR OF PEA PROTEIN ISOLATE - GUM ARABIC COMPLEX**

4.1 Abstract .....	39
4.2 Introduction.....	40
4.3 Materials and Methods.....	43
4.3.1 Materials.....	43
4.3.2 Identifying $pH_c$ , $pH_{\phi_1}$ , $pH_{opt}$ and $pH_{\phi_2}$ by turbidimetric analysis.....	43
4.3.3 Functional properties.....	43
4.3.3.1 Coacervate composition at 5.00% (w/w) Cp.....	44
4.3.3.2 Percent protein solubility (%PS).....	44
4.3.3.3 Emulsion stability.....	45
4.3.3.4 Percent foam expansion (%FE) and foam liquid stability (%FS).....	46
4.3.4 Statistical analysis.....	46
4.4 Results and Discussion.....	46
4.4.1 Complex coacervation between PPI and GA biopolymers.....	46

4.4.2 Emulsification properties.....	49
4.4.3 Foaming properties .....	53
4.5 Conclusion.....	55
4.6 Transition to the next study .....	55

## **5. PROTEIN-POLYSACCHARIDE ENCAPSULATION OF FLAX OIL**

5.1 Abstract.....	56
5.2 Introduction.....	57
5.3 Materials and Methods.....	58
5.3.1 Materials.....	58
5.3.2 Flax oil encapsulation under high speed mixing conditions (two-step emulsification).....	58
5.3.3 Flax oil encapsulation under low speed mixing conditions (one-step emulsification).....	59
5.3.4 Capsule characterization.....	60
5.3.5 Oxidative stability.....	62
5.3.6 Fatty acid profiles by gas chromatography.....	64
5.3.7 Statistical analysis.....	64
5.4 Results and Discussion.....	65
5.4.1 Flax oil encapsulation under high speed mixing conditions (two-step emulsification).....	65
5.4.1.1 Capsule formation.....	65
5.4.1.2 Characterization of gelatin-GA capsules.....	71
5.4.1.3 Oxidative stability of flax oil in gelatin-GA capsules.....	71
5.4.2 Flax oil encapsulation under low speed mixing conditions (one-step emulsification).....	74
5.4.2.1 Capsule formation.....	74
5.4.2.2 Characterization of PPI-alginate capsules.....	75
5.4.2.3 Oxidative stability of flax oil in PPI-alginate capsules.....	77
5.5 Conclusion.....	79



<b>6. GENERAL CONCLUSIONS</b> .....	<b>81</b>
<b>7. FUTURE STUDIES</b> .....	<b>82</b>
<b>8. REFERENCES</b> .....	<b>83</b>

## LIST OF TABLES

	<b>Page</b>
Table 2.1 Mechanical and chemical microencapsulation techniques.....	4
Table 2.2 Comparison of fatty acid profiles in dietary fats and oils from various sources (Adapted from Morris, 2007).....	22
Table 5.1 The characteristics of gelatin-GA capsules (Cp=2.00% w/v, wall-to-core ratio=50:50 w/w, homogenization rate=9000 rpm).....	71
Table 5.2 The effect of high speed mixing encapsulation (two-step emulsification) on the oxidative stability of flax oil in gelatin-GA capsules (Cp=2.00% w/v, wall-to-core ratio=50:50, homogenization rate=9000 rpm).....	72
Table 5.3 The characterization of PPI-alginate capsules as a function of biopolymer weight mixing ratio (Cp=2.00% w/v, wall-to-core ratio=50:50 w/w).....	76
Table 5.4 The characterization of PPI-alginate capsules as a function of wall-to-core ratio (Cp=2.00% w/v, PPI:alginate=1:1 w/w).....	77
Table 5.5 The effect of low speed mixing encapsulation (one-step emulsification) on the oxidative stability of flax oil in PPI-alginate capsules (Cp=2.00% w/v, PPI:alginate=1:1 w/w, wall-to-core ratio =70:30 w/w).....	78
Table 5.6 Fatty acid profiles of flax oil before and after encapsulation by low speed mixing (one-step emulsification).....	78

## LIST OF FIGURES

	Page
Figure 2.1 Microcapsules based on A) mononuclear and B) polynuclear designs (Adapted from Thies, 2005).....	5
Figure 2.2 A schematic of a generic lipid encapsulation procedure by simple coacervation.....	6
Figure 2.3 A schematic outlining various phase separation behaviours in admixtures of protein and polysaccharide (Adapted from Weinbreck, 2004).....	8
Figure 2.4 A schematic illustrating the complex coacervation process of admixture of protein (●) and polysaccharide (☞) (Adapted from Weinbreck, 2004).....	9
Figure 2.5 A typical phase diagram illustrating the effect of pH and ionic strength on critical pH values for a WPI–GA mixture (Adapted from Weinbreck et al., 2003a).....	10
Figure 2.6 A typical phase diagram illustrating the effect of biopolymer mixing ratio on the critical pH values for a WPI-GA mixture (Adapted from Weinbreck et al., 2003b).....	12
Figure 2.7 Schematic representations of three alternative effects of polysaccharide on the surface of protein-coated droplets: (a) bridging flocculation, (b) polysaccharide fully coat the droplet surface, and (c) polysaccharide form a weak gel-like network (adapted from Dickinson, 2003).....	15
Figure 2.8 Proposed structure of gum Arabic-GPI (glycosylphosphatidylinositol) (Adapted from Islam et al., 1997).....	20
Figure 2.9 Alginate units: β-D-mannopyranosyluronic acid (βDManpA) and α-L-gulopyranosyluronic acid (αLGulpA) (Adapted from BeMiller et al., 2008).....	21

Figure 3.1	Turbidity curve of PPI-GA mixture ( $C_p=0.05\%$ w/w, PPI:GA=1:1 w/w, NaCl=0 mM). $pH_c$ , $pH_{\phi_1}$ , $pH_{opt}$ and $pH_{\phi_2}$ represented the critical pH transitions during acid titration.....	30
Figure 3.2	Turbidity curves of PPI, GA and PPI-GA mixture ( $C_p=0.05\%$ w/w, PPI:GA=1:1 w/w) in the absence (a) and presence of 7.5 mM NaCl (b).....	30
Figure 3.3	Phase diagrams of critical pH transitions, $pH_c$ , $pH_{\phi_1}$ , $pH_{\phi_2}$ (a) and $pH_{opt}$ (b), as a function of NaCl ( $C_p=0.05\%$ w/w, PPI:GA=1:1 w/w).....	32
Figure 3.4	Turbidity curves of PPI-GA mixtures ( $C_p=0.05\%$ w/w, NaCl=0 mM) at biopolymer weight mixing ratios.....	32
Figure 3.5	Phase diagrams of critical pH transitions ( $C_p=0.05\%$ w/w, NaCl=0 mM), $pH_c$ , $pH_{\phi_1}$ , $pH_{\phi_2}$ (a), and $pH_{opt}$ (b); and peak optical density (c) as a function of biopolymer weight mixing ratio (PPI:GA). Dotted lines represent PPI:GA=1:1 .....	34
Figure 3.6	Zeta potential (mV) values for PPI, GA and mixed PPI-GA mixture ( $C_p=0.05\%$ w/w, PPI:GA=2:1 w/w, NaCl=0 mM) as a function of pH.....	35
Figure 4.1	Turbidity curves of PPI and PPI-GA mixture ( $C_p=0.05\%$ w/w, PPI:GA=2:1 w/w, NaCl=0 mM) and critical pH transitions of PPI-GA mixture.....	48
Figure 4.2	Percent protein solubility PPI and PPI- GA mixtures ( $C_p=1.00\%$ w/w, PPI:GA=2:1 w/w) as a function of pH.....	48
Figure 4.3	Percent emulsion stability of PPI and PPI-GA mixtures ( $C_p=5.00\%$ w/w, PPI:GA=2:1 w/w) as a function of pH.....	51
Figure 4.4	Percent foam expansion (solid) and stability (open) of PPI (circle) and PPI-GA mixtures (triangle) ( $C_p=5.00\%$ w/w, PPI:GA=2:1 w/w) as a function of pH.....	53
Figure 5.1	Gelatin-GA capsules observed by light microscopy as a function of homogenization rate: a) 3000; b) 6000; c) 9000; d) 12000 and e) 15000 rpm ( $C_p=2.00\%$ w/v, wall-to-core ratio=50:50 w/w).....	66

Figure 5.2 Gelatin-GA capsules observed by light microscopy as a function of Cp (% w/v): a) 1.00%; b) 1.25%; c) 1.50%; d) 1.75% and 2.00% (homogenization rate=9000 rpm, wall-to-core ratio=50:50 w/w).....	67
Figure 5.3 PPI-GA capsule formation experiments observed by light microscopy as a function of homogenization rate: a) 3000; b) 6000; c) 9000; d) 12000 and e) 15000 rpm (Cp=2.00% w/v, wall-to-core ratio=50:50 w/w).....	69
Figure 5.4 PPI-GA capsule formation experiments observed by light microscopy as a function of Cp (% w/v): a) 1.00%; b) 1.25%; c) 1.50%; d) 1.75% and 2.00% (homogenization rate=9000 rpm, wall-to-core ratio=50:50 w/w).....	70
Figure 5.5 Oxidative stability of free and encapsulated flax oil (Cp=2.00% w/v, wall-to-core ratio=50:50 w/w, homogenization rate=9000 rpm) maintained at room temperature over a 25 d period (Data represent the mean ± one standard deviation n=2). Asterisks indicate the day in which significant oxidation occurred.....	73
Figure 5.6 Oxidative stability of free and encapsulated flax oil (Cp=2.00% w/w, wall-to-core ratio=70:30 w/w, PPI:alginate=1:1 w/w) maintained at room temperature over a 20 d period (Data represent the mean ± one standard deviation n=2) .....	80

## LIST OF ABBREVIATIONS

ALA	$\alpha$ -linolenic acid
AV	p-anisidine value
A <sub>w</sub>	Water activity
BHT	Butylated hydroxytoluene
$\beta$ -LG	$\beta$ -lactoglobulin
CD	Conjugated diene
C <sub>p</sub>	Total polymer concentration
EFA	Essential fatty acids
ES	Emulsion stability
FE	Foam expansion
FS	Foam stability
GA	Gum Arabic
GC	Gas Chromatography
LA	Linoleic acid
MDA	Malondialdehyde
PF	Pea flour
pH <sub>c</sub>	pH where soluble complex forms
pH <sub><math>\phi</math>1</sub>	pH where insoluble complex forms
pH <sub><math>\phi</math>2</sub>	pH where complex dissociates
pH <sub>opt</sub>	pH where maximum complex forms
pI	Isoelectric point
PPI	Pea protein isolates
PV	Peroxide value
TBARS	2-thiobarbituric acid reactive substances
WPI	Whey protein isolates

## **Chapter 1**

### **Introduction**

#### **1.1 Summary**

With increased consumer awareness, market trends within the food industry are shifting towards food products that have additional health benefits, commonly referred to as functional food. According to Health Canada (1998), “A functional food is similar in appearance to, or may be, a conventional food, is consumed as part of a usual diet, and is demonstrated to have physiological benefits and/or reduce the risk of chronic disease beyond basic nutritional functions.” Essential fatty acids (EFA) (i.e.,  $\alpha$ -linolenic acid), commonly found in functional food, are well known bioactive ingredients for their potential to reduce the risk of coronary heart disease (Li et al., 2003) and prevent certain types of cancer (Bougnoux and Chajès, 2003). However, the wide spread use of this bioactive ingredient is significantly hindered by, a) the lack of miscibility in aqueous food systems; b) the lack of stability during processing and storage; and c) the difficulty in delivering target doses to maximize its health benefiting effects. To circumvent these problems, the food industry has been using encapsulation technology with limited success. Microencapsulation is described “as a process of enclosing micron-sized particles of solids or droplets of liquids or gasses in an inert shell, which in turn isolates and protects them from the external environment” (Ghosh, 2006). The choice of encapsulating material and processing conditions has been found to drastically influence their protective ability. Presently, the preferred commercial encapsulating material is gelatin. However, with increased consumer concerns over the safety of animal-derived products, dietary preferences and religious choices, an alternative plant-based wall material is being sought. The focus of this research was to encapsulate EFA rich flax oil by complex coacervation employing PPI and GA or other anionic polysaccharides. The

developed capsules may also have the potential to serve as a platform delivery vehicle for other lipid-soluble bioactive compounds (i.e., lipid-soluble vitamins).

## **1.2 Objectives**

The overall goal of this research was to develop a suitable alternative to animal-based encapsulation materials for flax oil, using PPI-GA complexes or PPI in combination with other anionic polysaccharide. To achieve this goal, three objectives were established: first, to identify suitable biopolymer and solvent conditions for complex coacervation involving PPI and GA; second, to assess the effect of pH on the functional behaviour of PPI-GA complexes; and third, to develop methodologies for encapsulating flax oil by complex coacervation using PPI with anionic polysaccharides (i.e., GA or alginate).

## **1.3 Hypotheses**

To achieve these objectives, three main hypotheses were tested: first, the formation of PPI-GA complexes will strongly depend on both solvent condition (i.e., pH and ionic strength) and biopolymer weight mixing ratio; second, the functional behaviour of PPI-GA complexes will be improved in mixture systems relative to protein alone; and third, the chemical properties and oxidative stability of encapsulated flax oil within PPI-polysaccharide capsules will depend on the wall material and processing condition employed.



## **Chapter 2**

### **Literature review**

#### **2.1 Encapsulation technology**

Encapsulation is a process whereby active ingredients are entrapped or coated by a polymeric matrix, and then dried to obtain a free flowing powder (Dziezak, 1988). Typically, the entrapped agent is referred as the “core material”, whereas the outer coating is referred as the “wall material”. Capsules can be classified, according to size, into three broad categories: macro-capsules ( $>5000 \mu\text{m}$ ), micro-capsules ( $0.2\sim 5000 \mu\text{m}$ ) and nano-capsules ( $<0.2 \mu\text{m}$ ) (King, 1995). Depending on the core material and processing conditions, microcapsules can be spherical, oval or irregular in shape (Madene et al., 2006). A summary of mechanical and chemical encapsulation techniques are presented in Table 2.1. Microcapsules typically have mononuclear or polynuclear structure (Figure 2.1). In the former, the core material is concentrated at the center of the capsule, surrounded (or coated) by the biopolymer wall material. In the latter, the core material exists as phase-separated inclusions, dispersed throughout the biopolymer wall matrix. Regardless of capsule design, both function to delay degradative reactions (i.e., oxidation) of the entrapped core material. Advantages of using encapsulation technology in the food industry include: a) increasing the stability and bioavailability of sensitive core materials; b) improving miscibility within aqueous-based food products; c) masking off-flavours and odours; and d) controlling and targeting the release of entrapped core materials at a desired rate to optimize site- and dose-delivery (Desai and Park, 2005).

#### **2.2 Encapsulation by coacervation**

Coacervation is defined as the phase separation of a mixture system into biopolymer-rich and biopolymer-deficient phases (de Kruif et al., 2004). The use of the biopolymer-rich phase as an encapsulating material has been done for both simple and

**Table 2.1 Mechanical and chemical microencapsulation techniques.**

<b>Type</b>	<b>Technique</b>	<b>Summary of process</b>	<b>Applications</b>
Mechanical	a) Spray drying (5-5000 $\mu\text{m}$ ) <sup>a</sup>	A core-wall emulsion is spray dried to give wall hardening. <sup>b</sup>	Lipids Flavours
	b) Extrusion (250-2500 $\mu\text{m}$ ) <sup>a</sup>	Liquid core is passed through a center orifice, while the wall is passed through the outer annulus of the concentric orifices. The wall material is then hardened. <sup>b</sup>	Flavours
	c) Spinning disk (5-1500 $\mu\text{m}$ ) <sup>a</sup>	A core-wall emulsion is loaded onto a spinning disk; the spinning action allows coating of the core component with the wall material; cooling results in wall hardening. <sup>a</sup>	Flavours
Chemical	a) Coacervation (2-1200 $\mu\text{m}$ ) <sup>a</sup>	Interactions of polymer(s) to form wall material; coacervate coated droplets are dried to give wall hardening. <sup>b</sup>	Dyes Flavours Lipids
	b) Molecular inclusion (5-50 $\mu\text{m}$ ) <sup>c</sup>	Encapsulation of apolar molecules by cyclodextrins, which have a hydrophobic hollow center. <sup>b</sup>	Flavours
	c) Interfacial polymerization (0.5-1000 $\mu\text{m}$ ) <sup>a</sup>	A nonpolar polymerizable monomer and the core material are dispersed within a polar phase; a catalyst induces polymerization of monomers to surround the core material. <sup>b</sup>	Lipids

<sup>a</sup> Adapted from Ghosh, 2006.

<sup>b</sup> Adapted from Jackson and Lee, 1991.

<sup>c</sup> Adapted from Madene et al., 2006.

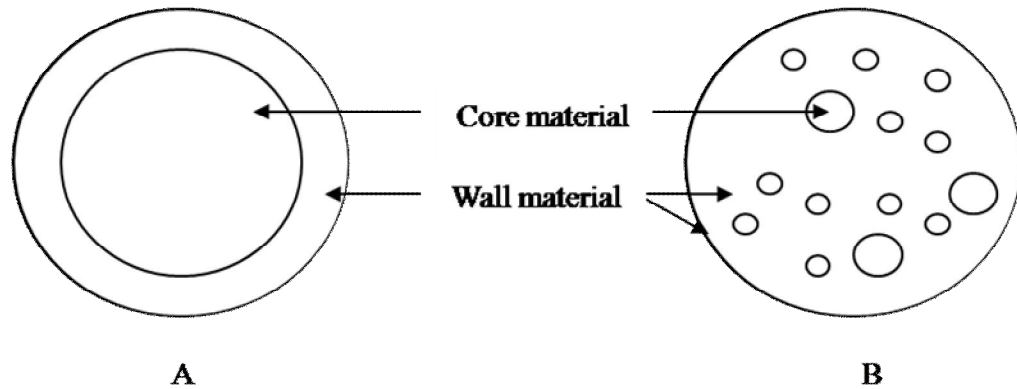


**Figure 2.1 Microcapsules based on A) mononuclear and B) polynuclear designs (Adapted from Thies, 2005).**

complex processes. The former involves the use of a single polymer as the wall material to entrap the bioactive core ingredient, whereas the latter involves two oppositely charged polymers (typically a protein and a polysaccharide) as the wall material. Since complex coacervation was the primary technique used in this research, simple coacervation will be discussed briefly.

### **2.2.1 Simple coacervation**

Phase separation by simple coacervation involves only one polymeric material. The separation of the biopolymer from its solvent is induced by the addition of a more hydrophilic compound, such as sodium sulphate, which leads to salting-out of the biopolymer; or the separation can be achieved by desolvation through addition of a water miscible non-solvent such as ethanol (Gander et al., 2002). Unlike complex coacervation, systematic studies on the simple coacervation process of protein under different solvent conditions is not well-established in literature. Mohanty and Bohidar (2003) investigated alcohol-induced simple coacervation of gelatin. The addition of alcohol was found to reduce the level of gelatin-water interactions, which led to an

overall reduced spatial extension of gelatin chains in solution. Eventually, phase separation of gelatin-rich and solvent-rich phases occurred. Encapsulation by simple coacervation has been studied using several different biopolymer systems, such as gelatin (Keipert and Melegari, 1993), wheat gliadin (Mauguet et al., 2002) and soy glycinin (Lazko et al., 2004a) to encapsulate lipophilic materials. A typical encapsulation process is illustrated in Figure 2.2.

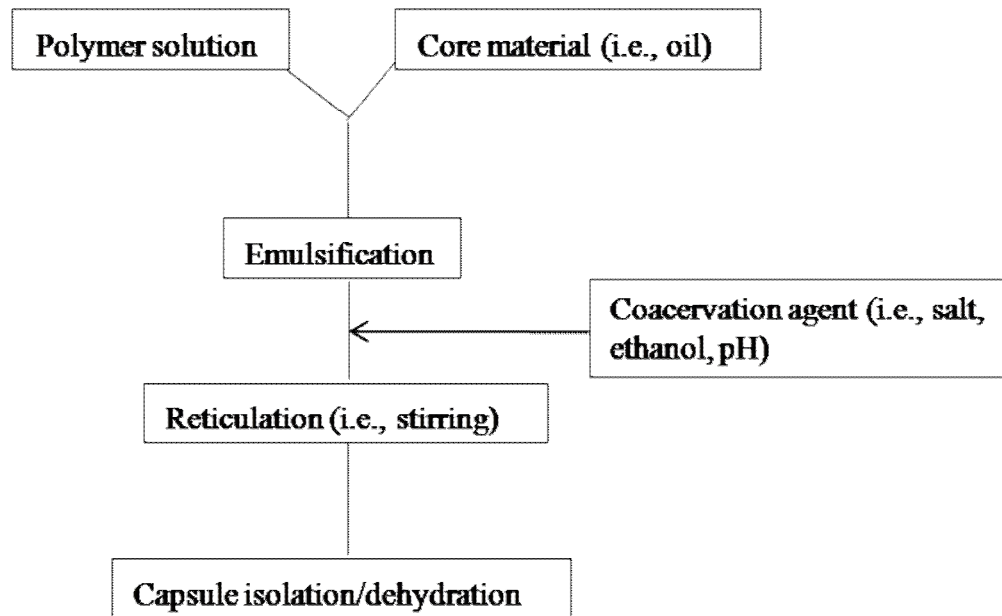


**Figure 2.2 A schematic of a generic lipid encapsulation procedure by simple coacervation.**

### **2.2.2 Complex coacervation**

Microencapsulation by complex coacervation involves three main stages: a) complex formation involving two oppositely charged polyelectrolytes; b) film formation around a lipid core material; and c) solidification (or hardening) of the wall material to produce the microcapsule shell (Jackson et al., 1991). The latter involves cross-linking and/or drying processes (Dziezak, 1988). Although this technique can

produce capsules with high payloads, the process is more expensive and complex than simple coacervation.

### **2.2.2.1 Formation of complex coacervate**

Complex coacervation involves liquid-liquid phase separation of a concentrated polymer phase (also known as complex) and a polymer-deficient solvent phase. Complex formation results from the interaction between two oppositely charged polyelectrolytes, which are defined as biopolymers bearing multiple charged groups (i.e., polysaccharide and protein) (Weinbreck, 2004). Depending on biopolymer and solvent conditions, phase separation of a biopolymer mixture may result in three outcomes, as depicted in Figure 2.3. Under very dilute conditions, biopolymers are solvent suspended and are co-soluble with little interaction (Figure 2.3a). As the total biopolymer concentration ( $C_p$ ) increases, repulsive or attractive interaction takes place. When the protein and polysaccharide have similar charges, electrostatic repulsion keeps the two biopolymers apart, resulting in separation into protein-rich and polysaccharide-rich phases (Figure 2.3b). This incompatibility between two biopolymers is also referred to as segregative phase separation. In contrast, when two oppositely charged polyelectrolytes are mixed, they undergo electrostatic attraction to form a zero net surface charge complex which results in phase separation into biopolymer- (coacervate phase) and solvent-rich (solvent phase) phases (Figure 2.3c). This phenomenon is referred to as complex coacervation or associative phase separation. During the past few decades, researchers have proposed several explanations for complex coacervation which were reviewed briefly by Weinbreck (2004). Bungenberg (1929, 1949a-c) suggested that complex coacervation is due to the absence of charge and solvent. The neutral complex formed undergoes desolvation and separation from the solvent phase. Overbeek and Voorn (1957) proposed that coacervation is a spontaneous process. When the charge density ( $\sigma$ ) and the molar mass ( $r$ ) reach the critical condition of  $\sigma^3 r \geq 0.53$ , complex coacervation occurs. Later, Veis and co-workers (1960, 1961, 1963, 1967) developed an alternative theory to suggest a gradual process for coacervate formation, where initial protein-polysaccharide interactions occur at  $\sigma^3 r < 0.53$ , prior to substantial

coacervate formation at  $\sigma^3 r \geq 0.53$ . The most recent theory was developed by Tainaka (1979, 1980).

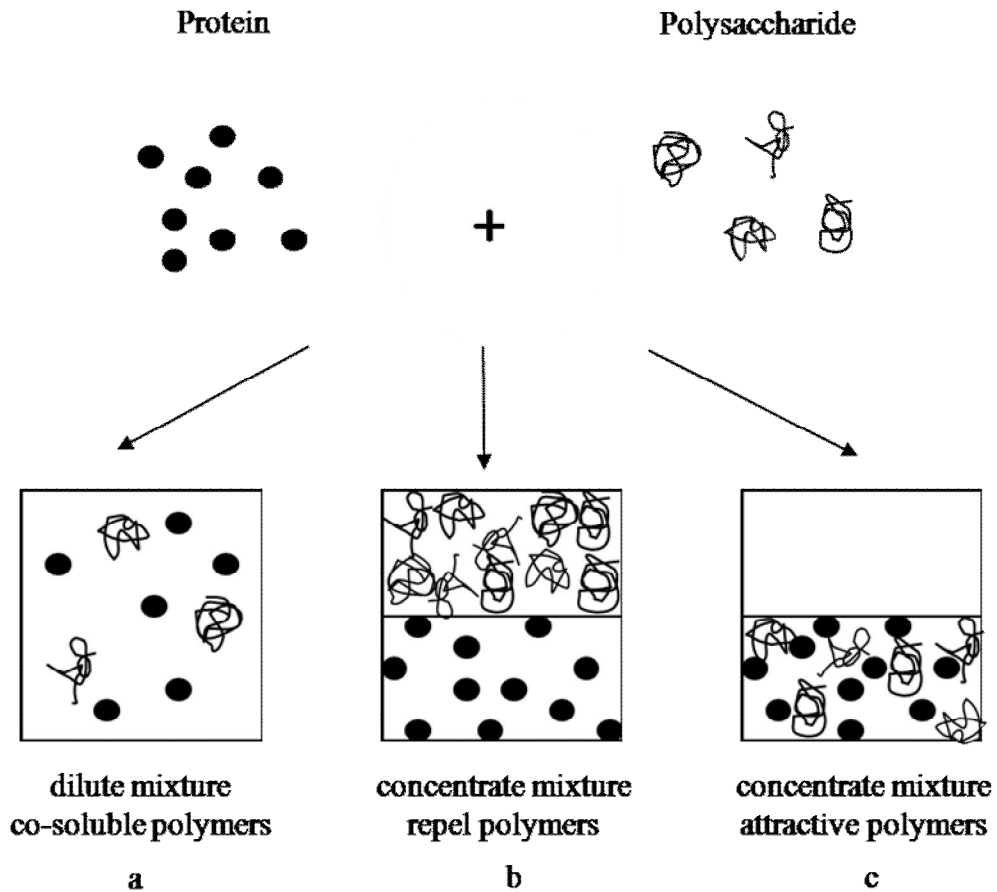


**Figure 2.3 A schematic outlining various phase separation behaviours in admixtures of protein and polysaccharide (Adapted from Weinbreck, 2004).**

He adapted the Veis-Aranyi theory and proposed that coacervation occurs within a critical charge density and molar mass range. When the charge density or molar mass is higher than this range, precipitation occurs. In contrast, when they are lower than this range, biopolymers are co-soluble in solution and coacervation is inhibited.

The fundamental step in complex coacervation is the attractive interaction between oppositely charged biopolymers. This attraction reduces the overall charge due to neutralization; in other words, it decreases the polarity of the protein-polysaccharide

complex. When reaches neutral net surface charge, the solubility of complex declines and maximum coacervation is achieved.

### Factors affecting coacervate formation

Although a variety of factors influence the formation of complex coacervate, the three major factors investigated in this research are pH, biopolymer weight mixing ratio (i.e., protein-to-polysaccharide ratio) and the presence of salts. Complex coacervation can occur in the presence of a oppositely charged protein and polysaccharide. Functional groups (i.e., carboxyl or amine groups) along the biopolymer backbone become charged depending on solution pH, in relation to the pKa of these groups and the isoelectric point (pI) of the protein. In addition, the presence of salts can drastically influence repulsive and attractive electrostatic forces involved to promote biopolymer attraction/repulsion and charge screening. Figure 2.4 depicts a typical phase separation occurring during complex coacervation.

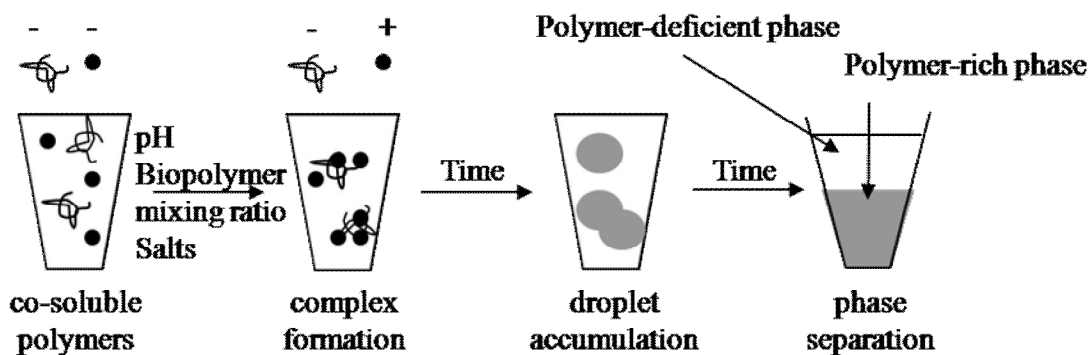


**Figure 2.4** A schematic illustrating the complex coacervation process of admixture of protein (●) and polysaccharide (⌘) (Adapted from Weinbreck, 2004).

#### (a) Effect of pH

It is essential in coacervate formation that oppositely charged polyelectrolytes interact with each other. Polyelectrolytes bearing positive charges are called polycations, whereas those with negative charges are called polyanions. Like weak acids, the degree

of ionization of their functional groups strongly depends on their environment pH. When the pH of the solution is close to the pI of the protein, the polyelectrolyte has minimal net charge, thereby inhibiting coacervate formation. Since complex coacervation involves more than one polyelectrolyte, it is crucial to work at pH values where the biopolymers have opposite charges. Studies suggested that complex coacervation tends to fall into a very narrow pH range (Weinbreck et al., 2003a; Ducel et al., 2004). According to the Veis-Arvanyi theory (1960), the pH value where the initial soluble complex is formed is  $pH_c$ , the pH value where phase separation occurs is designated as  $pH_{\phi_1}$ , and the pH value where complex is dissociated is  $pH_{\phi_2}$ . For example, Weinbreck and co-workers (2003a) reported for a whey protein isolate (WPI) and GA system (Cp of 0.1% w/w, WPI:GA=2:1 w/w, [NaCl]=12.5 mM),  $pH_c$ ,  $pH_{\phi_1}$  and  $pH_{\phi_2}$  were 5.3, 4.8 and 2.3 respectively. Below a pH of 2.3, the carboxyl groups ( $pK_a=2.2$ ) on GA become protonated and the WPI carries a net positive charge; whereas above pH 5, both GA and WPI ( $pI \approx 5$ ) have net negative charge. In both instances, these biopolymers will not attract each other and complex coacervation is inhibited. Figure 2.5 is a schematic phase diagram illustrating the effect of pH and salt on the phase separation of a WPI-GA mixture.

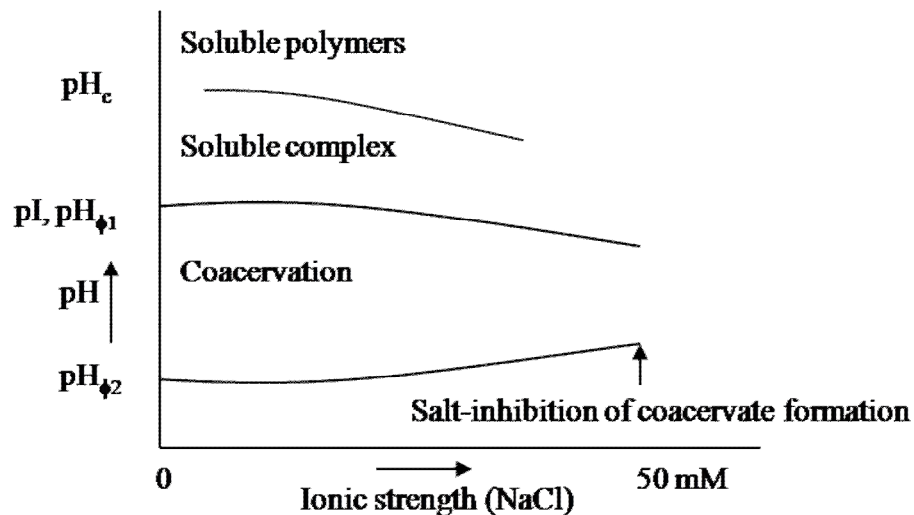


**Figure 2.5** A typical phase diagram illustrating the effect of pH and ionic strength on critical pH values for a WPI-GA mixture (Adapted from Weinbreck et al., 2003a).



### **(b) Ionic strength**

The influence of ionic strength on coacervate formation has been intensively studied (Burgess and Carless, 1984; Mattison et al., 1995; Weinbreck et al., 2003a). Weinbreck and co-workers (2003a) found that for a WPI-GA mixture, ionic strength had a significant effect on the phase boundaries,  $\text{pH}_c$  and  $\text{pH}_{\phi 1}$ . In general, ionic strength has two main effects: a) at high levels ( $>50$  mM NaCl), bound and unbound ions screen surface charges on both WPI and GA, resulting in reduced electrostatic attractive forces and suppression of complex coacervation; and b) at low levels ( $<50$  mM NaCl), ions associate with the protein structure, altering its conformation to expose additional charged groups. Consequently, this can lead to an apparent increase in linear charge density and enhance complex coacervation between the protein and polysaccharide. Figure 2.5 shows that as ionic strength increases, the coacervation region becomes narrower up to a critical point, where coacervation is completely inhibited by ionic strength. This ionic strength was found to be 54 mM NaCl for the WPI-GA system studied by Weinbreck and co-workers (2003a).

### **(c) Biopolymer weight mixing ratio**

As discussed previously, complex coacervation is optimized when opposite charges on the protein and polysaccharide become neutralized. In general, biopolymers have a fixed charge density at a given pH and ionic strength. By adjusting the biopolymer weight mixing ratio, the total charges available for coacervate formation can be modified. Weinbreck and co-workers (2003b) studied the effect of pH and biopolymer weight mixing ratio using WPI and the polysaccharide EPS B40. They found that biopolymer weight mixing ratios WPI:EPS B40 ranging from 1:1 to 25:1 did not change the initial soluble complex formation pH ( $\text{pH}_c$ ). In contrast, as WPI:EPS B40 increased from 1:1 to 9:1, the pH at which insoluble coacervate formed ( $\text{pH}_{\phi 1}$ ) increased. The authors also found that as WPI:EPS B40 increasing from 9 to 25,  $\text{pH}_{\phi 1}$  was constant due to the saturation of polysaccharide EPS B40 (Figure 2.6).

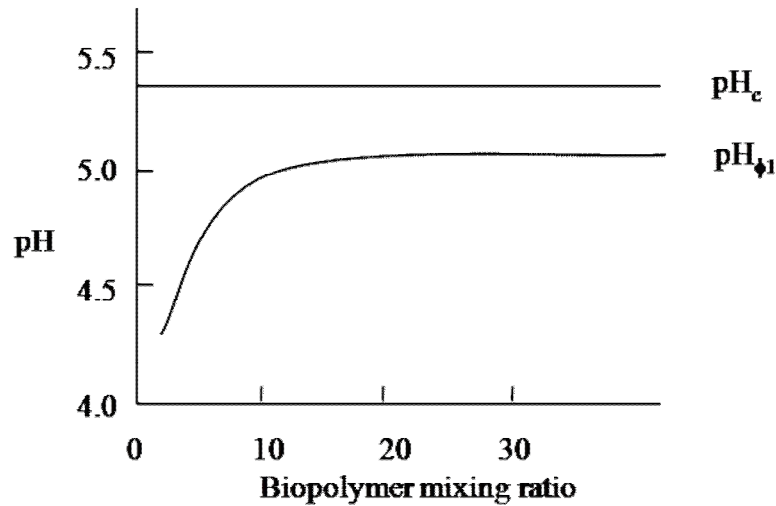


**Figure 2.6** A typical phase diagram illustrating the effect of biopolymer mixing ratio on the critical pH values for a WPI-GA mixture (Adapted from Weinbreck et al., 2003b).

#### **2.2.2.2 Structure-function relationship of complex coacervate**

Formation of protein-polysaccharide complex coacervate (also known as complex) may alter the conformation of the protein and/or modify its physicochemical properties. In literature, researchers have employed direct techniques (i.e., circular dichroism, small angle neutral scattering, infrared spectroscopy and nuclear magnetic resonance) and indirect (i.e., light scattering) techniques to obtain information on the changes in protein conformation as a result of complexation (Schmitt et al., 1998). Van de Weert and co-workers (2004) studied the complex formed between lysozyme and heparin using Fourier-transform infrared spectroscopy and fluorescence spectroscopy. Analytical results revealed that there was a very small change in the lysozyme's secondary and tertiary structure upon complexation with heparin. In contrast, differential scanning calorimetry suggested that thermal stability (i.e., as described by the denaturation temperature) of lysozyme significantly decreased from 77 to 61°C after complex formation. They postulated that heparin favoured interaction with the unfolded lysozyme state rather than the native form. Chourpa and co-workers (2006) monitored conformational changes of pea globulin upon complexation with GA using raman

microspectroscopy. Pea globulin, under acidic conditions, mainly consisted of  $\beta$ -sheet and random coil conformations, however when complexed with GA,  $\beta$ -sheets dominated.

Changes to protein conformation upon complexation can alter the exposed surface chemistry of the protein in the solvent, as well as the spatial extensibility. Consequently, the attributes of the new biopolymer complex may have a net positive, neutral or negative effect on its functional properties, relative to the protein alone. In addition, through this process, protein functionality may be modified to a degree to avoid the use of chemical modifying agents or time/temperature sensitive enzymatic treatments (Schmitt et al, 1998). Some important functionalities of protein in food industry include, but are not limited to, solubility, emulsification and foaming.

### **a) Solubility**

Protein solubility depends on the balance between protein-protein and protein-solvent interactions. The solubility of proteins increases when solvent interactions are favoured over protein-protein interactions. The type of interaction is highly affected by the protein's surface charge, surface hydrophobicity as well as its conformation. In general, proteins with high surface charge and low surface hydrophobicity exhibit high solubility. For example, when solvent pH is far away from the pI, a protein exhibits a high net charge. Consequently, the protein has greater solubility than at its pI. Electrostatic interaction between charged groups on the protein and polysaccharide reduces the protein's ability to interact with water; reducing their solubility. Furthermore, complex formation results in conformational changes to the protein which may lead to the exposure or concealment of hydrophobic groups. Therefore, conformational changes may contribute positively or negatively to protein solubility. The solubilities of soy protein isolate, pea legumin and potato protein isolate were found to be increased by complexation with xanthan gum, chitosan and carboxymethylcellulose, respectively (Xie and Hettiarachchy, 1997; Braudo et al., 2001; Vikelouda and Kiosseoglou, 2004). In contrast, reduced protein solubility upon complexation with a polysaccharide has been used as a means to selectively recover protein. Whey proteins have been successfully fractionated into  $\beta$ -lactoglobulin and  $\alpha$ -lactoalbumin by complexation with carboxymethylcellulose at selected pHs (Hidalgo and Hansen, 1971).

## **b) Emulsion stability**

Emulsions play an important role in the food industry in terms of product appearance, texture, flavour and stability. By definition, an emulsion is comprised of a mixture of two immiscible liquids with one liquid dispersed as small droplets within the other; formed after applying mechanical agitation (i.e., homogenization) in the presence of an emulsifier. Depending on the nature of the dispersed liquid, emulsions can be classified as water-in-oil (W/O) or oil-in-water (O/W). An emulsifier is a small (i.e., lecithin) or large (i.e., protein) amphiphilic molecule that migrates to the oil-water interface to lower interfacial tension. Small emulsifiers diffuse quickly to the interface, promoting emulsion formation and short-term stability. Large emulsifiers migrate at a slower pace, then re-align (undergoing a conformational change) at the interface to form a viscoelastic film around the dispersed droplets. Depending on the nature of the emulsifier present and solvent conditions, coalescence may be inhibited by steric hindrance and electrostatic repulsion between neighbouring droplets.

Emulsion stability is dependent on several parameters, including: (i) type of emulsifier present; (ii) droplet size (smaller droplets are more stable); (iii) continuous phase viscosity (a viscous continuous phase reduces the rate of creaming); and (iv) the volume ratio of dispersed versus continuous phase. In general, proteins aid in emulsion stability by interacting with the oil-water interface and by increasing the continuous phase viscosity, whereas polysaccharide functions primarily by the latter mechanism (Dickinson, 2003). For admixtures of proteins and polysaccharides, emulsion stability or instability may be favoured depending on the biopolymer present, solvent conditions and the method of emulsification. Biopolymers can be mixed prior to emulsification (i.e., biopolymer complexes interact with the oil-water interface) or one biopolymer is added (i.e., polysaccharide) to an already protein stabilized emulsion (i.e., biopolymers interact through a layer-by-layer assembly approach, with only one biopolymer interacting with the interface) (Jourdain et al., 2008). In the latter case, emulsion stability becomes concentration dependent. At a dilute polysaccharide concentration, bridging flocculation between protein-coated droplets may occur and lead to emulsion destabilization (Figure 2.7a). In contrast, emulsion stability is enhanced when the polysaccharide concentration is sufficiently high to completely cover protein-coated droplets (Figure 2.7b); or if in

excess, a weak gel-like network may form that immobilizes the droplets (Figure 2.7c) (Dickinson, 2003).

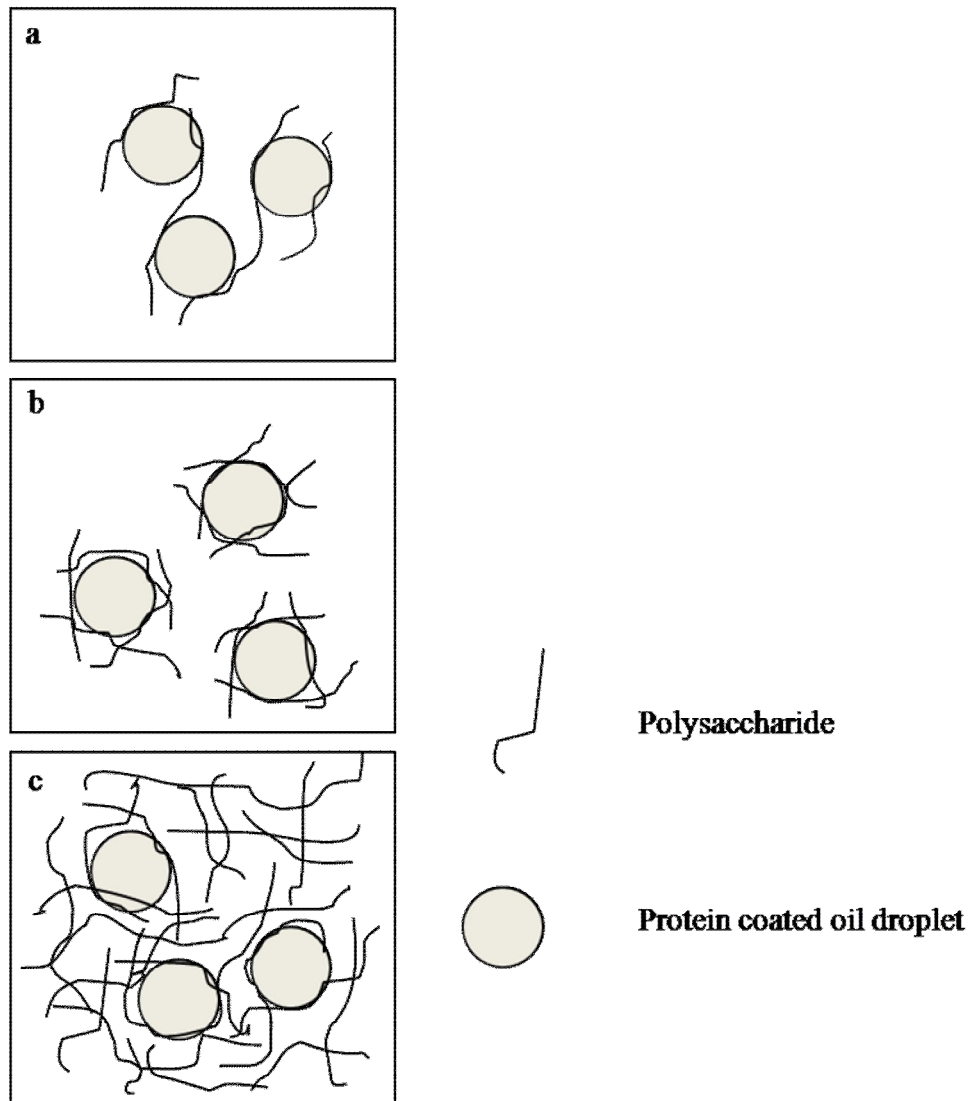


**Figure 2.7 Schematic representations of three alternative effects of polysaccharide on the surface of protein-coated droplets: (a) bridging flocculation, (b) polysaccharide fully coat the droplet surface, and (c) polysaccharide form a weak gel-like network (adapted from Dickinson, 2003).**

### **c) Foaming properties**

Foam is a two-phase system with air as the dispersed phase and an aqueous solution as the continuous phase. Similar to emulsions, foam formation requires surface active agents, such as proteins to reduce the surface tension and to stabilize the interface (i.e., formation of a viscoelastic film). However, foams are more difficult to control and are thermodynamically less stable than emulsions. In general, foam formation involves protein diffusion from the continuous phase to the air-water interface, followed by the conformational change and alignment at the interface to form a viscoelastic film around the dispersed air bubbles. Admixtures of proteins and polysaccharides have been shown to improve foam formation and stability. For instance, foam stabilized by whey protein-carboxymethylcellulose complexes was significantly more stable than that stabilized by protein alone (Mann and Malik, 1996). Stability was enhanced by the electrostatic repulsion between air bubbles and the increase in continuous phase viscosity (which inhibits liquid drainage). Complexation with polysaccharides may cause conformational changes to the protein structure from compact and rigid, to less compact and more flexible, which favours adsorption at the air/water interface (Xie and Hettiarachchy, 1998).

### **2.2.2.3 Encapsulation by complex coacervation**

Formation of microcapsules is accomplished by emulsifying a lipid phase (core material) within an aqueous biopolymer complex coacervate phase (wall material). During emulsification, biopolymer complexes are deposited around the surface of individual oil droplets to form a protective film. Spray or freeze drying is then used to harden the wall material and produce a dry powder. Encapsulation efficiency (the ratio of encapsulated oil to total oil) is dependent on the core and wall materials, total biopolymer concentrations, and emulsification properties of the wall material, which are described as follows:

#### **a) Core-to-wall ratio**

The core-to-wall ratio is an important parameter to control, and maximize the encapsulation efficiency without compromising the wall's protective and mechanical

stability. A general trend is that microencapsulation efficiency decreases as the core-to-wall ratio increases (Hogan et al., 2001). For example, as the core-to-wall ratio of sodium caseinate encapsulated soybean oil increased from 0.25 to 3.0, encapsulation efficiency decreased from 89.15% to 18.80% (Hogan et al., 2001). Madene and co-workers (2006) in a review paper suggested a typical core-to-wall ratio of 1:4 for encapsulating flavouring oils with various wall materials using spray drying.

### **b) Total biopolymer concentration**

The total polymer concentration ( $C_p$ ) has a direct impact on the biopolymer coacervate phase viscosity. To date, studies examining the rheological properties of coacervate phase have been limited. In general, as the  $C_p$  (and hence viscosity) increases, the wall material takes less time to dry (Soottitantawat et al., 2005). However, the viscosity must not become too high so that the wall thickness becomes problematic for core material release (Weinbreck et al., 2004a). Weinbreck and co-workers (2004a) reported that the optimal droplet morphology of encapsulated orange oil (5% w/w oil, pH=4.0, WPI:GA = 2:1) occurred at  $C_p$  between 0.5% to 1% (w/w). However, for a WPI-GA coacervate at a biopolymer weight mixing ratio (WPI:GA) of 2:1 and pH 4.0, maximum coacervation was achieved at a  $C_p$  of 32.8% (w/w) (Weinbreck et al., 2004e). Therefore, the optimal  $C_p$  condition for complex coacervation may not be optimal for encapsulation efficiency.

### **c) Emulsification**

Barbosa and co-workers (2005) demonstrated that the use of an emulsifier (i.e., GA) enhanced emulsion stability, increased microencapsulation efficiency, and provided better protection for the oil-soluble pigment bixin (core material), compared to maltodextrin alone used as wall material. In addition, small emulsion droplet size (0.5  $\mu\text{m}$ ) resulted in reduced surface oil for milk fat encapsulation (Danviriyakul et al., 2002; Soottitantawat and Yoshii, 2003). Droplet size can be altered by changing the homogenization instrument, shearing speed and duration. Weinbreck and co-workers (2004a) reported that in WPI-GA complex coacervate encapsulated orange oil microcapsules, a magnetic stirrer created larger droplet size than that using a blender. In

addition, ultrasound has been suggested to produce higher encapsulation efficiency than using a homogenizer (Mongenot et al., 2000).

## **2.3 Choice of wall materials**

### **Overview of common wall materials**

Microcapsules prepared for the food industry most often consist of protein and/or polysaccharide. Both biopolymers under specific conditions have gel- and film-forming properties making them ideal wall materials. Proteins can also act as an emulsifying agent because they are amphiphilic (i.e., have both a hydrophilic and hydrophobic component). Gelatin alone or in combination with a polysaccharide is a commercial encapsulation agent. Recently, safety concerns about gelatin in food or biomaterial application has increased due to the potential contamination from Bovine spongiform encephalopathy (BSE) related animals. As such, the search for a plant-based alternative is of economic importance (Pierucci et al., 2006). In this research, pea protein and GA were employed as encapsulation materials. Pea protein was selected since it represents an underutilized plant protein ingredient and its superior nutritional value compared to gelatin. GA is known to have emulsifying properties and its branches have carboxyl reactive groups, capable of complexing with pea protein below its pI. Alginate is another potential polysaccharide that could be used to form complexes with pea protein. In contrast to GA, alginate is a linear polysaccharide containing a greater number (or linear charge density) of carboxyl groups per unit length. Therefore, alginate may interact more strongly (a consequence of a greater number of protein-polysaccharide linkages rather than bond strength) with pea protein leading to a different complex structure and wall matrix.

### **Pea protein**

Field pea (*Pisum sativum*) contains 20-30% protein, with the majority being the storage proteins, globulins and albumins (Schroeder, 1982). The globulin-type storage proteins: legumin and vicilin represent 65-80% of extractable pea protein (Schroeder, 1982). Legumin is a hexameric 11S protein (350-400 kDa), composed of six  $\alpha$ - $\beta$  subunit pairs arranged to form a trigonal bipyramid; vicillin is a trimer 7S protein, comprised of



three subunits with molecular mass of approximately 50 kDa each (Lampart-Szczapa, 2001). Functionally, pea legumin is non-gelling, while vicilin has gelling potential (Lampart-Szczapa, 2001). The pI of pea protein is ~ pH 4.5 (Koyoro and Powers, 1987). However, depending on the extraction process, the pI of pea protein can vary from 4 to 6. During complex coacervation, solution pH must be kept below the pI to ensure an overall net positive charge for pea protein. Initial studies of microencapsulation by complex coacervation involving pea protein globulin and GA for oil entrapment have been conducted by Ducel and co-workers (2004). Using a combination of zeta potential and turbidity measurements, they found that optimal coacervation conditions for pea protein globulin and GA was at pH 3.5 with a biopolymer weight mixing ratio of 50:50. However, the best oil droplet morphology was obtained at pH 2.75 with a biopolymer weight mixing ratio (pea protein globulin:GA) of 30:70.

### **Gum Arabic**

Gum Arabic is a natural exudate from *Acacia senegal* and *Acacia seyal* trees, widely used by the food and pharmaceutical industries. Its popularity is attributed to its excellent emulsifying properties and low viscosity at high concentrations. In order to optimize the utilization of GA, numerous studies on its structure-function relationships have been carried out to obtain a greater understanding of its emulsifying mechanism (Randall et al., 1989; Qi et al., 1991; Yadav et al., 2007). Gum Arabic is an anionic arabinogalactan polysaccharide, comprised of three fractions. The major fraction (~89% of the total; ~250 kDa) consists of a  $\beta$ -(1→3) galactopyranose (galactan) polysaccharide backbone that is highly branched with  $\beta$ -(1→6) galactopyranose residues terminating in arabinose and glucuronic acid and/or 4-O-methyl glucuronic acid units. The second fraction (~10% of the total) is comprised of an arabinogalactan-protein complex, where arabinogalactan chains are covalently linked to a polypeptide backbone. The remaining fraction (~1% of the total) consists of a glycoprotein similar to the arabinogalactan-protein complex, except with higher protein levels and comprised of different amino acid sequences (Dror et al., 2006). In a recent study by Yadav and co-workers (2007), it was proposed that GA contained trace lipid attached to the arabinogalactan-protein complex, referred as the glycosylphosphatidylinositol (GPI) lipid anchor, and that this

may assist in localizing the arabinogalactan-protein complex at the oil-water interface. The proposed structure of gum Arabic is shown in Figure 2.8. Matsumura and co-workers (2003) have found that peptide-bound polysaccharides, such as GA, may also have an inhibitory effect on lipid oxidation in a non-food emulsion. This observation was also reported by Park and co-workers (2005). Although this antioxidant effect in a food emulsion has not been confirmed, the use of GA as a wall material is proposed to be beneficial due to its emulsifying ability.

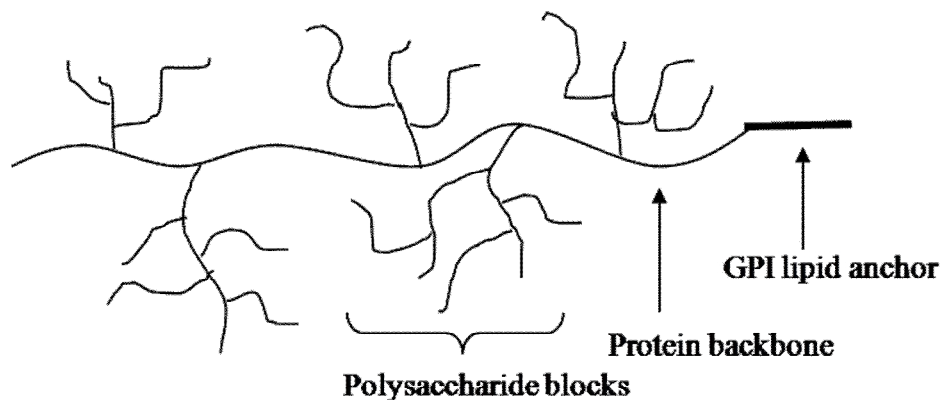


**Figure 2.8 Proposed structure of gum Arabic-GPI (glycosylphosphatidylinositol)**  
(Adapted from Islam et al., 1997).

### **Alginate**

Alginate, commercially known as sodium alginate, is the sodium salt of alginic acid, which is found in the cell wall of brown algae. Alginic acid is a linear polymer of two monomers,  $\beta$ -D-mannopyranosyluronic acid ( $\beta$ DManpA) and  $\alpha$ -L-gulopyranosyluronic acid ( $\alpha$ LGulpA) (Figure 2.9).  $\beta$ DManpA are linked  $\beta$ -(1-4) to form linear blocks, referred to as M blocks;  $\alpha$ LGulpA are linked  $\alpha$ -(1-4) to form linear blocks, referred to as G blocks (BeMiller and Huber, 2008). Alginate is commonly used in the food and pharmaceutical industries to increase viscosity and to form gels in the presence of calcium. Depending on the monomer content and distribution, alginate gels can

exhibit different strengths. Higher contents of  $\alpha$ LGulpA or G blocks results in the formation of stronger gel networks (BeMiller and Huber, 2008).

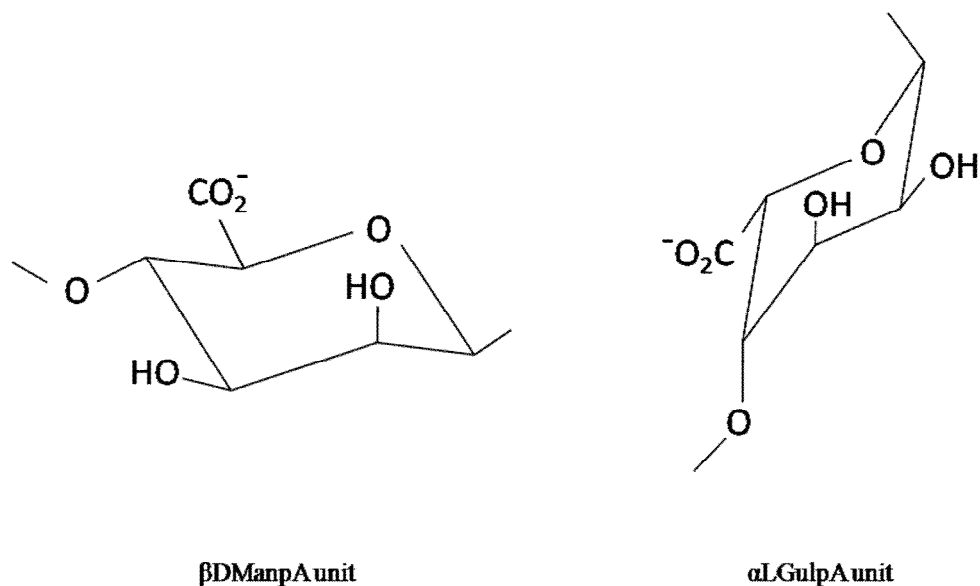


**Figure 2.9 Alginate units:  $\beta$ -D-mannopyranosyluronic acid ( $\beta$ DManpA) and  $\alpha$ -L-gulopyranosyluronic acid ( $\alpha$ LGulpA) (Adapted from BeMiller et al., 2008).**

#### 2.4 Flax oil as core ingredient

Flaxseed (*Linum usitatissimum*) is recognized as a valuable commercial crop because of its high nutritional composition, containing 41% lipid, 20% protein and 28% dietary fiber. Based on its fatty acid profile, flax oil is a rich source of  $\alpha$ -linolenic acid (ALA) relative to other plant-based oils (Table 2.2). Of the total fatty acid content, 57% w/w is ALA. ALA (C18:3 n-3), an omega-3 ( $\omega$ -3) fatty acid, and linoleic acid (LA) (C18:2 n-6), an omega-6 ( $\omega$ -6) fatty acid, are two essential fatty acids in the human diet. Omega-3 fatty acids are beneficial for normal brain and eye development, and for reducing the risks of chronic diseases, such as, coronary heart disease, certain types of cancers, and inflammatory disease (Bougnoux et al., 2003; Li et al., 2003; Cleland and James, 2003). LA is the precursor of prostaglandin E1 (PGE1) and E2 (PGE2); whereas prostaglandin E3 (PGE3) is synthesized from ALA. The anti-inflammatory PGE1 and

PGE3 work in combination with inflammatory PGE2 to ensure a healthy blood clotting system. However, excessive dietary LA can be problematic due to the high production of inflammatory PGE2 that has been correlated with artery hardening and stroke (Prasad, 2003).

**Table 2.2 Comparison of fatty acid profiles in dietary fats and oils from various sources (Adapted from Morris, 2007).**

Source	ALA <sup>a</sup>	LA <sup>b</sup>	SF <sup>c</sup>	MUF <sup>d</sup>
Flaxseed oil	57	16	9	18
Solin oil	2	71	9	18
Canola oil	11	21	7	61
Sunflower oil	1	71	12	16
Corn oil	1	57	13	29
Olive oil	1	9	15	75
Soybean oil	8	54	15	23
Peanut oil	Trace	33	19	48
Lard	1	9	43	47
Beef tallow	1	2	48	49
Palm oil	Trace	10	51	39
Butterfat	1	3	68	28

<sup>a</sup> ALA:  $\alpha$ -linolenic acid;

<sup>b</sup> LA: linoleic acid;

<sup>c</sup> SF: saturated fatty acids;

<sup>d</sup> MUF: monounsaturated fatty acids;

All values are based on percentage by weight of the total fatty acids.

## Chapter 3

### Effect of pH, salt and biopolymer ratio on the formation of pea protein isolate-gum Arabic complexes<sup>1</sup>

#### 3.1 Abstract

Optimal biopolymer and solvent conditions for complex coacervation between PPI and GA were investigated as a function of pH (6.00-1.50), NaCl (0-50 mM) and biopolymer weight mixing ratio (PPI:GA=0.25:1 to 10:1) by turbidimetric acid titration. For mixtures in the absence of salt and at a 1:1 biopolymer weight mixing ratio, two structure-forming transitions were observed as a function of pH. The first event occurred at pH 4.23, with the second at 3.63, indicating the formation of soluble and insoluble complexes, respectively. Sodium chloride at  $\leq 7.5$  mM was found to have no effect on biopolymer interaction, but interfered with interaction at higher levels ( $>7.5$  mM) due to substantial PPI aggregation. The pH at which maximum PPI-GA interactions occurred was 3.50, and was independent of NaCl levels ( $\leq 7.5$  mM). As PPI-GA ratios increased, structure-forming transitions shifted to higher pH and then became constant. The optimal biopolymer and solvent condition for complex coacervation was found to be at a 2:1 biopolymer weight mixing ratio at pH 3.60, and in the absence of added NaCl.

---

<sup>1</sup> Reproduced with permission from Liu, S., Low, N.H. and Nickerson, M.T. 2009. Effect of pH, salt, and biopolymer ratio on the formation of pea protein isolate-gum Arabic complexes. *Journal of Agricultural and Food Chemistry*, 57, 1521-1526. Copyright (2009) American Chemical Society.

### 3.2 Introduction

Protein-polysaccharide interactions play significant roles in controlling the structure, texture and stability in food systems (deKruif and Tuinier, 2001), coatings, and packaging materials (Weinbreck et al., 2004d). In order to control these interactions to give desired functionality (i.e., gel/film-forming, emulsifying, foaming), a greater understanding of the factors affecting protein-polysaccharide interactions is required (Dickinson, 1998). The nature of these interactions may lead to either segregative or associative phase behaviour, depending on biopolymer characteristics (i.e., their charge density, type and distribution of reactive groups, size), biopolymer concentration and ratio, and solvent conditions (i.e., pH, temperature, ionic strength) (Turgeon et al., 2003; Weinbreck et al., 2003a; Chourpa et al., 2006). In general, segregative phase behaviour occurs when both protein and polysaccharide carry similar charge, separating into protein- and polysaccharide-rich phases. Associative phase behaviour (also termed complex coacervation) typically occurs via an electrostatic attraction between protein and/or polysaccharide carrying opposing charges, leading to separation into biopolymer-rich (also known as 'coacervate-rich') and solvent-rich phases (Braudo et al., 2001; de Kruif et al., 2001; Turgeon et al., 2003). The former is comprised of electrostatically formed biopolymer complex with small amount of entrapped solvent. Since these interactions are dominated by electrostatic forces, interactions are generally reversible and highly dependent upon solvent pH and salt content, although irreversibility of the formed complexes may occur if non-Coulombic interactions are significant (Ye, 2008). During complex coacervate formation, both the conformational entropy of the biopolymers and the entropy associated with solvent mixing are reduced, which offsets the enthalpic contributions associated with the release of water and counter-ions during complexation, leading to the stabilization of the formed coacervate (biopolymer complex) phase (Schmitt et al., 1999; Singh et al., 2007; Ye, 2008).

Most of the studies on complex coacervation have investigated complexation between milk proteins, serum albumin (Kaibara et al., 2000; Glisenan et al., 2003), casein (de Kruif and Tuinier, 2001; Tuinier et al., 2002; Turgeon et al., 2003),  $\beta$ -lactoglobulin (Schmitt et al., 1999, 2000; Girard et al., 2002; Wang et al., 2007) or whey (Weinbreck et al., 2003a; Weinbreck et al., 2004b-d) with anionic polysaccharides.

Although the mechanisms driving complexation have not been fully elucidated, it is believed that two-structure forming transitions occur as a function of pH, associated with the formation of soluble, and then insoluble complexes via a nucleation and growth-type mechanism (Girard et al., 2004; Sanchez et al., 2006). In a recent paper by Turgeon and co-workers (2007), advances associated with complex formation between protein and polysaccharide were reviewed. Soluble protein-polysaccharide complex form near the protein's pI, as evident by a slight increase in turbidity (denoted as  $\text{pH}_c$ ), followed by macroscopic phase separation at  $\text{pH}_{\phi_1}$  and the formation of insoluble protein-polysaccharide complex (de Kruif and Tuinier, 2001; Turgeon et al., 2003; Weinbreck et al., 2003a). The critical pH ( $\text{pH}_c$ ) signifies the initial non-covalent attraction experimentally detected between the protein and the polysaccharide, whereas at  $\text{pH}_{\phi_1}$ , macroscopic phase separation occurs as the net charge on each biopolymer becomes opposite (Ducel et al., 2004). Conditions for complexation are considered optimal at a pH where both biopolymers reach their electrical equivalence (denoted as  $\text{pH}_{\text{opt}}$ ), and complexation ceases at a lower pH ( $\text{pH}_{\phi_2}$ ), where reactive groups along the polysaccharide become protonated (giving both biopolymers a similar net charge). Weinbreck and co-workers (2003a) and Mekhloufi and co-workers (2005) using whey protein isolate and  $\beta$ -lactoglobulin ( $\beta$ -LG) observed a two-step structure-forming event upon acid titration with a polysaccharide similar to that used in the present study. Due to the electrostatic nature of the interactions, investigation of the effects of salt, degree of ionization and mixing ratio (i.e., achieving conditions where biopolymers are electrically equivalent) on these critical pH values is crucial to understanding their complexation.

To our knowledge, studies focused on understanding mechanisms for complexation involving plant protein with anionic polysacchrides have been limited, especially as it relates to initial PPI-GA interactions (i.e., formation of soluble complexes). The aim of this study was to advance our understanding of mechanisms underlying associative phase behaviour between PPI and GA, by investigating the effects of salt, pH and biopolymer weight mixing ratio on the formation of soluble and insoluble complexes. Previous work by Ducel and co-workers (2004) on pea globulin-GA complexation involved studying solvent and biopolymer effects under conditions showing maximum protein-polysaccharide interactions, as it relates to a potential

encapsulating material, rather than investigating their effects on the formation of soluble and insoluble complexes.

### **3.3 Materials and Methods**

#### **3.3.1 Materials**

Pea flour (PF) (Fiesta Flour, Lot #: F147X, 2008) and GA (Gum Arabic FT Pre-Hydrated, Lot #: 11229, 2007) were kindly donated by Parrheim Foods (Saskatoon, SK) and TIC Gums (Belcamp, MD), respectively. The composition of the PF was 7.80% moisture, 21.78% protein (%N x 6.25), 1.00% lipid, 65.26% carbohydrate and 4.16% ash (mineral content (w/w): 0.02% sodium, 0.88% potassium, 0.09% calcium, 0.12% magnesium, 0.34% phosphorus). In contrast, GA was comprised of 9.56% moisture, 0.86% protein (%N x 6.25), 0.11% lipid, 84.28% carbohydrate and 5.19% ash (mineral content (w/w): 0.50% sodium, 0.24% potassium, 1.03% calcium, 0.12% magnesium). Chemical analyses on all materials were performed according to AOAC Methods 925.10 (moisture), 923.03 (ash), 920.87 (crude protein) and 920.85 (lipid) (AOAC, 2003). Carbohydrate content was determined based on percent differential from 100%.

PPI was prepared by dissolving PF into a 0.1 M phosphate buffer (pH 8.0) containing 6.4% KCl at a 1:10 (w/v) ratio, followed by mixing at 500 rpm using a magnetic stirrer (Heidolph MR 3003 control stir plate, Heidolph Instruments GmbH & Co., DEU) for 24 h at room temperature (~21-22°C) (Créviu et al., 1996). Insoluble residues were then removed by centrifugation at  $3840 \times g$  for 20 min. The supernatant was dialyzed (Spectro/Por® tubing, 6-8 kDa cut off, Spectrum Medical Industries, Inc, USA) for salt removal using Milli-Q™ water (Millipore Corporation, MA) at 4°C; refreshing every 30 min until dialysis water conductivity reached 2.1 mS/cm. De-salted supernatant was freeze dried (Labconco Corporation, MO) and stored at 4°C. The composition of the PPI was determined to be comprised of 8.92% moisture, 82.80% protein (%N x 6.25), 1.06% lipid, 0.75% carbohydrate and 6.47% ash (mineral content (w/w): 0.17% sodium, 0.69% potassium, 0.08% calcium, 0.13% magnesium, 0.58% phosphorus). PPI and GA powders were used without further purification. Biopolymer concentrations used in this study reflect the protein (PPI) or carbohydrate (GA) content rather than powder weight.



### 3.3.2 Turbidimetric analysis during an acid titration

Stock solutions (0.50%, w/w; pH 8.0) of PPI and GA were prepared by dissolving each powder in Milli-Q<sup>TM</sup> water under constant stirring (500 rpm) for 2 h at room temperature (21-22°C), and then overnight at 4°C to help facilitate protein solubility. Mixtures of PPI and GA were prepared by mixing appropriate masses of stock solutions, at the desired ratio, with Milli-Q<sup>TM</sup> water to achieve a Cp of 0.05% (w/w) (adjusted to pH 8.0 with 0.1M NaOH). Turbidimetric titration upon acidification was achieved via the addition of an internal acidifier (0.05% (w/w) glucono-delta-lactone, GDL) to slowly lower the mixture pH to 3.9, followed by the dropwise addition of HCl (Weinbreck et al., 2003a; Weinbreck et al. 2004b). Diluting effects were kept to a minimum using a gradient of HCl concentrations based on pH (0.05M>pH 3.30; 0.5M>pH 2.70; 1M>pH 2.20; 2M>pH 1.50). Dilution was thought to not significantly influence complex formation based on findings, and because critical pH values ( $pH_c$ ,  $pH_{\phi_1}$  and  $pH_{opt}$ ) measured in this study corresponded to conditions where no or minimal HCl addition occurred. For instance, within the pH range (4.23-3.50) corresponding to  $pH_c$ ,  $pH_{\phi_1}$  and  $pH_{opt}$ , the rise in conductivity (~150 mS/cm) and level of dilution (<0.5%) was considered insignificant. In contrast, at pH 2.6 (corresponding to  $pH_{\phi_2}$ ) the change in conductivity (1900 mS/cm) and dilution (<3%) was much greater. The rise in conductivity measured in this study is associated with addition of acidulants and the release of counter ions during complexation (Schmitt et al., 1999; Singh et al., 2007; Ye, 2008). Changes in the optical density of the solution were recorded over a pH range of 6.00 to 1.50 using a UV/Vis spectrophotometer (Mecasys Co, Daejeon, South Korea) at 600 nm using plastic cuvettes (1 cm path length). The effect of salt (NaCl) and biopolymer weight mixing ratio on turbidimetric acid titrations were investigated systematically, testing: a) the effect of added NaCl (0-50 mM) for a 1:1 PPI-GA mixture; and b) the effect of biopolymer weight mixing ratio (PPI:GA) (1:4, 1:2, 1:1, 2:1, 4:1, 6:1, 8:1 and 10:1) in the absence of added NaCl. Homogenous PPI and GA solutions were used as blanks under the same solvent conditions, and at corresponding protein or polysaccharide concentrations. Structure-forming transitions ( $pH_c$ ,  $pH_{\phi_1}$  and  $pH_{\phi_2}$ ) were determined graphically as the intersection point of two curve tangents (Weinbreck et al., 2003a), whereas  $pH_{opt}$  corresponded to the maximum optical density at 600 nm (Figure

3.1). All measurements were made in triplicate, using separate stock solutions. All chemicals used in this study were reagent grade, and purchased from Sigma-Aldrich Canada Ltd. (Oakville, ON).

### 3.3.3 Electrophoretic mobility

To access the overall surface charge of the formed complexes, electrophoretic mobility ( $U_E$ ) for a 2:1 PPI-GA mixed system and its corresponding homogenous PPI and GA solutions during an acid titration from 6.5 to 1.5 was measured using a Zetasizer Nano with a MPT-2 autotitrator (Malvern Instruments, Westborough, MA). Sodium hydroxide (0.25 M) and HCl (0.25 M and 0.025 M) were used as titrants, to lower the pH. Samples were prepared as described in Section 3.2.2, but were diluted 10-fold to a final Cp of 0.005% (w/w). Electrophoretic mobility (i.e., velocity of a particle within an electric field) was related to the zeta potential ( $\zeta$ ) using the Henry equation:

$$U_E = \frac{2\varepsilon \times \zeta \times f(\kappa\alpha)}{3\eta} \quad [3.1]$$

where  $\eta$  is the dispersion viscosity,  $\varepsilon$  is the permittivity, and  $f(\kappa\alpha)$  is a function related to the ratio of particle radius ( $\alpha$ ) and the Debye length ( $\kappa$ ). Using the Smoluchowski approximation  $f(\kappa\alpha)$  equaled 1.5. All measurements were made in duplicate.

### 3.3.4 Statistical analysis

A one-way analysis of variance (ANOVA) with a Scheffe Post-Hoc test was used to measure statistical differences within state diagrams for each  $\text{pH}_c$ ,  $\text{pH}_{\phi 1}$ ,  $\text{pH}_{\text{opt}}$ , and  $\text{pH}_{\phi 2}$  as a function of salt, and biopolymer weight mixing ratio. All statistical analyses were performed using Systat software (SPSS Inc., Ver. 10, 2000, Chicago, IL, USA).

### 3.4 Results and Discussion

#### 3.4.1 Associative phase behaviour as a function of NaCl

Control of pH and ionic strength is critical to maximizing the strength of protein-polysaccharide interactions during complex coacervation. Solvent pH influences the number of charged reactive groups on the biopolymers surface, whereas the ionic strength acts to promote solubility at low concentrations, but interferes with electrostatic attractive forces at higher levels (Schmitt et al., 1999). The effect of NaCl (0-50 mM) on complexation between PPI and GA were studied during an acid titration at a 1:1 biopolymer weight mixing ratio in aqueous solution. Mixtures in the absence of NaCl, displayed two structure-forming transitions corresponding to the formation of soluble ( $\text{pH}_c=4.23$ ) and insoluble ( $\text{pH}_{\phi 1}=3.63$ ) complexes (Figure 3.1). For pHs higher than  $\text{pH}_{\phi 1}$ , all solutions were transparent. The rise in optical density signifies an increase in size and number of PPI-GA or PPI (aggregated)-GA complexes being formed. The highest amount of biopolymer interactions occurred at pH 3.47 ( $\text{pH}_{\text{opt}}$ ), followed by a disassociation of complexes near pH 2.58 ( $\text{pH}_{\phi 2}$ ) where both biopolymers carried a similar overall net positive charge. Under the same conditions, PPI alone gave only a weak scattering intensity (optical density  $<0.2$ ), whereas GA had none (Figure 3.2a). Ducel and co-workers (2004) reported a similar  $\text{pH}_{\text{opt}}$  for a 1:1 pea globulin-GA mixture. The observed two-step structure forming events have been previously reported for WPI-GA (Weinbreck et al., 2003a), WPI-EPS B40 (Weinbreck et al., 2003b), WPI-carrageenan (Weinbreck et al., 2004b),  $\beta$ -LG-pectin (Girard et al., 2004),  $\beta$ -LG-GA (Mekhloufi et al., 2005), and gelatin-agar (Singh et al., 2007) systems, as a consequence of increased electrostatic attractive interactions. The peak intensity for the homogenous PPI solution at pH  $\sim 4.0$  in the current study, although minor, is thought to correspond to a rise in protein-protein aggregation. The broad nature of the peak reflects the polydispersity of the isolate and its various protein components.

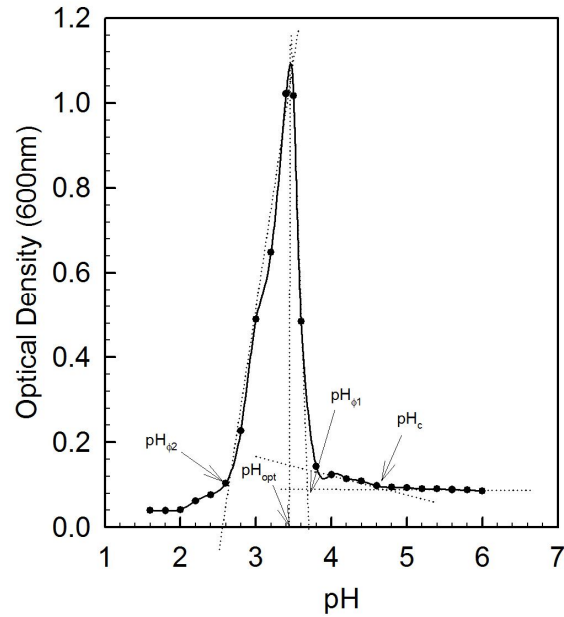


**Figure 3.1** Turbidity curve of PPI-GA mixture ( $C_p=0.05\%$  w/w, PPI:GA=1:1 w/w, NaCl=0 mM).  $pH_c$ ,  $pH_{\phi 1}$ ,  $pH_{opt}$  and  $pH_{\phi 2}$  represented critical pH transitions during acid titration.

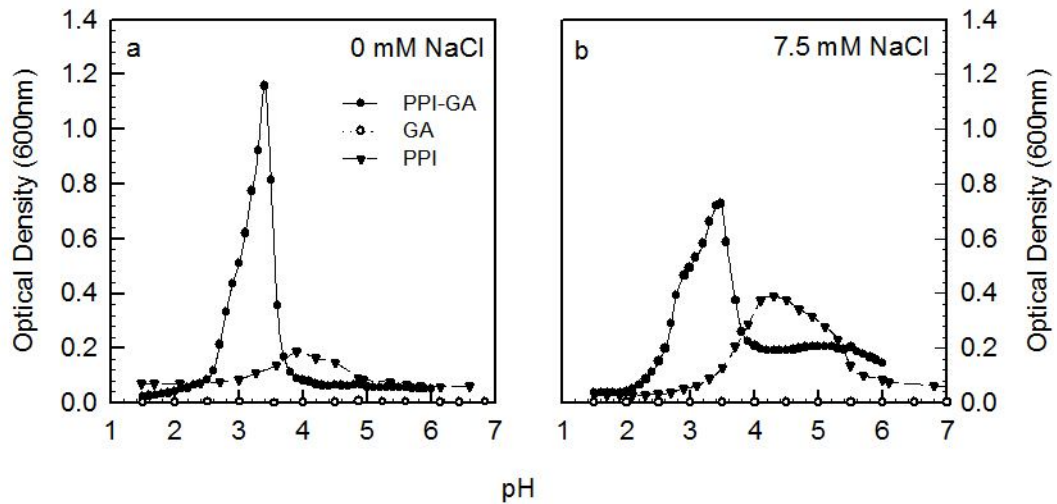


**Figure 3.2** Turbidity curves of PPI, GA and PPI-GA mixture ( $C_p=0.05\%$  w/w, PPI:GA=1:1 w/w) in the absence (a) and presence of 7.5 mM NaCl (b).

At a NaCl level of 7.5 mM, optical density of the PPI blank became more pronounced as charges on the protein's surface became screened (Figure 3.2b). At NaCl levels >7.5 mM, the aggregation phenomenon dominated the scattering spectrum preventing reliable estimates of critical pH transitions (data not shown). Higher salt levels are also expected to interfere with coacervate formation. Ducel and co-workers (2004) investigated the effect of NaCl on the coacervation of pea globulin and GA at a 1:1 mixing ratio (pH 3.47), and found that ionic strengths <50 mM did not alter the process, however they were unable to determine a critical ionic strength that inhibited coacervation due to protein precipitation. A state diagram describing changes to critical pH values for PPI-GA mixed systems as a function of NaCl is shown in Figure 3.3. PPI-GA mixtures were considered to be co-soluble at solvent  $\text{pH} > \text{pH}_c$  and  $< \text{pH}_{\phi 2}$ . Within the pH range (~4.20-2.50) where coacervation occurred, all critical pH values were found to be independent of NaCl levels at concentrations  $\leq 7.5$  mM, despite being dominated by electrostatic forces (Figure 3.3a). Maximum PPI-GA interactions at a biopolymer ratio of 1:1 occurred at a solvent pH of 3.47 (Figure 3.3b). Singh and co-workers (2007) observed similar trends for gelatin-agar mixtures, where  $\text{pH}_c$  remained independent of NaCl levels (0-200 mM) and  $\text{pH}_{\phi 1}$  remained constant until reaching a critical value (~50 mM), before shifting to a lower pH as the ionic strength increased to 200 mM. Weinbreck and co-workers (2004b) also observed a similar phenomenon in WPI-carrageenan mixtures.

### **3.4.2 Associative phase behaviour as a function of biopolymer mixing ratio**

Biopolymer weight mixing ratio is critical for controlling the charge balance between proteins and polysaccharides, the intensity of interactions and the degree of self-aggregation during complexation (Ye, 2008). The effect of PPI-GA mixing ratio (1:4 to 10:1) on complex coacervation was investigated during an acid titration, in the absence of added salt and at a constant  $C_p$  (0.05%, w/w). Under conditions where PPI-GA ratios were <1, the turbidity curves shifted to lower pH and the overall scattering intensity was reduced relative to the 1:1 ratio at  $\text{pH}_{\text{opt}}$  (Figure 3.4a). Interactions were almost negligible at a PPI-GA ratio of 1:4; likely due to the large concentration of GA

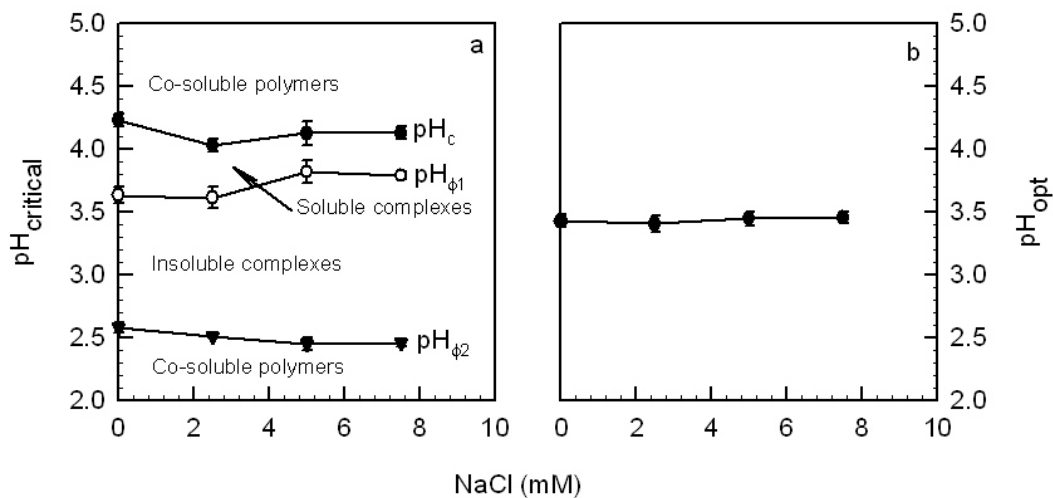


**Figure 3.3** Phase diagrams of critical pH transitions,  $pH_c$ ,  $pH_{\phi_1}$ ,  $pH_{\phi_2}$  (a) and  $pH_{opt}$  (b), as a function of NaCl ( $C_p=0.05\%$  w/w, PPI:GA=1:1 w/w) .

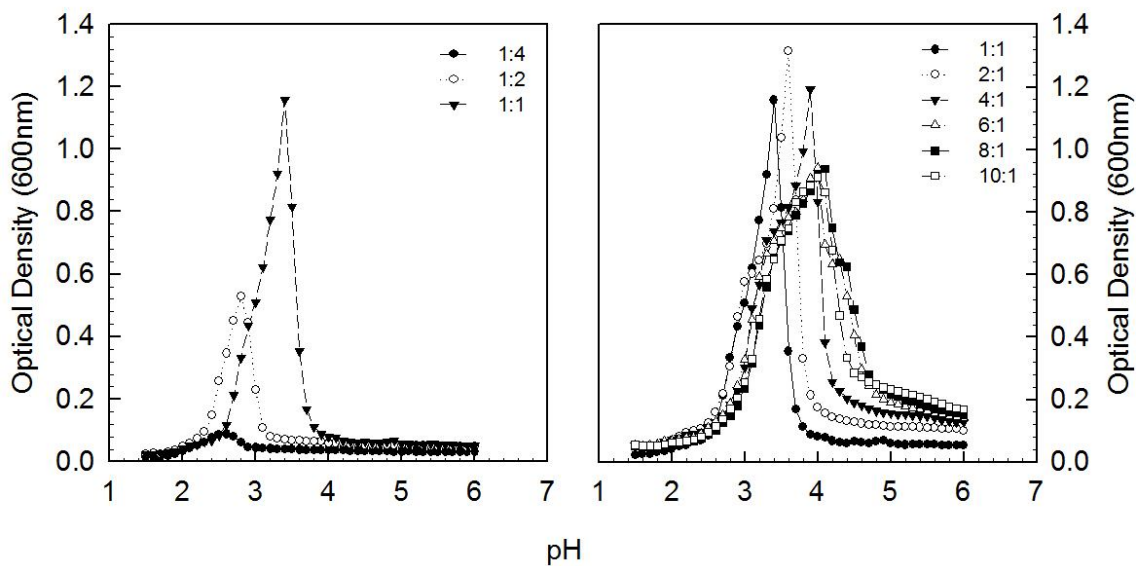


**Figure 3.4** Turbidity curves of PPI-GA mixtures ( $C_p=0.05\%$  w/w, NaCl=0 mM) at different biopolymer weight mixing ratios.

present in the system, which is a poor scatterer by itself. Blanks for both PPI and GA solutions contributed little to the scattering spectrum (optical density <0.2) for PPI-GA ratios <1:1 (data not shown). In contrast, at PPI-GA mixing ratios >1:1, scattering curves shifted to higher pH until reaching a mixing ratio of 4:1, after which turbidity curves overlapped (Figure 3.4b). Schmitt and co-workers (1999) reported a similar phenomenon when acacia gum or  $\beta$ -LG was in excess.

A state diagram depicting the effect of biopolymer weight mixing ratio on critical pH values associated with the structure-forming transitions is shown in Figure 3.5a. At PPI-GA mixing ratios <1, the critical transition pHs ( $\text{pH}_c$  and  $\text{pH}_{\phi 1}$ ) shifted considerably to lower pH as the protein content is decreased, suggesting that inter-polymer interactions were significantly reduced. Complex formation could not be detected at a PPI-GA ratio of 1:4 possibly because of the reduced protein levels present (Figure 3.4a). At mixing ratios where the protein content was greater, critical values shifted to higher pH as biopolymer weight mixing ratio increased, until reaching a ratio of 4:1 where it then became stable, showing no statistical differences ( $p>0.05$ ) for PPI-GA mixing ratios up to 10:1 (Figure 3.5a).

A similar trend was evident for  $\text{pH}_{\text{opt}}$  as a function of biopolymer weight mixing ratio (Figure 3.5b), however its corresponding maximum optical density was observed at 2:1 PPI-GA ratio before declining and reaching a plateau at ratios of 6:1 to 10:1 (Figure 3.5c). These results suggest that the greatest amount of PPI-GA interactions occurred at a mixing ratio of 2:1. It was assumed that at this ratio proteins became saturated by GA chains and, at mixing ratios above 2:1, proteins were in excess as evident by a rise in protein-protein aggregation in the turbidity spectrum of the protein blank (data not shown). The increased contribution from PPI aggregates during complex formation at higher mixing ratios is also shown by shifts in  $\text{pH}_{\phi 1}$  and  $\text{pH}_{\text{opt}}$  closer to the isoelectric point of PPI, as the mixing ratio increased from 1:1 to 4:1. This phenomenon can be attributed to an increase in the number of proteins interacting with the same number of GA chains, as a result of reduced protein charge (Schmitt et al., 1999; Koh and Tucker, 1988). Electrophoretic mobility measurements for a 2:1 PPI-GA ratio estimated a net neutral surface charge of formed complexes (zeta potential=0 mV) occurred at a solvent

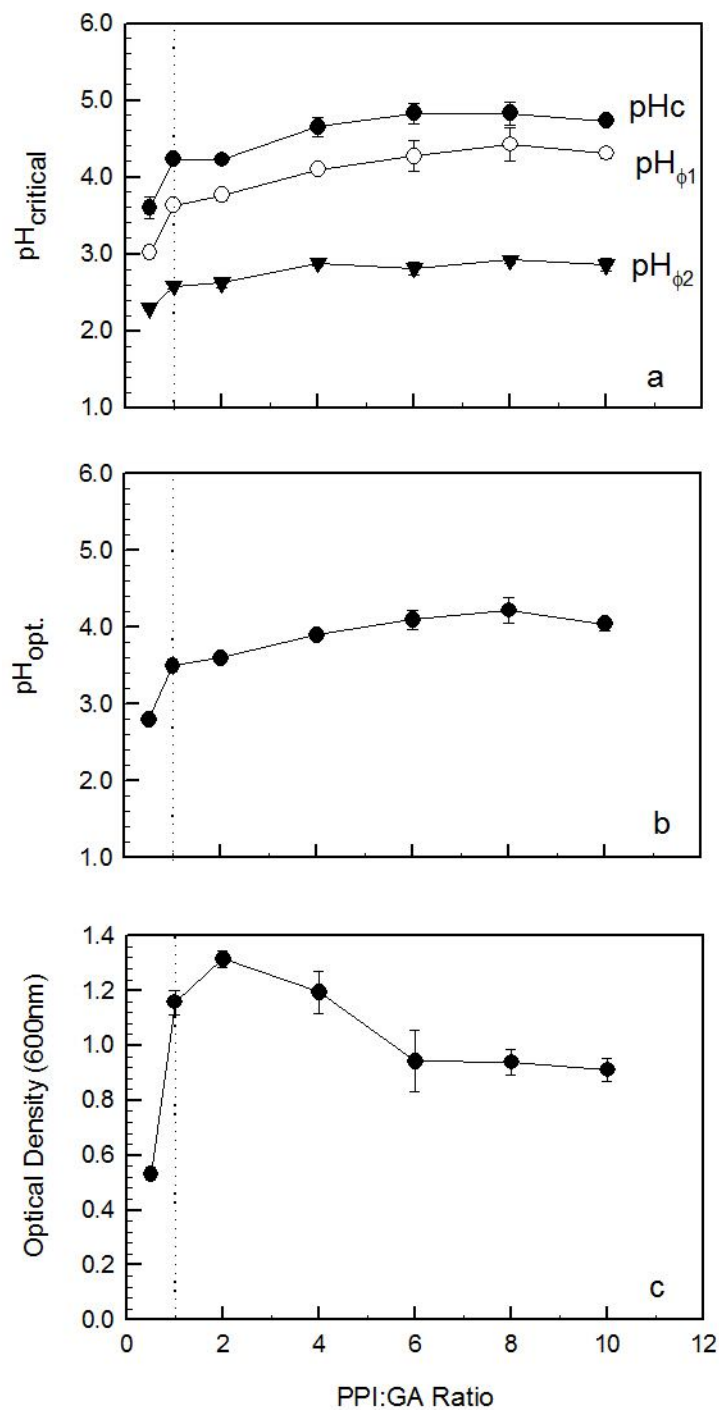


**Figure 3.5** Phase diagrams of critical pH transitions ( $C_p=0.05\%$  w/w,  $\text{NaCl}=0$  mM):  $\text{pH}_c$ ,  $\text{pH}_{\phi_1}$ ,  $\text{pH}_{\phi_2}$  (a), and  $\text{pH}_{\text{opt}}$  (b); and peak optical density (c) as a function biopolymer weight mixing ratio (PPI:GA). Dotted line represent PPI:GA=1:1.



pH of 3.57 (Figure 3.6, which was equivalent to the  $pH_{opt}$  of the system Figure 3.5b). At  $pH > 3.57$ , formed complexes carried a net negative charge (zeta potential  $< 0$  mV) as the charge contribution from the GA dominates over that of PPI despite being the less prevalent biopolymer present. In contrast, at  $pH < 3.57$  a net positive charge of complex occurs (zeta potential  $> 0$  mV) where the positive charge contribution from PPI dominates, as glucuronic acid residues on the GA start to become protonated. Neutrality of homogenous PPI and GA solutions occurred at a solvent pH of 5.60 and 1.88, respectively, and corresponded to the pI of the PPI and the protonation of the carboxyl group on the GA molecule, respectively.

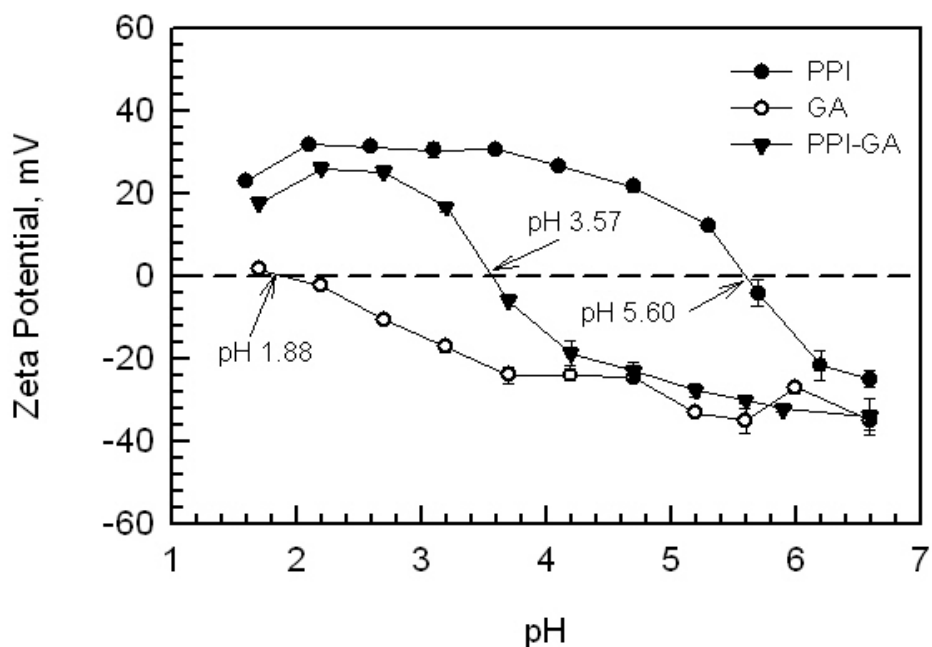


**Figure 3.6 Zeta potential (mV) values for PPI, GA and PPI-GA mixture ( $C_p=0.005\%$  w/w, PPI:GA=2:1 w/w, NaCl=0 mM) as a function of pH.**

Weinbreck and co-workers (2003a-b) for WPI (aggregate-free)-polysaccharide, and Girard and co-workers (2004) for  $\beta$ -LG (aggregate-free)-pectin systems reported a constant  $\text{pH}_c$  as a function of biopolymer weight mixing ratio, suggesting the formation of soluble complexes occurred between a single polysaccharide chain and a given amount of protein. In contrast, in the present study  $\text{pH}_c$  was found to be dependent upon biopolymer weight mixing ratio  $<4:1$  which skews from the current view in literature (Weinbreck et al., 2003b, 2004b; Girard et al., 2004; Sanchez et al., 2006).

Determination of the  $\text{pH}_c$  is based on the first detectable evidence of biopolymer interactions occurring within the scattering spectrum (as noted by a small inflection point within a turbidimetric vs. pH curve during acidification). In the current study, the role of protein-protein aggregates seems to play a significant role during complexation. In Figure 3.2a, optical density for the homogenous PPI system is  $\sim 0.2$  within the pH region of 3.5-4.2, effectively overlapping within the region where complexes initially form for the 1:1 mixing ratio. Findings suggest that during complexation, GA chains are interacting with protein-protein aggregates rather than single (or a few) molecules. Similar observations were made for homogenous PPI systems corresponding to higher mixing ratios except optical densities were  $>0.2$  (not shown), suggesting the protein-protein aggregates were larger at the time of initial complexation (at  $\text{pH}_c$ ). It is presumed as a result, a mixing ratio dependence of  $\text{pH}_c$  emerges at low ratios. At mixing ratios  $>4:1$ , protein-protein aggregates are thought to reach a critical size leading to similar turbidimetric pH profiles (Figure 3.4) and constant critical values. Singh and co-workers (2007) using type-A and type-B gelatin with agar also reported a similar trend where a strong dependence of  $\text{pH}_c$  was found with gelatin-agar mixing ratios  $<2$ , followed by independence of  $\text{pH}_c$  at mixing ratios  $>2$ . Of note, this was despite showing NaCl independence for low NaCl levels (also similar to the current study). However, Singh and co-workers (2007) provide no explanation for the phenomenon. Evidence of a mixing ratio dependence of  $\text{pH}_c$  in the literature is limited, and warrants further investigation to help elucidate mechanistic differences to the well studied milk protein-polysaccharide complexation.

In the case of  $\text{pH}_{\phi 1}$ , Weinbreck and co-authors (2003b; 2004b) observed a shift to higher pH until a critical biopolymer weight mixing ratio was reached where it then

became stable. The movement of  $\text{pH}_{\phi_1}$  to higher pH as a function of increasing biopolymer ratio reflects the greater amount of protein molecules available per polysaccharide chain (Weinbreck et al., 2003b). Schmitt and co-workers (1999, 2000) reported that the presence of  $\beta$ -LG aggregates during coacervation contributed to the complexity of  $\beta$ -LG and GA interactions, as non-Coulombic interactions became more pronounced. In the present study, the shift in critical pH transitions as biopolymer weight mixing ratio was increased from 1:1 to 4:1 is attributed to the presence of PPI aggregates in the formed complexes. Although not measured in the present study, the effect of increasing the  $C_p$  (at a constant biopolymer weight mixing ratio) on the coacervation process is well documented (Schmitt et al., 1998; Weinbreck et al., 2003a; Ye, 2008). Weinbreck and co-workers (2003a) found in WPI-GA systems, increasing the  $C_p$  caused a shift in  $\text{pH}_{\phi_1}$  to higher values, until reaching an upper concentration limit. Afterwards coacervation is suppressed thought due to the thermodynamic incompatibility of the mixture as biopolymers compete for solvent (Schmitt et al., 1998; Ye, 2008) and/or due to a higher content of released counter ions in solution that function to reduce electrostatic attractive forces between biopolymers based on charge screening (Weinbreck et al., 2003a).

### **3.5 Conclusion**

Findings from this study described the effect of salts and biopolymer weight mixing ratio on the formation of soluble and insoluble complexes involving PPI and GA. Critical structure forming transitions ( $\text{pH}_c$ ,  $\text{pH}_{\phi_1}$ ,  $\text{pH}_{\text{opt}}$  and  $\text{pH}_{\phi_2}$ ) were found to be independent of NaCl at  $\leq 7.5$  mM, whereas at concentrations between 7.5 and 50 mM, protein-protein aggregation overwhelmed protein-polysaccharide interactions. Critical structure forming transitions were found to shift to higher pH as protein content increased, to a PPI-GA ratio of 4:1. Maximum biopolymer interactions occurred at a ratio of 2:1.

### **3.6 Transition to the next study**

Complex coacervation between PPI and GA was found to occur over a narrow pH range (4.23 to 2.58) independent of the presence of salt (at levels  $\leq 7.5$  mM NaCl).

Formed complexes also displayed significant difference in surface charge as a function of pH, at the pH where the biopolymer(s) were electrically neutral, relative to homogenous PPI and GA solutions. Although not measured in this study, complexation is thought to be accompanied by a change in protein conformation. The focus of the next study was to characterize the functional properties of formed complex within the pH regime where coacervation occurred. Specifically, pH effects on solubility, emulsification and foaming ability were assessed. Findings could lead to commercial use of the complex systems as novel food and biomaterial ingredients.

## Chapter 4

### Effect of pH on the functional behaviour of pea protein isolate-gum Arabic complex<sup>2</sup>

#### 4.1 Abstract

The functional behaviours (i.e., emulsion stability, foam expansion and stability, and solubility) of mixtures of PPI and GA were investigated as a function of pH (4.30-2.40) within a region dominated by complex coacervation. For a 2:1 PPI-GA system, soluble and insoluble complexes were formed at pH 4.23 and 3.77, respectively; maximum biopolymer interaction occurred at pH 3.60 and complex disassociation occurred at pH 2.62. Functional properties were tested at or in between these critical pH transitions. In the case of emulsion stability, one vs. two-step emulsification procedures were tested. Emulsion stability was greater for mixed systems relative to PPI alone at pH values between 3.10 and 4.00; and greatest in those prepared using the one-step emulsification procedure. Foam expansion was independent of both biopolymer content and pH, whereas foam stability was improved for the mixed system between pH 3.10 and 4.00. The pH-solubility minimum was broadened for the mixed system relative to PPI alone to more acidic pH values. Findings suggest that admixtures of PPI and GA under complexing conditions could represent a new blended food and/or biomaterial ingredient, and has potential as an encapsulating agent.

---

<sup>2</sup> Reproduced with permission from Liu, S., Elmer, C., Low, N.H. and Nickerson, M.T. 2009. Effect of pH on the functional behaviour of pea protein isolate-gum Arabic complexes. Food Research International. Copyright (2009) Elsevier.

## 4.2 Introduction

In recent years, the protein ingredient industry has been turning towards plants as a preferred alternative to animal-based sources (i.e., gelatin, whey and casein), due to increased consumer concerns over the safety of animal-derived products (i.e., prion diseases), and their dietary preferences and food choices based on moral, religious and cultural dietary prohibitions/decisions. Controlled protein-polysaccharide interactions through complex coacervation may offer a means for improving their functional role as ingredients, without chemical or enzymatic modification.

In mixed biopolymer system, complex coacervation (also known as associative phase separation) occurs over a narrow pH range depending on the biopolymer characteristics (i.e., type and distribution of reactive groups, and molecular weight), biopolymer concentration and ratio, and solvent conditions (i.e., pH and salt) (Turgeon et al., 2003; Weinbreck et al., 2003a; Chourpa et al., 2006). Complex coacervation involves primarily the electrostatic attraction between biopolymers of opposing charges, which results in separation into solvent- and biopolymer-rich phases (Braudo et al., 2001; de Kruif et al., 2001; Turgeon et al., 2003). Although the exact mechanism of this interaction has not been elucidated, complexation is thought to follow nucleation and growth-type mechanism (Weinbreck et al., 2003b; Girard et al., 2004; Sanchez et al., 2006), initiated from non-Coulombic interactions near the protein's pI and the formation of soluble complex. This structure-forming event (denoted as  $\text{pH}_c$ ) is based on an initial increase in turbidity that can be experimentally detected during an acid titration. This event is followed by the formation of insoluble complex, which is accompanied by larger changes in the scattering spectrum (denoted as  $\text{pH}_{\phi_1}$ ) (de Kruif et al., 2001; de Vries et al., 2003; Turgeon et al., 2003). Biopolymer interactions reach a maximum at their electrical equivalence (denoted as  $\text{pH}_{\text{opt}}$ ), before the disassociation of complex at  $\text{pH}_{\phi_2}$  due to the protonation of reactive groups along the polysaccharide backbone at lower pH, giving rise to biopolymers with similar net charges. Turgeon and co-workers (2003) and Chourpa and co-workers (2006) reported that the adsorption of a polysaccharide to a protein's surface induces changes to the secondary conformations of the protein. During an acid titration, it is thought that polysaccharide- and pH-induced

changes to the protein's conformation could lead to different surface properties of the formed complex, and thus new functional attributes.

Admixtures of proteins and polysaccharides under conditions favouring associative phase separation affect the solubility profile of proteins differently depending on the biopolymer-biopolymer and biopolymer-solvent characteristics. Solubility is highly dependent on the overall surface charge of the formed complex, which relates to the level of surface hydrophobicity, biopolymer ratio and solvent conditions (Schmitt et al., 1998). In general, highly charged polysaccharides, low levels of surface hydrophobicity or biopolymer mixtures far from their electrical equivalence ratios, can exert an overall net negative charge on the formed complexes to improve their solubility relative to protein alone (especially at its pI) (Schmitt et al., 1998). However, depending on the biopolymers involved and complexation conditions, deviations from this behaviour can occur. Ortiz and co-workers (2004) studied solubility profiles for soy protein isolate-carrageenan complex and found that as the polysaccharide level increased, the range of pH from which minimum solubility occurred broadened towards more acidic pHs.

The addition of polysaccharides to a protein-stabilized oil-in-water emulsion leads to either stabilization or destabilization, depending on the nature of the biopolymer, solvent conditions and degree of complexation with the protein adsorbed to the interface. In the case of adsorbing polysaccharides, a destabilization phenomenon called 'bridging flocculation' may occur at a low biopolymer concentration (Jourdain et al., 2008). In this instance, there is insufficient polysaccharide present to span the entire oil droplet's surface, favouring complexation (or linking) to protein on more than one oil droplets (Dickinson, 2003). In contrast, at higher concentrations of adsorbing polysaccharides, 'steric stabilization' is favoured as polysaccharides complex to proteins on the interface, and to saturate the protein-stabilized oil droplet (Dickinson and Pawlowsky, 1998; Dickinson, 2003). The protective polysaccharide outer layer improves the viscoelastic properties of the interfacial film, alters the surface charge on the dispersed droplets, and creates steric hindrance inhibiting the coalescence of neighbouring droplets. Vikelouda and Kiosseoglou (2004) reported improved emulsion stability due to steric repulsive forces between droplets for a carboxymethylcellulose-potato protein isolate stabilized

interface. As polysaccharide levels increase, emulsion stability can be enhanced further through the formation of a ‘network-like’ structure within the continuous phase (Papalamprou et al., 2005). Jourdain and co-workers (2008) investigated the steps of emulsion preparation involving a complexing system of sodium caseinate and dextran sulphate. Emulsions prepared using pre-formed complexes were more stable than those formed via a layer-by-layer assembly (or bilayer) whereby polysaccharide is triggered to adsorb to an already formed protein-stabilized interface. The difference in observed stabilities is most probably related to the biopolymer film structure at the interface. In either case, stability was enhanced in the presence of dextran sulphate.

The foam forming properties of proteins relate to its ability to diffuse to the air-water interface, adsorb at the interface, and re-align or undergo conformational changes at the interface to lower surface tension (Ganzevles et al., 2006; Martinez et al., 2007). In general, globular proteins act as good foam stabilizers but weak foam forming agents. As in emulsions, partial unraveling of the protein structure to expose hydrophobic moieties promotes greater interactions at the air-water interface. The addition of polysaccharides and subsequent formation of complexes contributes to foam stability through enhanced adsorption at the interface and the formation of a viscoelastic film between neighbouring air bubbles (Marki and Doxastakis, 2007). The degree of stabilization by formed complexes is highly dependent on the characteristics of the biopolymer interactions (and solvent conditions) present. Polysaccharides themselves also contribute to foam stabilization, typically through increases in bulk phase viscosity (Schmitt et al., 1998; Dickinson, 2003; Martinez et al., 2007), which results in higher cohesive forces among biopolymers (Marki et al., 2007). The foaming properties of biopolymer admixtures have been studied for  $\beta$ -LG with pectin (Ganzevles et al., 2006), soy protein with hydroxylpropylmethylcellulose,  $\lambda$ -carrageenan and locust bean gum (Martinez et al., 2007), common bean protein isolates with xanthan gum, and locust bean gum and GA (Marki et al., 2007). Mechanisms for foam destabilization include coalescence, Ostwald ripening, and drainage of the bulk phase (Marki et al., 2007).

The aim of this study was to characterize the functional behaviour of formed PPI-GA complexes relative to PPI alone, at solution pH corresponding to the presence of soluble and insoluble complexes, complexes considered to be at their electrical



equivalent, and complexes close to their dissolution pH (near  $\text{pH}_{\phi 2}$ ). In section 3.0, the effects of salts (0-50 mM), pH (6.00-1.50) and biopolymer weight mixing ratio (PPI:GA) (1:4 to 10:1) on PPI-GA complex formation were characterized at a  $C_p$  of 0.05% (w/w). Findings indicated that optimal conditions for complexation between the two biopolymers occurred at a weight mixing ratio of 2:1 in the absence of added NaCl. Functional attributes (solubility, emulsification and foaming abilities) of formed complexes in this study were based on these conditions, except at higher  $C_p$  due to the difficulty of functionality study at very low  $C_p$ . Emulsions prepared using one- and two-step processes were also investigated.

### **4.3 Materials and methods**

#### **4.3.1 Materials**

Materials used in this study were previously described in section 3.3.1. Flax oil (peroxide value <10) was kindly donated by Bioriginal Food & Science Corp. (Saskatoon, SK).

#### **4.3.2 Identifying $\text{pH}_c$ , $\text{pH}_{\phi 1}$ , $\text{pH}_{\text{opt}}$ and $\text{pH}_{\phi 2}$ by turbidimetric analysis**

Turbidimetric measurements used in this study were previously described in section 3.3.2. A pH-acid titration was only performed for a 2:1 PPI-GA biopolymer weight mixing ratio, in the absence of added NaCl ( $C_p=0.05\%$ , w/w) for this study. In addition, changes to turbidity were also measured for both the homogenous PPI and GA systems as controls.

#### **4.3.3 Functional properties**

The functional behaviour of PPI alone and PPI-GA mixtures were investigated as a function of pH within the regime associated with complex formation (section 4.3.2). However, in contrast to the turbidimetric analysis, the  $C_p$  was increased from 0.05% (w/w) to 1.00% (w/w) for protein solubility study and 5.00% (w/w) for emulsion and foaming studies.

#### **4.3.3.1 Coacervate composition at 5.00% (w/w) Cp**

Mixed PPI-GA biopolymer solutions were prepared in a similar manner as for the turbidimetric studies, except at a Cp of 5.00% (w/w). Biopolymer weight mixing ratio and solvent pH were kept constant at 2:1 and 3.60, respectively to simulate conditions where maximum biopolymer interactions occurred (section 3.4.2). Coacervate composition was determined according to a modified method of Koh and co-worker (1988). Briefly, the PPI-GA mixture was held static for 10 min at room temperature, followed by centrifugation (Sorvall Inc., Norwalk) at  $270 \times g$  for 10 min. The mixture was then held at 4°C for 20 h, followed by a second centrifugation step at  $270 \times g$  for 20 min. The supernatant was then decanted into a 10 mL graduate cylinder. The volume of supernatant recovered, and the weight of the resulting pellet were recorded. The pellet was subsequently dissolved in 0.1 N NaOH to a total volume of 10 mL for protein and carbohydrate analyses. The GA concentrations in both the supernatant and pellet were determined using a phenol-sulphuric acid colorimetric test (Dubois et al., 1956), whereas PPI content was measured by the micro-Kjeldahl method (AOAC, 2003).

#### **4.3.3.2 Percent protein solubility (%PS)**

Percent protein solubility was determined for a Cp of 1.00% (w/w) and PPI:GA of 2:1 PPI:GA mixing ratio as a function of pH (2.0-10.0) according to Morr and co-worker (1985). Dispersions were adjusted to their desired pH using 0.1 N HCl or NaOH, and allowed to stir for 1 h at room temperature to facilitate solubilization. An aliquot (~12 g) of the dispersion was then centrifuged (Beckman Instruments Inc., Palo Alto, CA) at  $6260 \times g$  for 10 min at room temperature to remove insoluble residues. The supernatant was filtered through a 0.2  $\mu\text{m}$  nylon syringe filter (Chromatographic Specialties Inc., Brockville, ON) directly into a micro-Kjeldahl digestion tube. Nitrogen content within the biopolymer dispersions were measured using a micro-Kjeldahl digestion and distillation system (Labconco Corp., Kansas City, MO) according to AOAC Official Method (960.52) (%N x 6.25). Percent protein solubility was determined by dividing the water soluble protein content by the total protein content (x100%).

Homogenous PPI solutions were also tested at an equivalent concentration as found in the mixed system (0.67%, w/w). All measurements were performed in triplicate.

#### 4.3.3.3 Emulsion stability

Initially, 5.00% (w/w) PPI and GA stock solutions were prepared as previously described (section 3.3.2). Emulsion stability was tested for a 40/60 oil-in-water emulsion (3.2 mL oil/4.8 mL aqueous protein solution), using flax oil. The Cp in the aqueous phase was 5.00% (w/w) with a 2:1 biopolymer weight mixing ratio (PPI:GA). Emulsions were prepared using two different methods: one-step and two-step emulsification. In the one-step method, PPI and GA solutions were mixed at 700 rpm with a magnetic stirrer. The pH was then adjusted to a pre-determined value of 4.30, 4.00, 3.70, 3.60, 3.10 and 2.40 using 0.1N HCl. These pHs corresponded to solvent pH >pH<sub>c</sub>; in between pH<sub>c</sub> and pH<sub>φ1</sub>; in between pH<sub>φ1</sub> and pH<sub>opt</sub>; at pH<sub>opt</sub>; in between pH<sub>opt</sub> and pH<sub>φ2</sub>; and <pH<sub>φ2</sub>, respectively. After the addition of flax oil, the sample was homogenized (Omni International, Inc., Marietta, GA) at 6000 rpm for 3 min. In the two-step method, flax oil was initially added to the PPI solution and stirred at 700 rpm for 5 min, followed by the addition of GA. Solution pH was then adjusted to the same pre-determined values with 0.1 N HCl. The final emulsion was homogenized at 6000 rpm for 3 min. Emulsions prepared by either method were then transferred into individual 10 mL graduate cylinders (inner diameter=10.80 mm; height=100.24 mm; as measured by a digital caliper) and allowed to separate for 3 d. A homogenous PPI system was used as a blank at each concentration equivalent to that used in the mixed system (3.33% w/w). All measurements were performed in triplicate. The %ES was determined using eq. 4.1, where V<sub>B</sub> and V<sub>A</sub> are the volumes of the aqueous (or serum) layer before emulsification (4.8 mL) and after 3 d of drainage.

$$\%ES = \frac{V_B - V_A}{V_B} \times 100\% \quad [4.1]$$

#### 4.3.3.4 Percent foam expansion (%FE) and foam stability (%FS)

Foaming studies were performed under similar biopolymer conditions as were used in the emulsification stability study. Eight milliliters ( $V_{li}$ , initial volume of biopolymer solution used to make the foam) of the PPI and PPI-GA solutions were foamed using an Omni Macro Homogenizer at 8,000 rpm for 5 min, and then poured into a 25 mL graduated cylinder (inner diameter=18.57 mm; height=85.05 mm; as measured by a digital caliper). Percent FE and FS were determined using eq. 4.2 and eq. 4.3, respectively, where  $V_{fo}$  is the foam volume generated initially after homogenization,  $V_{lo}$  is the initial liquid volume immediately after foaming ( $t=0$ ) and  $V_{lt}$  is the liquid volume after time  $t$  (Wilde and Clark, 1996). Foam stability was measured after an arbitrary time of 30 min. All measurements were performed in triplicate.

$$\%FE = \frac{V_{fo}}{V_{li}} \times 100\% \quad [4.2]$$

$$\%FS = \frac{(V_{li} - V_{lt})}{(V_{li} - V_{lo})} \times 100\% \quad [4.3]$$

#### 4.3.4 Statistical analysis

A two-way analysis of variance (ANOVA) was performed to test the effect of pH and biopolymer systems (PPI alone and PPI-GA) on the functional properties studied (%ES (one- and two-step emulsion preparation), %FE or %FS), followed by a one-way ANOVA with a Scheffe Post-Hoc test to identify mean differences in pH for each biopolymer system. Statistical analysis was performed using Systat software (SPSS Inc., Ver. 10, 2000, Chicago, IL.).

### 4.4 Results and Discussion

#### 4.4.1 Complex coacervation between PPI and GA biopolymers

Composition analyses of the mixed PPI-GA system revealed ~65% and ~77% of the total GA and PPI were associated with the pellet, respectively; with the remaining

~35% and ~23% of the GA and PPI associated with the supernatant, respectively. In the case of the homogenous GA solution (control), no phase separation occurred. GA was found to be evenly distributed through the entire solution. In contrast, for the homogenous PPI solution (control), some protein precipitation occurred leaving approximately half in the supernatant and half in the collected pellet. Based on this analysis, coacervate formation between PPI and GA chains occurred at the 5.00% (w/w) Cp.

PPI-GA complex formation is primarily driven by electrostatic attractive forces arising between these two oppositely charged biopolymers. As such, control of solvent pH relative to the PPI's pI is critical for optimizing PPI-GA interactions. Optical density during turbidimetric analysis for homogenous PPI systems began to increase near its pI (pH=5.60), reached a maximum at ~pH 4.2, and then declined as the pH was lowered (Figure 4.1). The initial rise in absorbance corresponded to the solubility minimum in a U-shaped protein solubility pH profile (Figure 4.2) where surface charge was neutral (zeta potential=0 mV) (section 3.4.2). In contrast, GA alone had no optical density over the pH conditions examined (data not shown). In the mixed system, multiple structure-forming and deforming events (at critical pH transitions) were revealed, arising most likely between individual GA chain and small protein aggregates. The first interactions between PPI and the anionic GA polymer occurred at pH 4.23 (pH<sub>c</sub>), corresponding to the formation of soluble protein complexes. Despite significant protein-protein aggregation in the control (Figure 4.1), the presence of GA chains prevented significant PPI clustering at pH>pH<sub>c</sub> possibly due to electrostatic repulsion occurring between positively charged GA and PPI segments that were positively charged. Once the complex became sufficient in size and number, the solution transitions from transparent to turbid, as insoluble complex form at pH<sub>φ1</sub> (pH<sub>φ1</sub>=3.77). Optical density reached a maximum at a pH of 3.60, corresponding to solvent conditions where biopolymer interactions were optimal and charge neutralization occurred. As solvent pH was lowered below pH<sub>opt</sub>, PPI-GA complexes began to disassociate as the GA chains became less protonated as it neared carboxyl group pKa (pH=1.88). However, due to the presence of protein-protein aggregates and presumed stabilizing hydrophobic interactions, the dissociation process was slower (relative to association) resulting in a

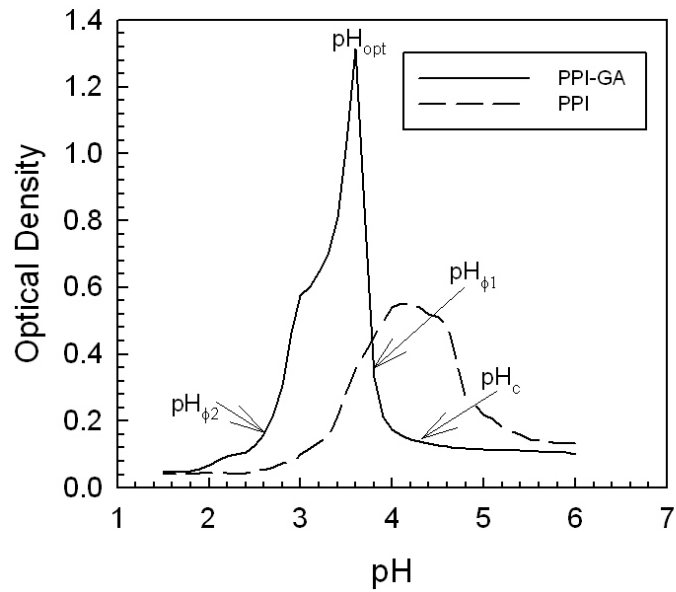


**Figure 4.1** Turbidity curves of PPI and PPI-GA mixture ( $C_p=0.05\%$  w/w, PPI:GA =2:1 w/w, NaCl=0 mM) and critical pH transitions of PPI-GA mixture.

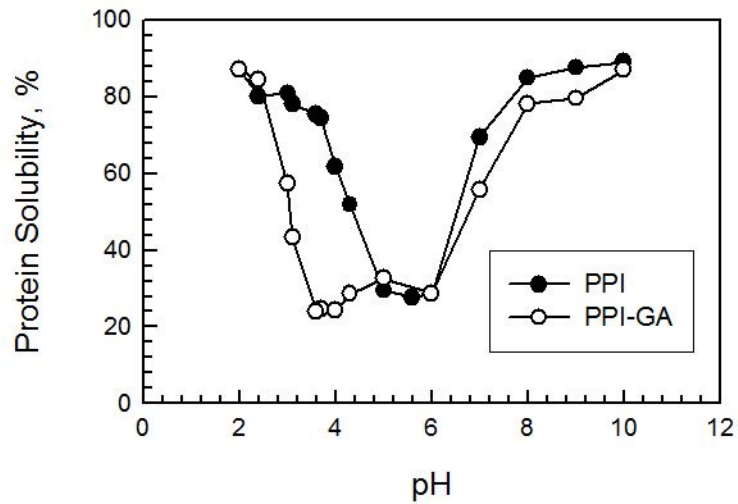


**Figure 4.2** Percent protein solubility of PPI and PPI-GA mixtures ( $C_p=1.00\%$  w/w, PPI:GA=2:1 w/w) as a function of pH.

non-Gaussian curve with a pronounced shoulder near pH 3.00 (Figure 4.1). Disassociation of complex structures occurred at pH 2.62. At solution pH below  $pH_{\phi_2}$  and above  $pH_c$ , biopolymers are thought to be co-soluble. In contrast to the homogenous PPI system, the protein solubility curve for the mixed system had two pH minimums (Figure 4.2). The first occurred at pH 5.60, which was similar to that observed for PPI, under conditions where biopolymers were co-soluble ( $pH > pH_c$  and  $pH < pH_{\phi_2}$ ). The second corresponded to a region where soluble and insoluble complexes were present (4.00-3.60), where  $pH > pH_{opt}$ . The reduction and shift in minimum solubility in the mixed system is most likely due to the expanded pH range where surface charge was neutralized. Complexation induced changes to protein solubility is well documented in literature (Samant et al, 1993; Wang et al., 1996; Vikelouda et al., 2004; Moure et al., 2006). Ortiz and co-workers (2004) reported for soy protein isolate-carrageenan systems that the presence of polysaccharides caused a broadening of the pH range where minimum solubility occurred with a shift towards more acidic pH values. In general, complexation with acidic polysaccharide shifts the solubility minimum towards lower pHs, whereas basic polyelectrolyte shifts the minimum towards higher pHs (Braudo et al., 2001). Furthermore, depending on the biopolymer and solvent conditions, solubility may increase or decrease relative to a homogenous protein solution. Xie and co-workers (1997) reported increased solubility in admixtures of soy protein and xanthan gum, whereas Hansen and co-workers (1971) and Vikelouda and co-workers (2004) reported decreased solubility in mixtures of whey proteins and carboxymethylcellulose and, potato protein isolates and carboxymethylcellulose, respectively.

#### **4.4.2 Emulsification properties**

Oil-in-water emulsion formation is dependent on the ability of a biopolymer (or emulsifier) to rapidly adsorb to the oil-water interface, and then undergo a conformational change to form a viscoelastic film that surrounds the oil droplets (Uruakpa and Arntfield, 2005). Emulsions formed using PPI alone, PPI-GA one-step method, and PPI-GA two-step method had significant differences in terms of their stabilizing effect at each pH tested. Stabilities were greatest for emulsions prepared using the one-step preparation method, followed by the two-step procedure and PPI

alone at all pHs tested (Figure 4.3). Differences in %ES between the mixed systems and PPI alone is thought to be associated with the structure of the biopolymer at the interface and the viscosity of the continuous phase. Although not measured in the present study, viscosity of the biopolymer solution was expected to be higher for the mixed systems, as the Cp was prepared at 5.00% (w/w) versus 3.33% (w/w) for the PPI control. It has been shown that continuous phase that had higher viscosity tend to inhibit the rate of creaming within an emulsified system (Jourdain et al., 2008). Differences in the structure of the biopolymer interface may also influence emulsion stability. In the case of the one-step emulsification procedure, PPI-GA complex should form prior to their interaction with the oil-water interface. Upon complex formation, a partial unfolding of the protein may occur, to allow greater exposure of hydrophobic moieties for more rapid adsorption at the interface. Turgeon and co-workers (2003) using circular dichroism, observed changes to secondary structures upon complexation of  $\beta$ -LG with GA, and faba bean legumin with chitosan. Chourpa and co-workers (2006) also reported similar findings with pea globulin- and wheat gliadin-GA mixtures. Ducel and co-workers (2005a) reported increased adsorption of a pea globulin-GA complex at the oil-water interface relative to pea globulin alone, resulting in a lowering of interfacial tension which was attributed to the increased hydrophobic nature of the formed complex. Consequently, complexes formed by the one-step method are thought to interact better at the oil-water interface. In contrast, in the two-step procedure, PPI interacts with the oil-water interface first to form a viscoelastic film, which is then subsequently strengthened by a layer of GA chains stabilized via electrostatic interactions, similar to film formation in layer-by-layer biopolymer assemblies. The bilayer functions to improve the stability of the biopolymer interface relative to PPI alone, but less so than the one-step method.



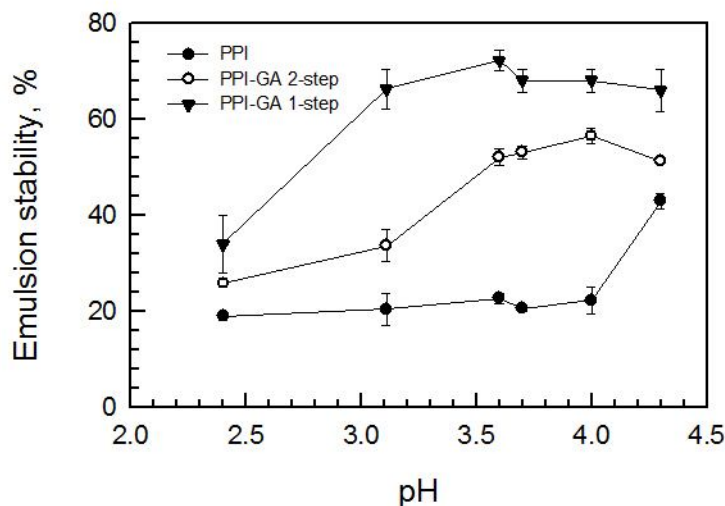


**Figure 4.3 Percent emulsion stability of PPI and PPI-GA mixtures ( $C_p=5.00\%$  w/w, PPI:GA=2:1 w/w) as a function of pH.**

The effect of pH was examined for each emulsion system. Emulsion stability was found to be highest and relatively independent of pH over the ranges of 4.30-3.10, and 4.30-3.60 for the one- and two-step preparation methods, respectively. The lack of pH dependence in these regions is thought to be due to the low surface charge on the formed complexes as a result of chain neutralization. Liu and co-workers (2009) reported no net charge at pH 3.60 for a 2:1 PPI-GA mixture. Therefore, steric stabilization and the continuous phase viscosity at the higher biopolymer concentrations (5.00% w/w) were thought to inhibit the coalescence of neighboring oil droplets, rather than electrostatic repulsive forces. Emulsion stability was significantly reduced at pH 2.4 for both preparation methods, as the PPI-GA complexes/bilayer underwent dissolution as the carboxyl groups on the GA approached their pKa. The formed complexes (one-step method) are thought to be more stable than the bilayer structure, as supported by its retained stability under acidic conditions (pH 3.10) (Figure 4.3). Of note, this pH corresponded to a shoulder in the PPI-GA turbidity curve, which is thought to be associated with hydrophobic interactions occurring within protein-protein aggregates within the complex that leads to improved stability under acidic pH. In the case of the bilayer, biopolymer interactions/spatial distribution would differ from the complex

prepared by the one-step procedure. In the case of PPI-stabilized emulsions, %ES was greatest at pH 4.30 (Figure 4.3), which corresponded to the turbidity maximum (Figure 4.1) and neared the solubility minimum (Figure 4.2).

Ducel and co-workers (2005) reported that the adsorption of pea globulin-GA to the oil-water interface was not pH dependent over the range of 2.75-9.00, but was influenced by the Cp as interfacial tension decreased as protein levels increased from 0.5 to 10 mg/mL at pH 2.75. In addition, the elastic behaviour of pea globulin-GA films at the oil-water interface was greater near the protein's pI due to the importance of hydrophobically driven lateral protein organization (and/or protein complexes) at the interface.

Jourdain and co-workers (2008) found that emulsions formed using the one-step method were more stable than those formed using the two-step approach for sodium caseinate-dextran sulphate. The authors demonstrated that bridging flocculation occurred only in multi-layer stabilized emulsions at low dextran sulphate concentrations (0.1% w/w), whereas at higher concentrations (1.0% w/w) steric stabilization and electrostatic repulsive forces prevailed that led to emulsion stability. For the one-step method, emulsions were stabilized by single layer, no bridging flocculation was observed. Emulsion stability was found to be reduced as the pH was lowered to more acidic values in both the one- and two-step preparation methods. Guzey and co-workers (2004) reported that oil-in-water emulsions stabilized by  $\beta$ -LG-pectin multi-layer membranes showed improved stability at pHs near the protein's pI relative to systems without pectin. The authors attributed these observations to increased complex pH stability as the adsorption of pectin chains to the protein-stabilized interface resulted in greater droplet surface charge. The improved stability of emulsions using biopolymer admixtures have also been reported for faba bean legumin-carrageenan (Galazka et al., 1999), faba bean legumin-chitosan (Plashchina et al., 2001), potato protein isolates-carboxymethylcellulose (Vikelouda and Kiosseoglou, 2004), pea globulin-GA and  $\alpha$ -gliadin-GA (Ducel et al., 2005), and canola protein-hydrocolloids (Uruakpa and Arntfield, 2005).

#### 4.4.3 Foaming properties

Percent foam expansion for PPI and PPI-GA systems as a function of pH is shown in Figure 4.4. Results indicated that the foam forming abilities of both biopolymer systems were similar and independent of pH over the range examined ( $p > 0.05$ ). In contrast, the stability of the foams were significantly different and dependent upon pH ( $p < 0.001$ ). Foam stability was higher for mixed systems than PPI alone within the pH regime of 3.10-4.00 where complexation occurred, but similar at pHs where biopolymer attraction was less or non-existent (pH 2.40 and 4.30) (Figure 4.4). Foam stability was greatest in the mixed system at pH 3.10 (Figure 4.4).

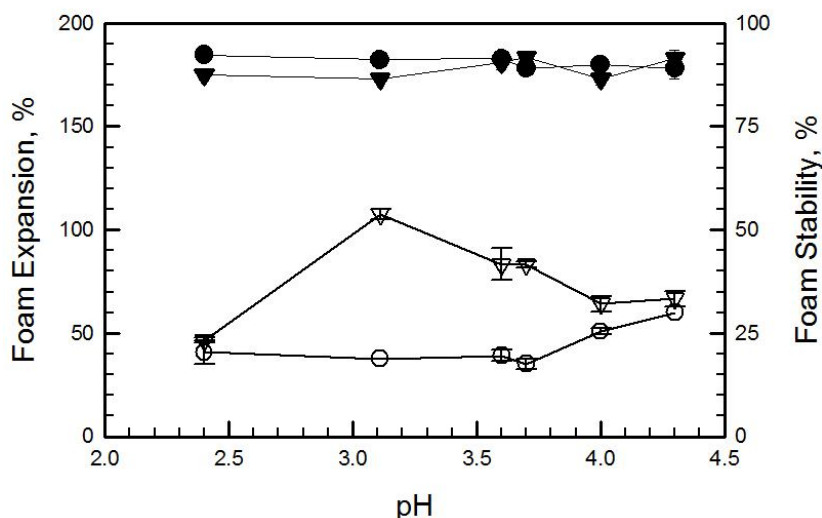


**Figure 4.4** Percent foam expansion (solid) and stability (open) of PPI (circle) and PPI-GA mixtures (triangle) ( $C_p=5.00\%$  w/w, PPI:GA=2:1w/w) as a function of pH.

Again, this pH corresponded to the shoulder observed in the turbidimetric analysis of dilute  $C_p$  (Figure 4.1). Similar to the oil-water interface, increased surface hydrophobicity of the formed complexes (due to polysaccharide-induced conformational changes of the protein upon binding) could result in greater adsorption at the air-water interface. Increased bulk phase viscosity is also expected to contribute to foam stability

due to differences in  $C_p$  between the mixed system and the PPI control. However, this effect is thought to be minor, as similar stability values were found at pH values of 2.40 and 4.00 in the two systems.

Ganzevles and co-workers (2006) proposed various mechanisms describing the use of polysaccharides to control protein adsorption at the air-water interface. In the first scenario, only free protein (un-complexed) is available to adsorb at the air-water interface and reduce surface tension. In the second case, adsorption at the interface involves a combination of protein-polysaccharide complexes and free protein in the continuous phase. Diffusion rates of the formed complexes would be lower than the free protein, resulting in slower migration from the bulk solution to the interface. Their last mechanism involves an additional association-dissociation step during protein adsorption from the complex. This theory suggested that complexes close to the air-water interface may undergo partial protein disassociation depending on the strength of the biopolymer interactions and solvent conditions, enabling 'released' protein to adsorb to the interface. In the present study, foam formation is probably based on the combined adsorption of free protein and PPI-GA complexes at the interface. Under non-complexing conditions (pH 2.40 and 4.30) free protein most likely stabilizes the interface in both the mixed systems and the PPI control. However, under complexing conditions (pH 3.10-4.00), a combined effect at the interface is probable, as a pH dependence of %ES emerged. In this case, electrostatic biopolymer interactions help strengthen the viscoelastic film at the interface, induced conformational changes in the protein for better integration at the interface, and increased bulk phase viscosity. Martinez and co-workers (2007) reported improved film properties at the air-water interface for soy protein stabilized foams in the presence of polysaccharide. In addition, Marki and co-workers (2007) found that admixtures of GA, locust bean gum and xanthan gum with common bean (*Phaseolus vulgaris* L.) and scarlet runner bean (*Phaseolus coccineus* L.) protein isolates improved foam stability, attributing their effect to increases in bulk phase viscosity and in the creation of a biopolymer network that prevented air bubble coalescence.

#### **4.5 Conclusion**

In the current study, the functional attributes of PPI and PPI-GA systems were investigated within the pH range dominated by associative phase separation. PPI-GA complexes were found to: expand the minimum pH-solubility profile of PPI, broadening it to more acidic pH values; and improve its emulsion and foam stabilities. The method of emulsion preparation (one- vs. two-step) was found to play an important role in controlling emulsion stability, with one-step emulsification giving greater stability. Findings from this study suggest that the complexation of GA to PPI improves the functional attributes of PPI over a finite pH range.

#### **4.6 Transition to the next study**

In this study, PPI-GA complexes were shown to have similar or improved functional properties relative to PPI alone over a very narrow pH range. In encapsulation, the ability for the wall material to stabilize the formed oil-in-water emulsion is essential to achieve high encapsulation efficiencies and possibly aid in core material (i.e. oil) stability. Mixed PPI-GA systems should improve emulsion stability over the narrow pH range where coacervation occurs, and as such may serve as a better wall material than PPI alone.

## Chapter 5

### Protein-polysaccharide encapsulation of flax oil

#### 5.1 Abstract

Experiments were conducted on the encapsulation of flax oil in animal- and plant protein-based capsules by complex coacervation, and their chemical properties and ability to delay flax oil oxidation were compared. Under high speed mixing process (two-step emulsification), gelatin-GA capsules exhibited low moisture content, water activity and surface oil content, and offered adequate protection against oxidation relative to free oil (non-encapsulated oil) over 25 d of storage. No capsule formation was observed using PPI-GA complex. An alternative encapsulation process using low speed mixing conditions (one-step emulsification) was employed for PPI-GA encapsulation, which also failed to produce acceptable capsules. In contrast, PPI-alginate capsules produced by low speed mixing, had similar chemical properties to the gelatin-GA capsules, with the exception of reduced total oil content (30% vs. 50% w/w), and although inconclusive, oxidative stability may be adversely affected by this encapsulation process.

## 5.2 Introduction

Flax oil offers a rich source of EFA, increasingly recognized for their role in reducing disease risk and maintaining human health. However, the incorporation of high levels of EFA into foods is hindered by their incompatibility (i.e., lack of solubility) with aqueous food ingredients and inherent instability against oxidation. Encapsulation technology offers a novel means to circumvent these problems and improve EFA bioavailability by ensuring stability and controlled release. This technology involves encasing or coating the core ingredient within a wall material (i.e., polysaccharide and/or protein), which is often cross-linked to improve its mechanical integrity. Depending on the formulation, desirable release and functional properties (i.e., stability, size and strength) can be achieved to suit a wide range of applications. Microencapsulation technology has been extensively used in the pharmaceutical and paint industries, however it remains underutilized in processed foods. Presently, gelatin is the main commercially used encapsulation material for oils (i.e., fish oil). However, with increased consumer concerns over the safety of animal-derived products (i.e., prion diseases), their dietary preferences and food choices based on moral, religious and cultural dietary prohibitions, scientists are seeking alternatives such as plant-based materials.

The focus of this research was to encapsulate flax oil within a protein-polysaccharide capsule by complex coacervation. Capsule design and processing were based on: a) the use of PPI-GA and gelatin-GA (control) mixtures as wall materials, with capsules formed under high speed (3000-15000 rpm) mixing conditions; and b) the use of PPI-alginate and PPI-GA mixtures as wall materials, with capsules formed under low speed (500 rpm) mixing conditions. A gelatin-GA based capsule served as a control since it has been well documented in literature (Yeo et al., 2005; Chang et al., 2006; Dong et al., 2007). Gelatin is a protein derived from partial hydrolysis of collagen that contains high levels of hydroxyproline, proline and glycine. It remains advantageous as a delivery matrix due to its inherent bio-compatibility, and ability to form thermally reversible gel networks, which melt below body temperature (37°C) (Nickerson et al., 2006). The potential replacement of gelatin with PPI is advantageous to the marketplace, as capsules could reach wider markets which restrict animal derived ingredients. The

aim of this study was to entrap flax oil within a comparable or superior plant-based (i.e., PPI) capsule, using a gelatin-GA capsule as a standard. The chemical properties of the resulting capsules were assessed, along with their ability to protect the core oil against oxidation over a defined (i.e., 25 d) time period.

## **5.3 Materials and Methods**

### **5.3.1 Materials**

Porcine gelatin (Type A, 300 Bloom, 9.47% moisture) and alginate (12.0% moisture) were purchased from Sigma–Aldrich Co. (Oakville, ON). PF and GA were kindly donated from Parrheim Foods (Saskatoon, SK) and TIC Gums (Belcamp, MD), respectively. Production of PPI, along with the chemical analyses of PPI and GA were presented in section 3.3.1. Flax oil (peroxide value <10), was kindly donated by Bioriginal Food and Science Corporation (Saskatoon, SK).

### **5.3.2 Flax oil encapsulation under high speed mixing conditions (two-step emulsification)**

PPI-GA and gelatin-GA capsules were prepared according to the published method of Yeo and co-workers (2005) at a 1:1 biopolymer weight mixing ratio (protein:GA), with the exception that the emulsion was slowly cooled to room temperature rather than cooled in a ice bath. Emulsion formation was studied systematically: first, as a function of homogenization rate (3000, 6000, 9000, 12000 and 15000 rpm) at a 2.00% (w/v) Cp, and second, as a function of Cp (1.00, 1.25, 1.50, 1.75 and 2.00% w/v) at a constant homogenization rate (9000 rpm). (a) *Gelatin-GA capsules*: Gelatin sols were prepared by dispersing appropriate amount of powder (depends on the Cp used) in 150 mL of Milli-Q™ water maintained at 50°C under stirring (500 rpm) until complete dissolution (~10 min). GA sols were prepared in a similar manner except at room temperature (21-22°C). Emulsions were formed by homogenizing 6.00 g of flax oil into the gelatin dispersion at pre-determined rates (rpm) for 3 min using an Omni Macro Homogenizer (Omni International, Inc., Marietta, GA). To visualize the formed capsules by microscopy, Nile Red, a lipid-soluble dye, was added (1 mg/g flax oil), which provided sufficient contrast from the aqueous biopolymer phase. The gelatin-



stabilized emulsion was then poured into a beaker kept at 50°C in a water bath under stirring at 500 rpm. The GA solution (150 mL) was then added dropwise to the gelatin-stabilized emulsion to a final volume of 300 mL. The emulsion was then allowed to stir for an additional 5 min at 50°C. Emulsion pH was lowered to 4.0 by the dropwise addition of 10% (v/v) acetic acid. The mixture was then allowed to cool slowly to room temperature (~1.5 h) in the same water bath without heating under constant stirring. Stirring was stopped once the emulsion reached room temperature. Phase separation occurred, leading to an upper aqueous phase and a lower microcapsule-rich phase. The upper phase was removed, and the lower phase was used for further analysis. (b) *PPI-GA capsules*: A PPI a stock solution (2.00% w/v, adjusted to pH 8.0 with 2.0 N NaOH) was prepared by dispersing PPI powder in Milli-Q™ water under constant stirring (500 rpm) for 2 h at room temperature and then overnight at 4°C to facilitate protein solubility. Capsules were prepared in a similar manner as for the gelatin-GA system, except the entire process was conducted at room temperature. Duplicate batches were prepared for each sample used for analyses. The microcapsule rich phase for protein-GA mixtures were visualized as a function of Cp and homogenization rate using a light microscope (Zeiss, Germany) to identify the optimal conditions for encapsulation. Emulsions were observed under an objective magnification of 10×, with images taken using a Nikon COOLPIX 990 camera (Tokyo, Japan). Once the optimal conditions were identified, samples were freeze dried (Labconco Corporation, Kansas City, MO) for 3 d to yield a free flowing powder.

### **5.3.3 Flax oil encapsulation under low speed mixing conditions (one-step emulsification)**

PPI-GA and PPI-alginate capsules were prepared according to the method of Lazko and co-workers (2004b). The method was modified to reflect conditions that promoted complex coacervation between PPI and GA. Capsule formation was systematically investigated: first, as a function of biopolymer weight mixing ratio (PPI:polysaccharide) (3:1, 2:1, 1:1 and 1:2) at a constant 50:50 (w/w) wall-to-core ratio; and second as a function of wall-to-core ratio (50:50, 60:40 and 70:30 w/w) at a constant biopolymer weight mixing ratio (1:1). In all cases, the Cp was kept constant at 2.00%

(w/v). A PPI stock solution was prepared as above (section 5.3.2). In contrast, alginate or GA solutions (2.00% w/v) were prepared by dispersing these powders in room temperature Milli-Q<sup>TM</sup> water under constant stirring for 20 min or until completely dissolved. Prior to emulsification, biopolymer stock solutions were mixed at appropriate masses depending on biopolymer weight mixing ratios, and brought to a total volume of 300 mL with Milli-Q<sup>TM</sup> water under constant stirring at room temperature for 5 min (2.00% w/v Cp). Flax oil of known weight (6.0 g (50:50 wall-to-core ratio), 4.0 g (60:40) and 2.6 g (70:30)) was then added to the biopolymer mixture under constant stirring (500 rpm) for 2.5 h using an overhead stirrer equipped with a square blade paddle (Caframon, Wiarton, ON). The emulsion pH (~8.0) was subsequently lowered to 4.0 by dropwise addition of 1 N HCl, and then allowed to stir for an additional 2.5 h to allow migration and alignment of the biopolymer complex to the oil-water interface. Emulsions were then frozen at -20°C, and then freeze dried (Labconco Corporation, Kansas City, MO) to yield a powder. Duplicate batches were prepared for each sample.

### **5.3.4 Capsule characterization**

#### **(a) Water activity ( $A_w$ ) and moisture content**

The water activity of freeze dried microcapsules were determined using an AquaLab CX-2 (Decagon Devices, Inc., Pullman, WA), whereas moisture content was determined gravimetrically, after drying the capsules in a oven at 105°C for ~12 h (Klaypradit and Huang, 2008).

#### **(b) Surface oil content**

Surface oil was determined using the published method of Heinzelmann and co-workers (2000). Briefly, 1 g of freeze dried capsules were dispersed in 30 mL of hexane in 50 mL flask followed by vigorous shaking for 30 s. The solvent was filtered with Whatman #41 filter paper into a 30 mL beaker, and the solvent was allowed to evaporate overnight in a fume hood. The beaker was then heated at 105°C for 30 min, followed by cooling in a desiccator for gravimetric analysis. The surface oil content, expressed as grams of oil per 100 g of capsules, was defined as oil that was readily

extracted by a single hexane wash. Three replicates were measured on each duplicate batch.

### **(c) Total oil content**

#### *(i) Gelatin-GA capsules*

Total oil was determined according to the Röse-Gottlieb method (AOAC, 2003). Briefly, 1 g of freeze dried capsules was dispersed in 20 mL of water at 65°C under constant stirring at 300 rpm. To help facilitate the degradation of the capsule wall, 2 mL of 28-30% (w/w) NH<sub>4</sub>OH was added during stirring. The mixture was then allowed to cool to room temperature, and transferred to a separatory funnel. Ten millilitres of 95% ethanol was added and the resulting solution was mixed gently. Lipid was extracted by the addition of 25 mL each of diethyl ether and hexane. After separation, the lower aqueous phase was removed. Extraction was repeated (2×) with a mixture containing 5 mL of ethanol, 15 mL of diethyl ether and 15 mL of hexane. The organic phases were combined, filtered through anhydrous sodium sulfate, and then evaporated overnight within a fume hood. The beaker was then heated at 105°C for 30 min, followed by cooling in a desiccator. Total oil content was determined gravimetrically, and it was calculated as the total amount of oil in grams extracted per 100 g of capsules. Three replicates were measured on each duplicate batch.

#### *(ii) PPI-polysaccharide capsules*

Attempts to measure the total oil content of PPI-polysaccharide capsules failed due to the difficulties encountered in disrupting the strong protein-lipid and/or polysaccharide-lipid interactions. Methods that were tried, but were unsuccessful included: Goldfish (petroleum ether) and Soxhlet (n-propanol/water) extractions, the Röse-Gottlieb method (ethanol/diethyl ether/hexane) and a chloroform/methanol/water extraction (Shahidi, 2005). Therefore, the total oil content in PPI-polysaccharide capsules was calculated based on the total oil used.

#### **(d) Encapsulated oil content**

The encapsulated oil, defined as the amount of non-readily extracted oil per 100 g capsules, was determined as the difference between the total oil and surface oil contents.

#### **5.3.5 Oxidative stability**

##### *(i) Gelatin-GA capsules*

Samples analyzed for their oxidative stability included: a) flax oil extracted from capsules immediately after freeze drying; b) flax oil extracted from 3 g aliquots of freeze dried capsules stored in an amber bottle at room temperature, drawn every 5 days over a 25 d period; and c) aliquots (1.5 mL) of non-encapsulated flax oil stored in an amber bottle at room temperature drawn every 5 days over a 25 d period. Flax oil extraction from capsules was similar to that of total oil content, except solvent was dried under a stream of nitrogen. The oxidative stabilities of encapsulated oil and non-encapsulated flax oil were determined using the following methods:

*(a) Conjugated diene (CD):* In brief, 0.01-0.03 g of sample oil was weighed into a 25 mL volumetric flask, dissolved and brought to volume with isooctane. The absorbance of the oil-isooctane mixture was made at 233 nm ( $A_{233}$ ) using isooctane as the blank. The CD value was calculated as:  $[CD = [c_{CD} \times (2.5 \times 10^4)] / W$ , where  $c_{CD}$  is the CD concentration (mmol/mL) equivalent to  $[A_{233} / (\epsilon * l)]$ , where  $\epsilon$  is the molar absorptivity of linoleic acid hydroperoxide ( $2.525 \times 10^4 \text{ M}^{-1} \text{ cm}^{-1}$ ),  $l$  is the cuvette path length (1 cm) and  $W$  is the oil sample weight (g) (Pegg, 2005).

*(b) p-Anisidine value (p-AV):* In brief, ~0.2 g of sample oil was weighed into a 25 mL volumetric flask and isooctane was used to dissolve the oil and bring the mixture to volume. Absorbance was determined at 350 nm with isooctane as the blank ( $A_b$ ). Then, exactly 1 mL of p-anisidine reagent was added to 5 mL of the oil-isooctane mixture, followed by mixing. After exactly 10 min, solution absorbance was made at 350 nm and recorded as  $A_s$ . The mixture of isooctane and p-anisidine (0.25 g/100 mL acetic acid) was used as a blank. The p-AV was calculated as:  $[p-AV = 25 \times (1.2A_s -$

$A_b/m]$ , where  $m$  is the weight of the oil sample (AOCS Official Method Cd 18-90, 1997).

(c) *Peroxide value (PV)*: In brief, ~0.2 g of sample oil was weighed into a 250 mL Erlenmeyer flask, followed by the addition of 30 mL of 3:2 acetic acid/chloroform (v/v) solution and 0.5 mL of saturated potassium iodide (KI). After vigorous shaking for exactly 1 min, 30 mL of Milli-Q™ water was added. Half a millilitre of 1% (w/v) starch indicator was then added to the mixture. The solution was titrated using 0.01N sodium thiosulfate ( $\text{Na}_2\text{S}_2\text{O}_3$ ) until the purple color disappeared. PV was calculated as:  $[PV = [(S - B) \times N \times 1000] / W]$ , where  $S$  is the volume of  $\text{Na}_2\text{S}_2\text{O}_3$  added to the sample,  $B$  is the volume of  $\text{Na}_2\text{S}_2\text{O}_3$  of the blank,  $N$  is the normality of  $\text{Na}_2\text{S}_2\text{O}_3$  solution, and  $W$  is the sample weight (g) (Pegg, 2005).

(ii) *PPI-polysaccharide capsules*

For oxidative stability studies, flax oil associated with PPI-polysaccharide capsules was extracted using the following method. Approximately 3 g of capsules were weighed into a 250 mL Erlenmeyer flask, followed by the addition of 35 mL each of diethyl ether and hexane. The mixture was homogenized at 5000 rpm for 30 s, followed by sonication for 15 min (modified from Shahidi, 2005). The mixture was filtered (Whatman #41) to remove residue protein and polysaccharide. The filtrate was dried under a stream of nitrogen. This method gave an oil recovery of ~30% of the total oil input. p-AV test was not performed on the PPI-polysaccharide capsules due to interferences at its respective wavelengths. The oxidative stability of the flax oil before and after encapsulation, and during a 20 d storage period was investigated as for section 5.3.5. (i). The oxidative stability of PPI-polysaccharide encapsulated oil was analyzed using following methods:

(a) *Conjugated diene (CD)*: As for section 5.3.5 (i).

(b) *2-thiobarbituric acid reactive substances (TBARS) test*: In brief, ~40 mg of sample oil was weighed into 10 mL volumetric flask and was dissolved and brought

to volume with n-butanol. To 2.0 mL Eppendorf tubes was added, 50  $\mu$ L of 8.1% (w/v) SDS, 375  $\mu$ L of 20% acetic acid, 375  $\mu$ L of 0.8% (w/v) TBA, 8.25  $\mu$ L of 0.02% (w/v) BHT (in DMSO) and 200  $\mu$ L of the oil-butanol mixture. Samples were then heated at 95°C for 1 h. After cooling in cold water, 0.9 mL of n-butanol/pyridine (15:1, v/v) was added, followed by vigorous shaking for 1 min. Samples were centrifuged at 4000  $\times$  g for 10 min, and the upper organic layer was transferred to a 1.5 mL cuvette and the absorbance at 532 nm was measured against a butanol blank. A standard curve was prepared using malondialdehyde (MDA) (5-40  $\mu$ M) under the same experimental conditions. TBA values were expressed as mg MDA eq/g oil, which equates to the MDA content (mg) / sample oil weight (g) (modified from Pegg, 2005).

### **5.3.6 Fatty acid profiles by gas chromatography**

Fatty acid profiles of flax oil before and after encapsulation were analyzed by capillary gas chromatography (Agilent Technologies 6890N, Santa Clara, CA), equipped with a flame-ionization detector under following conditions: fused silica capillary column DB 23 (60.0 m length, 250 internal diameter, and 0.25  $\mu$ m film thickness); helium as the carrier gas with a flow rate of 41 cm/s; oven temperature 240°C; injector temperature 250°C; split ratio of 40:1; detector temperature 250°C. Methyl esters were prepared from sample oil according to AOCS Official Method Ce 1b-89 (AOCS, 1997). Heptadecanoate (C17:0 methyl ester) was used as the internal standard. Three replicate samples were analyzed from two batches of capsules.

### **5.3.7 Statistical analysis**

A one-way analysis of variance using the Scheffe Post-Hoc test was used to test for differences in oxidative stability between free and entrapped oils before and after the encapsulation process (i.e., before and after encapsulation) and during storage. Statically analysis was performed using Systat software (SPSS Inc., Ver. 10, 2000, Chicago, IL).

## 5.4 Results and Discussion

### 5.4.1 Flax oil encapsulation under high speed mixing conditions (two-step emulsification)

#### 5.4.1.1 Capsule formation

##### *(i) Gelatin-GA capsule formation*

Successful formation of gelatin-GA capsules was achieved with similar findings as those published by Yeo and co-workers (2005). In Figure 5.1, the effect of homogenization rate on capsule formation was observed at a constant  $C_p$  (2.00% w/v) and wall-to-core ratio (50:50 w/w). Capsule morphology at low homogenization rates (i.e., 3000 rpm) revealed the formation of mononuclear capsules comprised of a single large oil droplet (stained with Nile red). Free oil droplets and gelatin-GA complex without entrapped oil were also prevalent at low homogenization rate. As homogenization rates increased, multiple small oil droplets became entrapped within the gelatin-GA complex (Figure 5.1b). From 9000 to 15000 rpm, large amounts of multinuclear capsules formed with multiple small oil droplets enclosed. It was also observed that the degree of oil droplet aggregation increased with homogenization rate, while capsule sizes were not much affected (Figure 5.1c-e). In Figure 5.2, the effect of  $C_p$  on capsule formation at a constant homogenization rate (9000 rpm) and wall-to-core ratio (50:50 w/w) is shown. It was found that the size of capsule clusters decreased substantially from  $>200\ \mu\text{m}$  to about  $100\ \mu\text{m}$  as biopolymer levels were raised from 1.00% to 2.00% (w/v). In addition, the presence of non-encapsulated oil, as indicated by the presence of uncoated red droplets, which was observed at  $C_p$  of 1.00% (w/v), was not observed at higher  $C_p$  (i.e., 2.00% w/v) (Figure 5.2). Furthermore, the thickness of the outer capsule wall increased with increasing  $C_p$ . Based on these findings, optimal conditions for gelatin-GA capsule formation occurred at a homogenization rate of 9000 rpm and a  $C_p$  of 2.00% (w/v). It has been suggested that multinuclear capsules are generally recognized for having better controlled release properties than mononuclear designs (Dong et al., 2007).

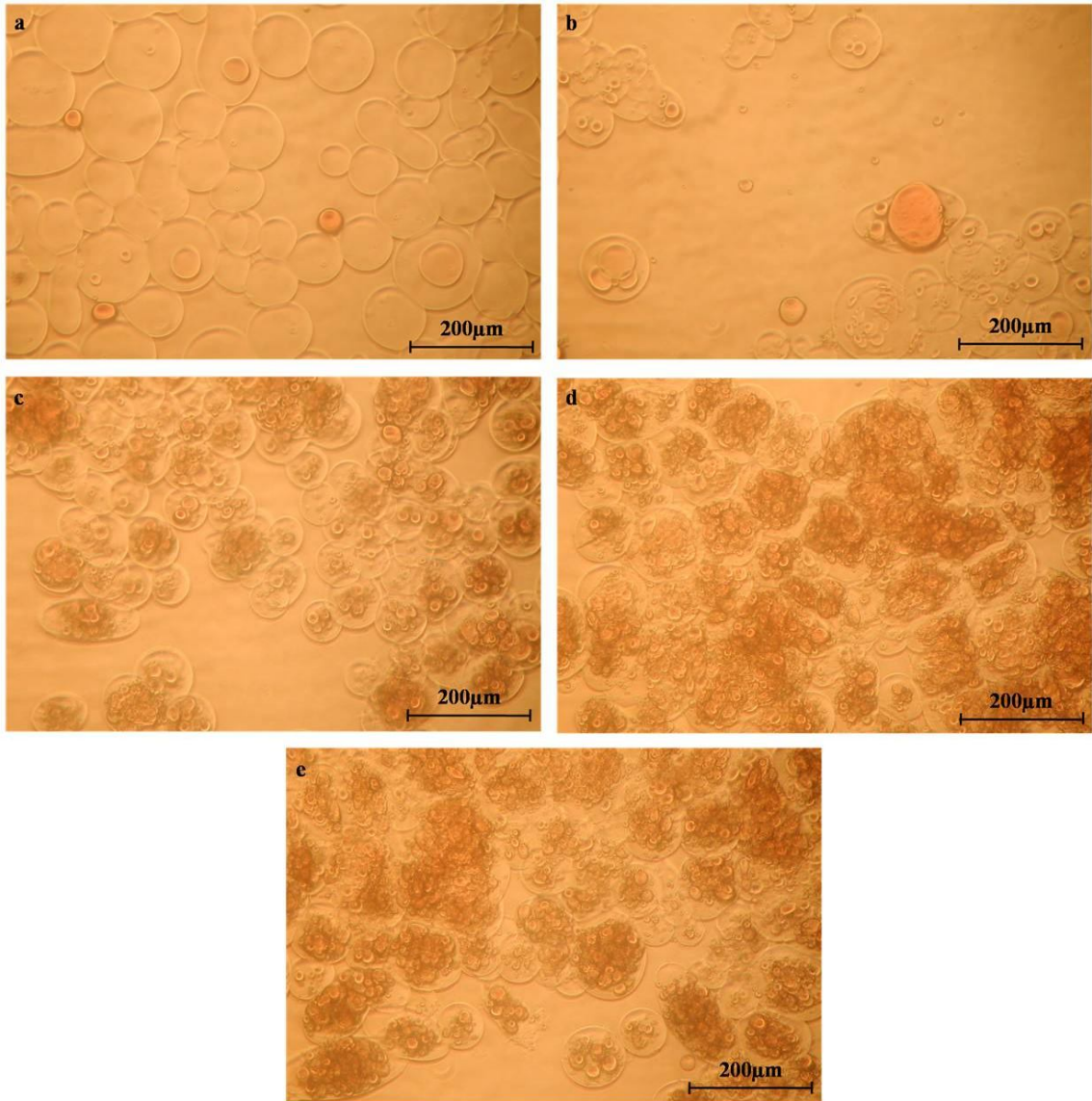


**Figure 5.1 Gelatin-GA capsules observed by light microscopy as a function of homogenization rate: a) 3000; b) 6000; c) 9000; d) 12000 and e) 15000 rpm ( $C_p=2.00\%$  w/v, wall-to-core ratio=50:50 w/w).**



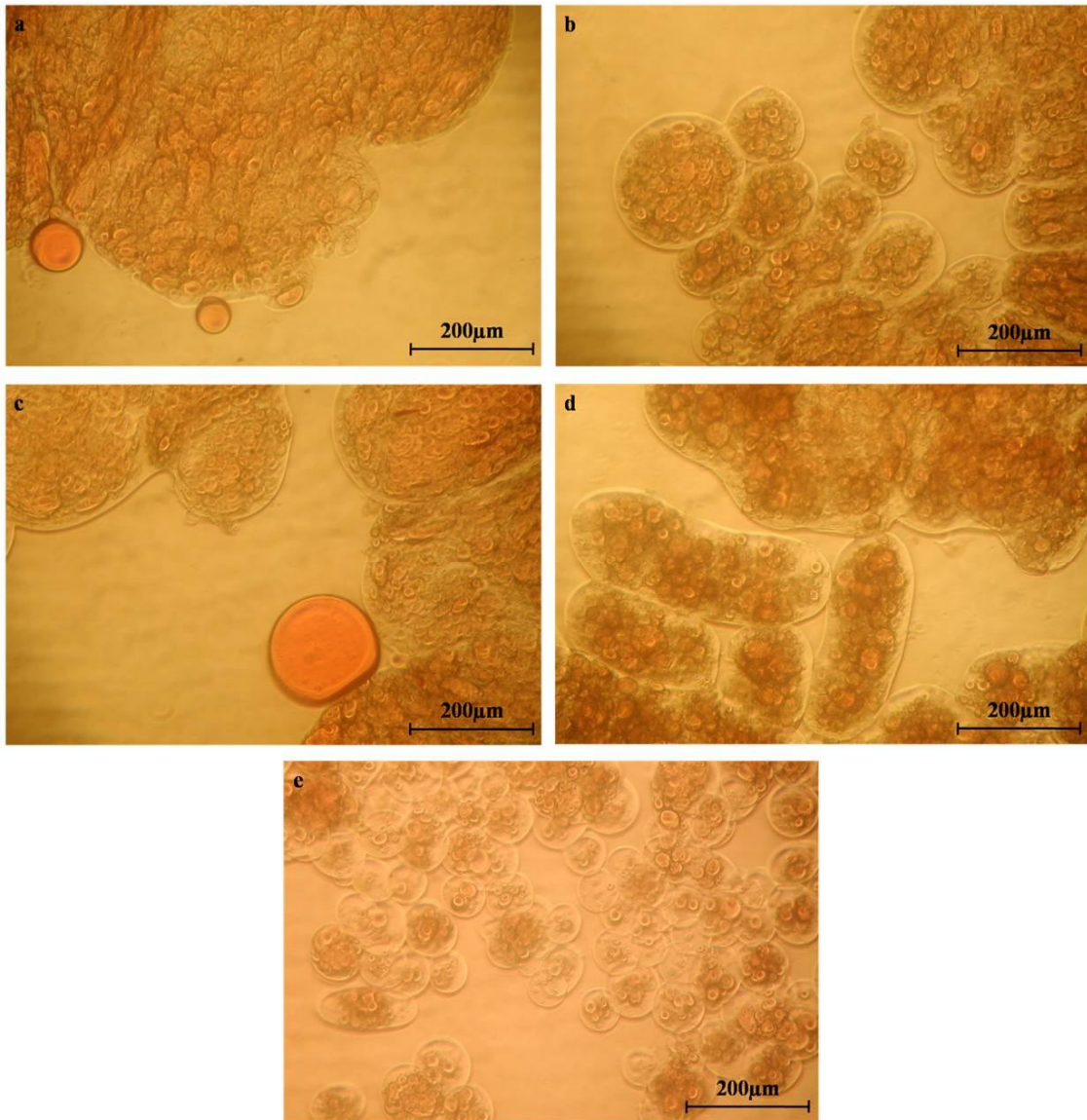


**Figure 5.2** Gelatin-GA capsules observed by light microscopy as a function of  $C_p$  (% w/v): a) 1.00%; b) 1.25%; c) 1.50%; d) 1.75%; and e) 2.00% (homogenization rate=9000 rpm, wall-to-core ratio=50:50 w/w).

*(ii) PPI-GA capsules formation*

Microcapsules comprised of gelatin-GA polymers have been well studied in literature (Yeo et al., 2005; Chang et al., 2006; Dong et al., 2007), and served as a benchmark for designing plant protein-polysaccharide capsules in this study. In the PPI-GA encapsulation experiments, emulsion formation followed a two-step process, in which a PPI-oil emulsion was produced via high speed short time homogenization, followed by the slow addition of GA. Finally, the mixture pH was adjusted to induce complexation between PPI and GA. Attempts of capsule formation as a function of homogenization rate (Figure 5.3) and  $C_p$  (Figure 5.4) revealed that the PPI-GA complex did not form a coating around oil droplets as the gelatin-GA complex did (Figures 5.1 and 5.2). Furthermore, upon ceasing stirring a significant oil layer was visible on the sample surface indicating entrapment within the PPI-GA matrix did not occur. In contrast, no such layer was visible with the gelatin-GA system. Depending on the processing conditions, commercial gelatin has an average MW ranging from 40 to 80 kDa (Jones, 2004), which is much smaller in size compared to legumin (~360 kDa) and vicillin (~150 kDa) present in PPI. In addition, compared to PPI's globular, rigid conformation, gelatin has linear chains which are more flexible. Therefore, gelatin can easily migrate to and align themselves at the oil-water interface in a short time compared to PPI molecules. Due to this fact, PPI may not have enough time to migrate and adsorb at the interface before GA addition, which resulted in complex formation rather than complex round the oil droplet. This possibly led to the unsuccessful encapsulation of PPI-GA under high speed mixing condition.

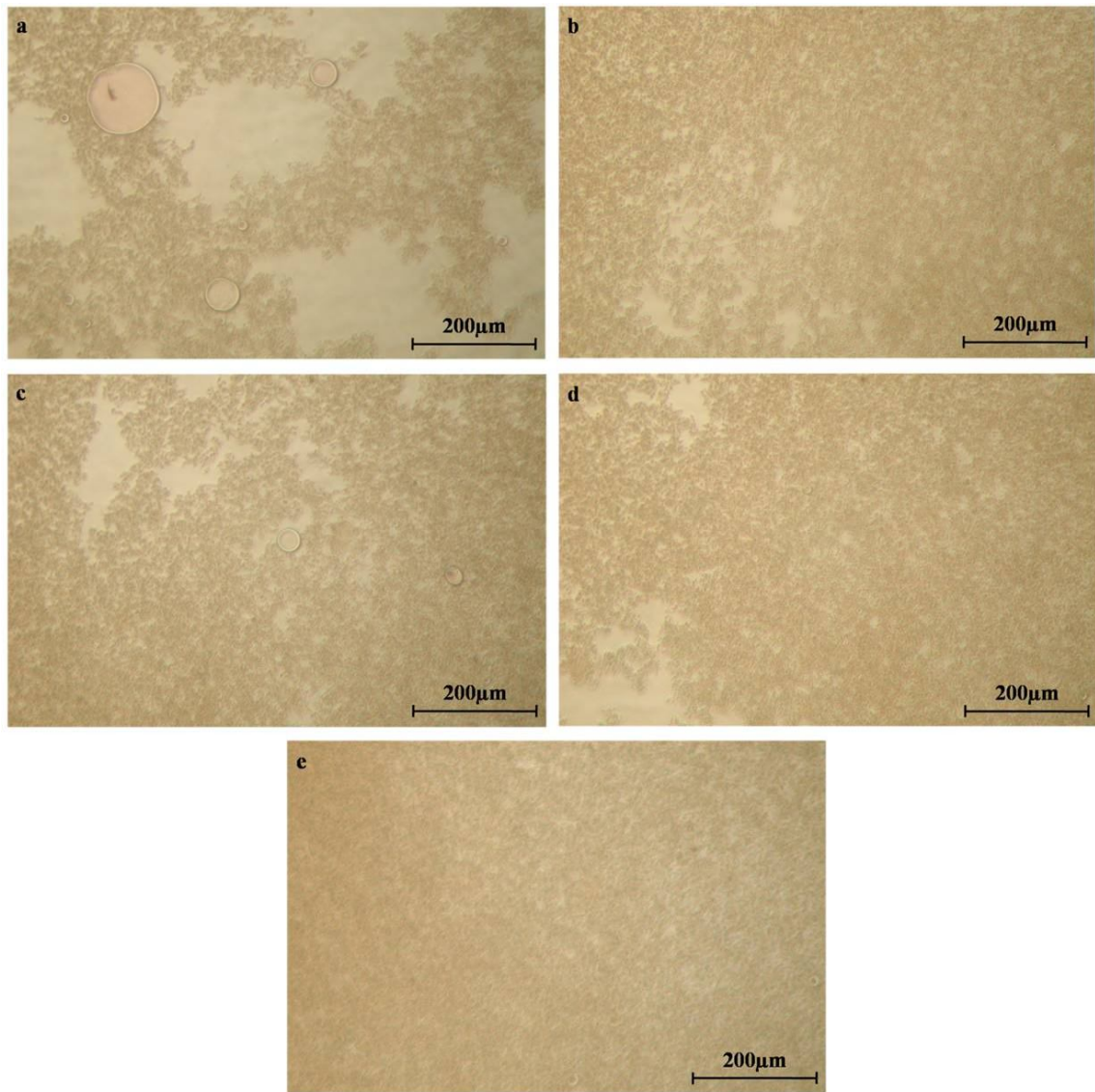


**Figure 5.3 PPI-GA capsule formation experiments observed by light microscopy as a function of homogenization rate: a) 3000; b) 6000; c) 9000; d) 12000 and e) 15000 rpm ( $C_p=2.00\%$  w/v, wall-to-core ratio=50:50 w/w).**

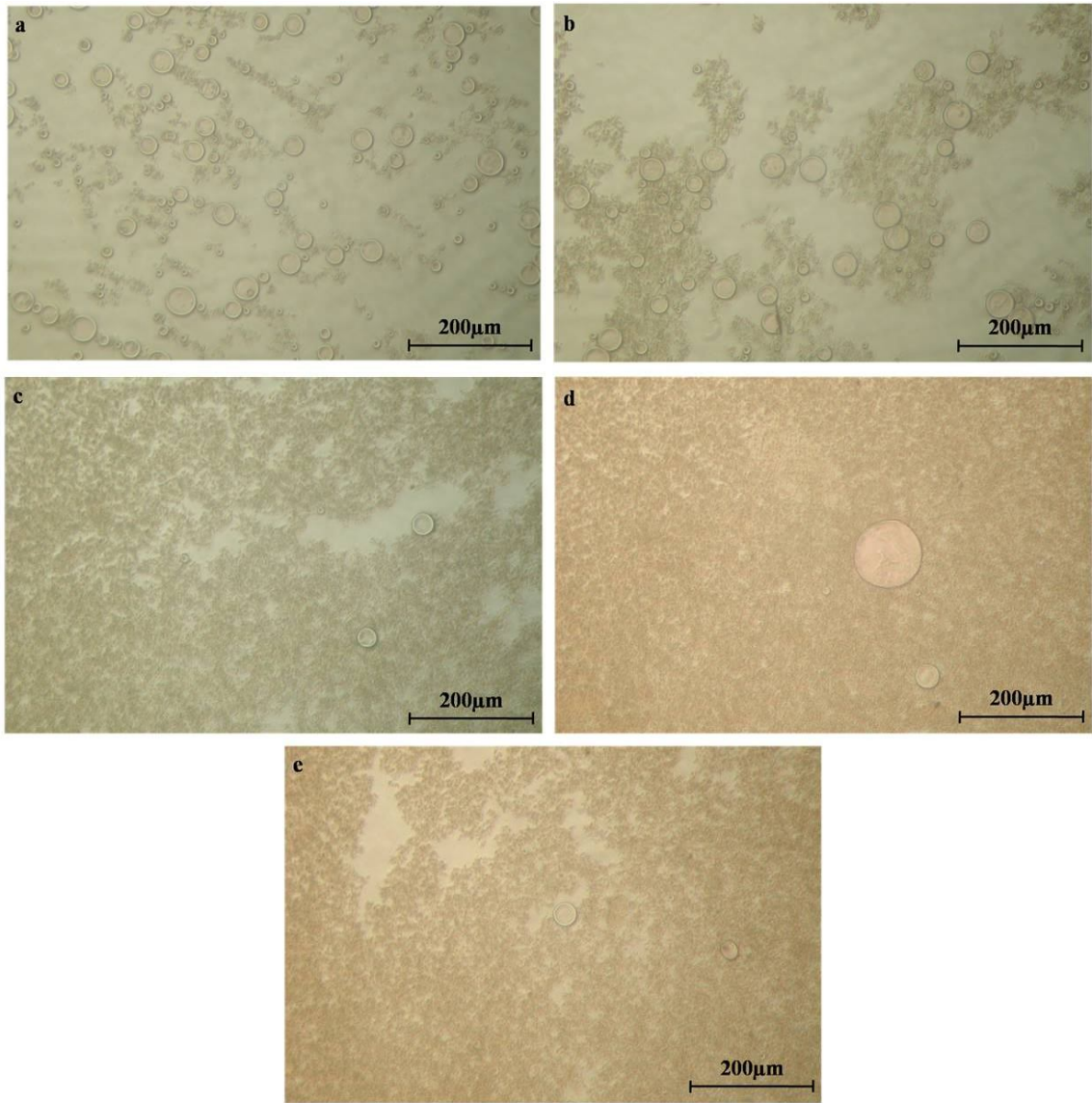


**Figure 5.4 PPI-GA capsule formation experiments observed by light microscopy as a function of  $C_p$  (% w/v): a) 1.00%; b) 1.25%; c) 1.50%; d) 1.75% and 2.00% (homogenization rate=9000 rpm, wall-to-core ratio=50:50 w/w).**

#### 5.4.1.2 Characterization of gelatin-GA capsules

Freeze drying of the gelatin-GA capsules with entrapped flax oil produced a free-flowing yellowish powder. Chemical parameters (Table 5.1) of the powder showed a low moisture content (3.17%) and water activity (0.18). In the food industry, the maximum moisture specification for a dried powder is 3-4% and an  $A_w$  of approximately 0.3 (Klaypradit et al., 2008). Encapsulated oil content reached 40.41 g flax oil per 100 g of capsules, with a surface oil content of 7.68 g. In the oil release study of Yeo and co-workers (2005), microcapsules without freeze drying or any treatment had similar free oil (surface) content as the capsules produced in this study.

**Table 5.1 The characteristics of gelatin-GA capsules ( $C_p=2.00\%$ w/v, wall-to-core ratio=50:50, homogenization rate=9000 rpm).**

Capsule characteristics	
Moisture content <sup>a</sup>	3.17 ± 0.07
Water activity	0.18 ± 0.00
Surface oil content <sup>a</sup>	7.68 ± 0.50
Total oil content <sup>a</sup>	48.08 ± 1.18
Encapsulated oil content <sup>a</sup>	40.41 ± 1.35

<sup>a</sup>gram per 100 g of freeze dried gelatin-GA capsules.  
Mean ± standard deviation (n=2).

#### 5.4.1.3 Oxidative stability of flax oil in gelatin-GA capsules

##### *Effect of the encapsulation process on oxidative stability*

One of the main reasons for entrapping flax oil in gelatin-GA capsules is to delay oxidation; this reaction results in the production of off-flavours and off-odours. Oxidation results in the production of primary and secondary oxidation products. Primary products, mainly peroxides, tend to be highly reactive; readily break down to free radicals, which propagate oxidation reactions. Peroxides also decompose to produce odorous secondary oxidation products, such as aldehydes and ketones. To access the



level of primary and secondary oxidative products arising from the encapsulation process, CD, p-AV and PV were measured. As shown in Table 5.2, flax oil extracted from freeze dried capsules had a CD of 10.04  $\mu\text{mol/g}$  of oil, p-AV of 1.89, and PV of 10.97 meq active  $\text{O}_2/\text{kg}$  oil. These results were similar to flax oil prior to encapsulation ( $p > 0.05$ ), which had a CD of 10.67  $\mu\text{mol/g}$  of oil, p-AV of 1.52, and PV of 8.44 meq active  $\text{O}_2/\text{kg}$  oil. These results indicated that the encapsulation process used in this study did not significantly affect the oxidative stability of flax oil.

**Table 5.2 The effect of high speed mixing encapsulation (two-step emulsification) on the oxidative stability of flax oil in gelatin-GA capsules (Cp=2.00% w/v, wall-to-core ratio=50:50, gelatin:GA=1:1, homogenization rate=9000 rpm).**

Oxidative tests	Before encapsulation	After encapsulation
Conjugated diene (CD), $\mu\text{mol/g}$	10.67 $\pm$ 1.62	10.04 $\pm$ 1.93
p-Anisidine value (p-AV)	1.52 $\pm$ 0.72	1.89 $\pm$ 0.71
Peroxide value (PV), meq active $\text{O}_2/\text{kg}$	8.44 $\pm$ 1.17	10.97 $\pm$ 1.76

Mean  $\pm$  standard deviation (n=2).

#### *Oxidative stability during storage*

The oxidative stability of free and encapsulated flax oil held at room temperature was monitored over a 25 d period using CD, p-AV and PV (Figure 5.5). Non-encapsulated oil and extracted capsule oil had similar CD values up to 15 d of storage, however the free oil oxidized at a much faster rate at day 20 (Figure 5.5a) than did the encapsulated oil, which showed no significant change ( $p > 0.05$ ) over the entire storage period (Figure 5.5a).

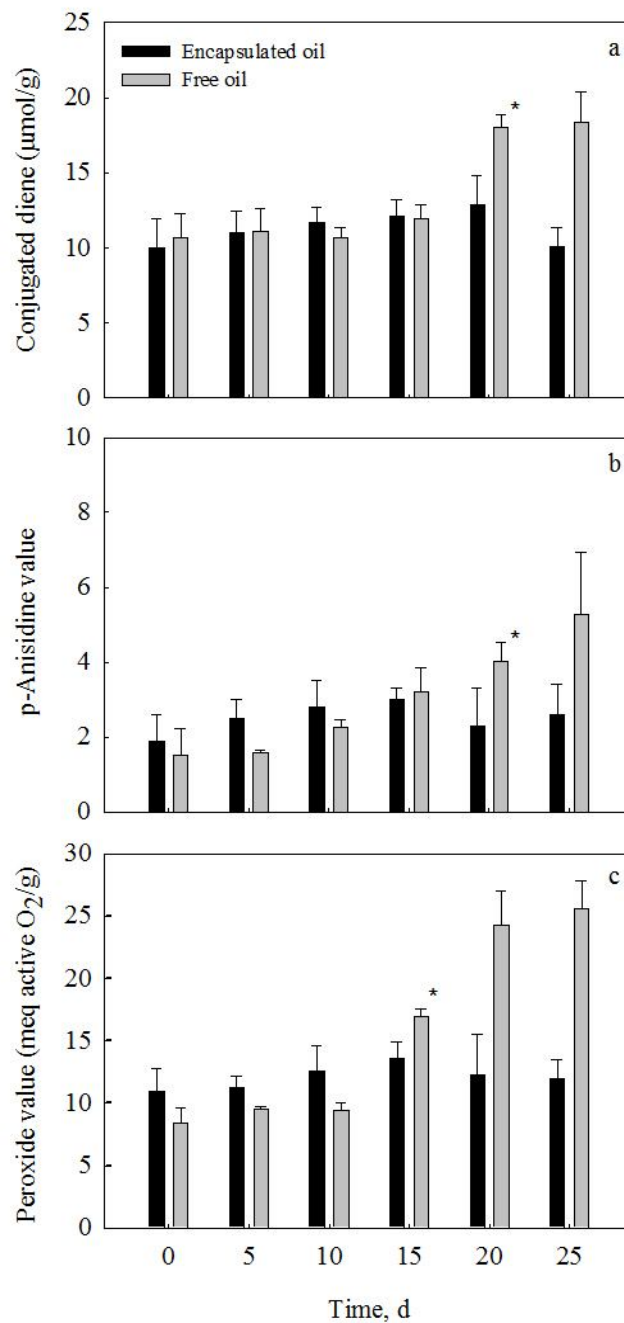


**Figure 5.5** Oxidative stability of free and encapsulated flax oil ( $C_p=2.00\%w/v$ , wall-to-core ratio=50:50 w/w, homogenization rate=9000 rpm) maintained at room temperature over a 25 d period (Data represent the mean  $\pm$  one standard deviation  $n=2$ ). Asterisks indicate the day in which significant oxidation occurred.

The p-AV results for extracted capsule oil were relatively constant over the storage period, whereas this value had slight increase over the entire storage period for free oil (Figure 5.5b). The PV of free oil showed no change ( $p > 0.05$ ) during the first 10 d of storage but significantly increased from day 15, indicating accelerated oxidation ( $p < 0.05$ ). In contrast, extracted capsule oil had similar PV ( $p > 0.05$ ) throughout the storage period (Figure 5.5c). Based on these results, free oil began to oxidize around day 15, whereas the gelatin-GA matrix protected the encapsulated oil from oxidation for 25 d at room temperature.

## **5.4.2 Flax oil encapsulation under low speed mixing conditions (one-step emulsification)**

### **5.4.2.1 Capsule formation**

#### *(i) PPI-GA capsule formation*

Early attempts to produce PPI-GA capsules under high speed mixing conditions failed (section 5.4.1.1). An alternative encapsulation procedure under low speed mixing conditions with a one-step emulsification was also unsuccessful as indicated by very high surface oil content resulting in large clumps of material after freeze drying. In this process, initial mixing of PPI and GA (pH 8.0) under non-attracting conditions due to charge repulsion, was followed by mixing with flax oil to allow adsorption of PPI to the oil-water interface. The pH of the mixture was lowered to 4.0 to afford PPI-GA complex formation. It was hypothesized that the strength of the electrostatic interactions between PPI and GA was insufficient, resulting in a capsule wall of weak integrity that broke down during the freeze drying process. Duce and co-workers (2004) encapsulated a model oil (mixture of medium chain triacylglycerols) in an emulsion state with pea globulin-GA; however, the researchers did not carry the process to the dried powder stage. The authors indicated that the encapsulation ability of the pea globulin-GA mixture was highly dependent upon solvent pH and the nature of the protein.



#### *(ii) PPI-alginate capsules formation and characterization*

Alginate was used to replace GA in this study due to the presence of a significantly higher number of carboxyl groups along its backbone relative to GA. It was hypothesized that this would most likely lead to a higher degree of biopolymer interaction and a stronger capsule wall. PPI-alginate capsules with encapsulated flax oil were formed at all biopolymer weight mixing ratios, yielding free-flowing yellowish powders after freeze drying. At pH 8.0, PPI (pI 5.60) and alginate are negatively charged. During the encapsulation process, stirring the biopolymer-oil mixture for 2.5 h under a solvent pH of 8.0 favours segregative phase association (i.e., where polymers carry a similar net charge and repel one another). This approach is hypothesized to improve the migration of one polymer to the oil-water interface resulting in its alignment at the interface of the emulsion. Stabilization of this emulsion is improved when the solvent pH was lowered to 4.0, favouring complex coacervation, as PPI-alginate chains are thought to adsorb at the oil-water interface and within the continuous aqueous phase. The latter results in an increase in the viscosity of the continuous phase, which inhibits further coalescence of oil droplets.

#### **5.4.2.2 Characterization of PPI-alginate capsules**

The effect of biopolymer weight mixing ratio (PPI:alginate) (3:1, 2:1, 1:1 and 1:2) on capsule formation was studied at a constant  $C_p$  (2.00% w/v) and wall-to-core ratio (50:50 w/w). Biopolymer weight mixing ratio and solvent pH are critical for controlling the charge balance between proteins and polysaccharides to form complex coacervates. PPI-alginate capsules were found to have low water activities and moisture contents (Table 5.3), and their dried powders met the specification for most powder ingredients used in the food industry (Klaypradit et al., 2008). Surface oil and encapsulated oil contents were used as markers in this study for optimization purposes, as they correlated positively with capsule shelf-stability (Anandaraman and Reineccius, 1987). Surface oil content was found to be the lowest (11.7 g per 100g of capsules) at a biopolymer weight mixing ratio (PPI:alginate) of 1:1, which also corresponded to the highest amount of oil encapsulated 38.3 g per 100g of capsules (Table 5.3). Using the identified optimal biopolymer weight mixing ratio (1:1), the effect of wall-to-core ratio (50:50, 60:40 and

70:30 biopolymer:oil) on the formation of capsules was investigated at constant Cp (2.00% w/v). The resultant dried powders had similar moisture contents and water activities as those previously reported (Tables 5.1 and 5.3).

**Table 5.3 The characterization of PPI-alginate capsules as a function of biopolymer weight mixing ratio (Cp=2.00% w/v, wall-to-core ratio=50:50 w/w).**

PPI:alginate	Moisture content <sup>a</sup>	Water activity	Surface oil content <sup>a</sup>	Encapsulated oil content <sup>a</sup>
3:1	1.34 ± 0.21 <sup>a</sup>	0.07 ± 0.01 <sup>a</sup>	19.41 ± 1.42 <sup>a</sup>	30.59 ± 1.42 <sup>a</sup>
2:1	1.32 ± 0.50 <sup>a</sup>	0.12 ± 0.05 <sup>a</sup>	20.90 ± 0.48 <sup>a</sup>	29.10 ± 0.48 <sup>a</sup>
1:1	1.66 ± 0.16 <sup>a</sup>	0.10 ± 0.03 <sup>a</sup>	11.70 ± 1.23 <sup>b</sup>	38.30 ± 1.23 <sup>b</sup>
1:2	3.53 ± 1.34 <sup>b</sup>	0.10 ± 0.03 <sup>a</sup>	14.63 ± 0.85 <sup>γ</sup>	35.37 ± 0.85 <sup>γ</sup>

<sup>a</sup> gram per 100 g of freeze dried PPI-alginate capsules.

Mean ± standard deviation (n=2).

Mean within columns followed by different letters differ significantly (p <0.05).

Capsule surface oil content was substantially reduced at the 70:30 wall-to-core ratio relative to the 60:40 and 50:50 ratios, however all ratios had encapsulated oil contents greater than 20 g per 100 g of capsules (Table 5.4). Surface oil content is an important parameter in the selection of optimal capsule design, since the readily extractable (unprotected) oil can become oxidized easily. This can cause product rancidity. Findings from this study suggest that the optimal PPI-alginate capsule design had a 1:1 biopolymer weight mixing ratio and a wall-to-core ratio of 70:30. Based on these results, oxidative stability tests were conducted using this capsule design.

**Table 5.4 The characterization of PPI-alginate capsules as a function of wall-to-core ratio (Cp=2.00% w/v, PPI:alginate=1:1 w/w).**

Wall-to-core ratio	Moisture content <sup>a</sup>	Water activity	Surface oil content <sup>a</sup>	Encapsulated oil content <sup>a</sup>
50:50	1.66 ± 0.16 <sup>α</sup>	0.10 ± 0.03 <sup>α</sup>	11.70 ± 1.23 <sup>α</sup>	38.30 ± 1.23 <sup>α</sup>
60:40	3.19 ± 0.06 <sup>β</sup>	0.10 ± 0.02 <sup>α</sup>	11.77 ± 0.79 <sup>α</sup>	28.23 ± 0.79 <sup>β</sup>
70:30	2.29 ± 0.22 <sup>γ</sup>	0.06 ± 0.01 <sup>β</sup>	7.79 ± 0.86 <sup>β</sup>	22.21 ± 0.86 <sup>γ</sup>

<sup>a</sup> gram per 100 g of freeze dried PPI-alginate capsules.

Mean ± standard deviation (n=2).

Mean within columns followed by different letters differ significantly (p <0.05).

#### 5.4.2.3 Oxidative stability of flax oil in PPI-alginate capsules

##### *Effect of encapsulation on oxidative stability*

Results from CD and TBARS tests suggest that oxidative products were produced during the encapsulation process (Table 5.5). While the TBA value only increased slightly (p <0.05), the CD value changed substantially (p <0.05) from approximately 8 to 45 μmol/g. In the case of the TBARS test, the MDA value directly relates to the amount of secondary oxidative products present. In contrast, the CD method measures the total amount of conjugated double bonds present, whether they arise from oxidation or were originally present. It has been shown (Reichert and MacKenzie, 1982) that pigments present in the pea material, such as carotenoids and xanthophylls may interfere with absorbance readings during CD analysis (Pegg, 2005). Extractions of empty capsules (without oil) were carried out with hexane-diethyl ether mixture. The organic solvent extracts showed high absorbance at 233 nm where CD value was measured. Therefore, the high CD value may possibly have resulted from both oxidation of entrapped flax oil and pigment presented in wall materials. At 532 nm, low absorbance was also observed in the extract of wall materials, which may contribute to the TBA value as well.

**Table 5.5 The effect of low speed mixing encapsulation (one-step emulsification) on the oxidative stability of flax oil in PPI-alginate capsules (Cp=2.00% w/w, PPI:alginate=1:1 w/w, wall-to-core ratio=70:30 w/w).**

Oxidative tests	Before encapsulation	After encapsulation
Conjugated diene (CD), $\mu\text{mol/g}$	$7.97 \pm 0.40^a$	$44.99 \pm 2.27^b$
TBA value, mg MDA eq/g	$2.15 \pm 0.05^a$	$2.95 \pm 0.27^b$

Mean  $\pm$  standard deviation (n=2).

Mean within rows followed by different letters differ significantly (p <0.05).

Fatty acid profiles of flax oil before and after encapsulation were determined and the results are presented in Table 5.6. The most abundant and oxidative labile fatty acid in flax oil is  $\alpha$ -linolenic acid due to the presence of three sites of unsaturation. Based on GC analysis, the concentration of  $\alpha$ -linolenic acid was not significantly different after encapsulation, indicating that the encapsulation process using low speeding mixing may not have adversely affected the oxidative stability of the flax oil. However, it is possible that lipid oxidation could occur prior to detectable changes in the fatty acid profile.

**Table 5.6 Fatty acid profiles of flax oil before and after encapsulation by low speed mixing (one-step emulsification).**

Flax oil	Palmitic acid (C16:0)	Stearic acid (C18:0)	Oleic acid (C18:1)	linoleic acid (C18:2)	$\alpha$ -linolenic acid (C18:3)
Before	$4.48 \pm 0.02$	$3.20 \pm 0.11$	$17.50 \pm 0.10$	$16.67 \pm 0.06$	$58.17 \pm 0.25$
After	$4.61 \pm 0.05$	$3.25 \pm 0.05$	$17.87 \pm 0.06$	$16.80 \pm 0.00$	$57.47 \pm 0.12$

All values are based on percentage by weight of total fatty acids.

Mean  $\pm$  standard deviation (n=2).

### *Oxidative stability during storage*

The oxidative stability of non-encapsulated and encapsulated flax oil as measured by CD value over a 20 d period is presented in Figure 5.6a. In general, encapsulated oil exhibited higher CD values compared to non encapsulated oil, although this was hypothesized to be strongly influenced by interfering compounds present within the pea material. CD values for non encapsulated oil increased steadily after 10 d storage and reached a maximum of 15.4  $\mu\text{mol/g}$  at 20 d (Figure 5.6a) ( $p < 0.05$ ). TBARS test results for both non-encapsulated and encapsulated flax oil were given in Figure 5.6b. At day 0, TBA values for the entrapped oils were slightly higher than that of free oils, this may be affected by the interfering compounds present in wall materials. At day 20, TBA value of free oil was significantly increased from day 0 ( $p < 0.05$ ); whereas TBA of encapsulated oil did not change over 20 d period ( $p > 0.05$ ).

### **5.5 Conclusion**

Gelatin-GA capsules produced in the present study had high (~40 g per 100 g of capsules) levels of encapsulated flax oil and low levels (~8 g per 100 g of capsules) of surface oil. The encapsulation process did not significantly affect the oxidative stability of flax oil in terms of conjugated diene, p-anisidine and peroxide values. Encapsulated flax oil was found to be stable over 25 d of storage at room temperature whereas free oil had undergone significant oxidation. Therefore, the oxidative stability of highly unsaturated oil, such as flax oil, can be improved by encapsulation using a gelatin-GA system. In the case of PPI-GA mixtures, no capsules could be formed under the experimental conditions studied. Among various PPI-alginate capsules formed in the present study, capsules with a wall-to-core ratio of 70:30 and PPI-to-alginate ratio of 1:1 exhibited the lowest surface oil (~8 g per 100 g of capsules) while retaining high encapsulated oil (~20g per 100 g of capsules). Encapsulation employing low speed mixing conditions may result in increase in the CD and TBA values of the flax oil.

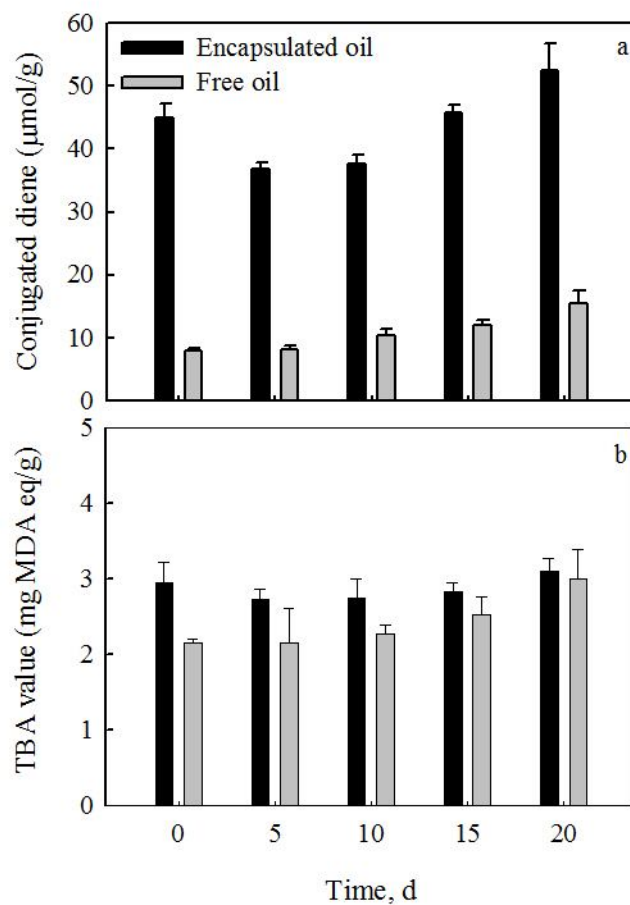


**Figure 5.6 Oxidative stability of free and encapsulated flax oil (Cp=2.00% w/w, wall-to-core ratio=70:30 w/w, PPI:alginate=1:1 w/w) maintained at room temperature over a 20 d period. (Data represent the mean  $\pm$  one standard deviation n=2).**

## Chapter 6

### General conclusions

The objective of this research was to encapsulate flax oil with plant-based materials (i.e., pea protein isolate-gum Arabic or another anionic polysaccharide) by complex coacervation. To accomplish this goal, a systematic study of complex formation involving PPI and GA biopolymers under different solvent and polymer conditions was carried out. The functional attributes of resulting PPI-GA complexes were then assessed for their potential as food/biomaterial ingredient or encapsulating agent. Complex coacervation between PPI-GA was found to be highly dependent upon solvent pH, salt, and biopolymer weight mixing ratio. Complexes only formed within a pH range where PPI and GA carried opposite charge, and was found to be optimal at a PPI-GA weight mixing ratio of 2:1 in the absence of added salt at pH 3.60. PPI-GA complexes were found to expand the minimum pH-solubility profile of PPI, broaden it to more acidic pH values; and improve its emulsion and foam stabilities. The method of emulsion preparation (one- vs. two-step) was found to play an important role in controlling emulsion stability, with one-step emulsification giving greater stability. Findings suggested that the complexation of GA to PPI improved the functional attributes of PPI over a finite pH range. PPI-GA complexes were found to be unable to form the wall material needed to coat flax oil droplets. It was hypothesized this may be attributed to the low degree of electrostatic attraction between PPI and GA biopolymers, resulting in weak wall integrity that broken down during freeze drying. In contrast, PPI-alginate capsules were formed under low speed mixing conditions (one-step emulsification). High encapsulated oil and low surface oil content was achieved at 1:1 biopolymer weight mixing ratio and 70:30 wall-to-core ratio. The encapsulated flax oil exhibited better oxidative stability compared to free oil during storage. However, the encapsulation process employed may adversely affect the oxidative stability of flax oil.

## **Chapter 7**

### **Further studies**

Although the formation of PPI-GA complex under different solvent and biopolymer conditions was intensively studied, biopolymer interactions involved in the formation and stability of PPI-GA complex are not well understood. In the present study, the significance of electrostatic interactions in complex formation was revealed, while other interactions were not known. As these interactions can affect the formation and stability of complex, it is important to investigate the nature of interactions involved and their roles in complex formation and disassociation. Since functionalities are different between biopolymer and biopolymer complexes, ingredients/materials can be made with desirable attributes.

Studies on the conformational changes of protein upon polysaccharide complexation may provide useful information on the structure of PPI-GA complex, as well as a better understanding of the different functionalities observed in the current research. This information will allow us to establish a structure-function relationship of the PPI-GA complex, which provides us the possibility to produce PPI-GA complex with tailor-made functionality.

Furthermore, modification is needed to minimize the effect of encapsulation process on the oxidative stability of PPI-alginate encapsulated flax oil before it can be used as a commercial process. Encapsulation of flax oil with PPI-GA complex was unsuccessful under the conditions studied in the research. The use of cross linking agent, which was not studied in the present research, may help strengthen the PPI-GA complex as wall material and achieve desirable encapsulation products.



## Chapter 8

### References

- AOAC. (2003). *Official Method of Analysis, 17<sup>th</sup> Edition*. Association of Official Analytical Chemists: Washington, DC.
- AOCS. (1997). *Official Methods and Recommended Practices of the AOCS*. AOCS Press: Illinois.
- Anandaraman, S., & Reineccius, G. A. (1988). Stability of encapsulated orange peel oil. *Food Technology*, 40, 88-93.
- Barbosa, M. I. M. J., Borsarelli, C. D., & Mercadante, A. Z. (2005). Light stability of spray-dried bixin encapsulated with different edible polysaccharide preparations. *Food Research International*, 38, 989-994.
- BeMiller, J. N., & Huber, K. C. (2008). Carbohydrates. In S. Damodaran, K. L. Parkin, & O. R. Fennema (Eds.), *Food Chemistry*. CRC Press: New York, NY. pp 83-154.
- Bougnoux, P., & Chajès, V. (2003).  $\alpha$ -Linolenic acid and cancer. In L. U. Thompson, & S. C. Cunnane (Eds.), *Flaxseed in Human Nutrition*. AOCS Press: Champaign, IL. pp 232-244.
- Braudo, E. E., Plashchina, L. G., & Schwenke, K. D. (2001). Plant protein interactions with polysaccharides and their influence on legume protein functionality - a review. *Nahrung*, 45, 382-384.
- Bungenberg de Jong, H. G., & Kruyt, H. R. (1929). Coacervation (Partial miscibility in colloid systems). *Proceedings of the Koninklijke Nederlandse Akademie van Wetenschappen*, 32, 849-856.

- Bungenberg de Jong, H. G. (1949a). Crystallisation-Coacervation-Flocculation. In Kruyt, H. R. (Ed), *Colloid Science*. Elsevier Publishing Company: Amsterdam, NL. pp 232-258.
- Bungenberg de Jong, H. G. (1949b). Complex colloid systems. In Kruyt, H. R. (Ed.), *Colloid Science*. Elsevier Publishing Company: Amsterdam, NL. pp 335-432.
- Bungenberg de Jong, H. G. (1949c). Morphology of coacervates. In Kruyt, H. R. (Ed.), *Colloid Science*. Elsevier Publishing Company: Amsterdam, NL. pp 433-480.
- Burgess, D. J., & Carless, J. E. (1984). Microelectrostatic studies of gelatin and acacia for the prediction of complex coacervation. *Journal of Colloid and Interface Science*, 98, 1-8.
- Chang, C. P., Leung, T. K., Lin, S. M., & Hsu, C. C. (2006). Release properties on gelatin-gum Arabic microcapsules containing camphor oil with added polystyrene. *Colloids and Surfaces B: Biointerfaces*, 50, 136-140.
- Chourpa, I., Ducel, V., Richard, J., Dubois, P., & Boury, F. (2006). Conformational modifications of alpha-gliadin and globulin proteins upon complex coacervates formation with gum Arabic as studied by Raman microspectroscopy. *Biomacromolecules*, 7, 2616-2623.
- Cleland, L. G., & James, M. J. (2003). Effect of flaxseed and  $\alpha$ -linolenic acid on inflammatory diseases and immune function. In L. U. Thompson, & S. C. Cunnane (Eds.), *Flaxseed in Human Nutrition*. AOCS Press: Champaign, IL. pp 333-340.
- Créviu, I., Bérot, S., & Guéguen, J. (1996). Large scale procedure for fractionation of albumins and globulins from pea seeds. *Nahrung*, 40, 237-244.
- Danviriyakul, S., McClements, D. J., Decker, E., Nawar, W. W., & Chinachoti, P. (2002). Physical stability of spray-dried milk fat emulsion as affected by emulsifiers and processing conditions. *Journal of Food Science*, 67, 2183-2189.
- de Kruif, C. G., & Tuinier, R. (2001). Polysaccharide protein interactions. *Food Hydrocolloids*, 15, 555-563.
- de Kruif, C., Weinbreck, F., & de Vries, R. (2004). Complex coacervation of proteins and anionic polysaccharides. *Current Opinion in Colloid & Interface Science*, 9, 340-349.

- Desai, K. G. H., & Park, H. J. (2005). Recent developments in microencapsulation of food ingredients. *Drying Technology*, 23, 1361-1394.
- de Vries, R., Weinbreck, F., & de Kruif, C. G. (2003). Theory of polyelectrolyte adsorption on heterogeneously charged surfaces applied to soluble protein-polyelectrolyte complexes. *Journal of Chemical Physics*, 118, 4649-4659.
- Dickinson, E., & Pawlowsky, K. (1998). Influence of  $\kappa$ -carrageenan on the properties of a protein-stabilized emulsion. *Food Hydrocolloids*, 12, 417-423.
- Dickinson, E. (2003). Hydrocolloids at interfaces and the influence on the properties of dispersed systems. *Food Hydrocolloids*, 17, 25-39.
- Dong, Z. J., Toure, A., Jia, C. S., Zhang, X. M., & Xu, S. Y. (2007). Effect of processing parameters on the formation of spherical multinuclear microcapsules encapsulating peppermint oil by coacervation. *Journal of Microencapsulation* 24, 634-646.
- Dror, Y., Cohen, Y., & Yerushalmi-Rozen, R. (2006). Structure of gum Arabic in aqueous solution. *Journal of Polymer Science Part B: Polymer Physics*, 44, 3265-3271.
- Dubois, M., Gilles, K. A., Hamilton, J. K., Rebers, P. A., & Smith, F. (1956). Colorimetric method for determination of sugars and related substances. *Analytical Chemistry*, 28, 350-356.
- Ducel, V., Richard, J., Saulnier, P., Popineau, Y., & Boury, F. (2004). Evidence and characterization of complex coacervates containing plant proteins: application to the microencapsulation of oil droplets. *Colloids and Surfaces A: Physicochemical and Engineering Aspects*, 232, 239-247.
- Ducel, V., Richard, J., Popineau, Y., & Boury, F. (2005). Rheological interfacial properties of plant protein – Arabic gum coacervates at the oil-water interface. *Biomacromolecules*, 6, 790-796.
- Dziezak, J. D. (1988). Microencapsulation and encapsulated ingredients. *Food Technology*, 42, 136-151.
- Galazka, V. B., Dickinson, E., & Ledward, D. A. (1999). Emulsifying behavior of 11S globulin *Vicia faba* in mixtures with sulphated polysaccharides: comparison of thermal and high-pressure treatments. *Food Hydrocolloids*, 13, 425-435.

- Gander, B., Blanco-Príeto, M. J., Thomasin, C., Wandrey, C., & Hunkeler, D. (2002). Coacervation/phase separation. In J. Swarbrick & J. C. Boylan (Eds.), *Encyclopedia of pharmaceutical technology* (2<sup>nd</sup> ed.). Marcel Dekker, Inc.: New York, NY. pp 481-496.
- Ganzevles, R. A., Stuart, C. M. A., van Vliet, T., & de Jongh, H. H. J. (2006). The use of polysaccharides to control protein adsorption to the air-water interface. *Food Hydrocolloids*, 20, 872-878.
- Ghosh, S. K. (2006). Functional Coatings by Polymer Microencapsulation: A General Perspective. In S. K. Ghosh (Ed), *Functional Coatings by Polymer Microencapsulation*. WILEY-VCH: Weinheim, GER. pp 1-28.
- Gilsenan, P. M., Richardson, R. K., & Morris, E. R. (2003). Associative and segregative interactions between gelatin and low-methoxy pectin: Part 1. Associative interactions in the absence of Ca<sup>2+</sup>. *Food Hydrocolloids*, 17, 723-737.
- Girard, M., Turgeon, S. L., & Gauthier, S. F. (2002). Interbiopolymer complexing between  $\beta$ -lactoglobulin and low- and high-methylated pectin measured by potentiometric titration and ultrafiltration. *Food Hydrocolloids*, 16, 585-591.
- Girard, M., Sanchez, C., Laneuville, S. I., Turgeon, S. L., & Gauthier, S. F. (2004). Associative phase separation of  $\beta$ -lactoglobulin/pectin solutions: a kinetic study by small angle static light scattering. *Colloids and Surfaces B: Biointerfaces*, 35, 15-22.
- Guzey, D., Kim, H. J., & McClements, D. J. (2004). Factors influencing the production of o/w emulsions stabilized by  $\beta$ -lactoglobulin-pectin membranes. *Food Hydrocolloids*, 18, 967-975.
- Hansen, P. M. T., Hidalgo, J., & Gould, I. A. (1971). Reclamation of whey protein with carboxymethylcellulose. *Journal of Dairy Science*, 54, 830-834.
- Health Canada. (1998). Nutraceuticals/Functional Foods and Health Claims on Foods. Retrieved May 12, 2009, from [http://www.hc-sc.gc.ca/fn-an/label-etiquet/claims-reclam/nutra-funct\\_foods-nutra-fonct\\_aliment-eng.php](http://www.hc-sc.gc.ca/fn-an/label-etiquet/claims-reclam/nutra-funct_foods-nutra-fonct_aliment-eng.php).
- Heinzelmann, K., Franke, K., Velasco, J., & Marquez-Ruiz, G. (2000). Microencapsulation of fish oil by freeze-drying techniques and influence of

- process parameters on oxidative stability during storage. *European Food Research and Technology*, 211, 234-239.
- Hidalgo, J., & Hansen, P. M. T. (1971). Selective precipitation of whey proteins with carboxymethylcellulose. *Journal of Dairy Science*, 54, 1270-1274.
- Hogan, S. A., McNamee, B. F., O'Riordan, E. D., & O'Sullivan, M. (2001). Microencapsulating properties of sodium caseinate. *Journal of Agricultural and Food Chemistry*, 49, 1934-1938.
- Islam, M., Phillips, G. O., Sljivo, A., Snowden, M. J., & Williams, P. A. (1997). Review of recent developments on regulatory, structural and functional aspects of gum Arabic. *Food Hydrocolloids*, 11, 493-505.
- Jackson, L. S., & Lee, K. (1991). Microencapsulation and the food industry. *Lebensmittel-Wissenschaft Technologie*, 24, 289-297.
- Jones, B. E. (2004). Gelatin: manufacture and physico-chemical properties. In F. Podczek, & B. E. Jones (Eds), *Pharmaceutical Capsules* (2<sup>nd</sup> Ed.). Pharmaceutical Press: London, UK. pp 23-60.
- Jourdain, L., Leser, M. E., Schmitt, C., Michel, M., & Dickinson, E. (2008). Stability of emulsions containing sodium caseinate and dextran sulfate: relationship to complexation in solution. *Food Hydrocolloids*, 22, 647-659.
- Kaibara, K., Okazaki, T., Bohidar, H. B., & Dubin, P. L. (2000). pH-Induced coacervation in complexes of bovine serum albumin and cationic polyelectrolytes. *Biomacromolecules*, 1, 100-107.
- Keipert, S., & Melegari, P. (1993). Preparation and characterization of oil containing microparticles. *Drug Development and Industrial Pharmacy*, 19, 603-621.
- King, A. H. (1995). Encapsulation of food ingredients. In S. J. Risch & G. Reineccius (Eds.), *Encapsulation and controlled release of food ingredients*. American Chemical Society: Washington, DC. pp 26-39.
- Klaypradit, W., & Huang, Y. W. (2008). Fish oil encapsulation with chitosan using ultrasonic atomizer. *LWT-Food Science and Technology*, 41, 1133-1139.
- Koh, G. L., & Tucker, I. G. (1988). Characterization of sodium carboxymethylcellulose-gelatin complex coacervation by chemical analysis of the coacervate and equilibrium fluid phases. *Journal of Pharmacy and Pharmacology*, 40, 309-312.

- Koyoro, H., & Powers, J. K. (1987). Functional properties of pea globulin fractions. *Cereal Chemistry*, 64, 97-101.
- Lampart-Szczapa, E. (2001). Legumin and Oilseed Protein. In Z. E. Sikorski (Ed.), *Chemical and Functional Properties of Food Proteins*. CRC Press: Boca Raton. pp 407-436.
- Lazko, J., Popineau, Y., & Legrand, J. (2004a). Soy glycinin microcapsules by simple coacervation method. *Colloids and Surfaces B: Biointerfaces*, 37, 1-8.
- Lazko, J., Popineau, Y., Renard, D., & Legrand, J. (2004b). Microcapsules based on glycinin-sodium dodecyl sulphate complex coacervation. *Journal of Microencapsulation*, 21, 59-70.
- Li, D., Attar-Bashi, N., & Sinclair, A. J. (2003).  $\alpha$ -Linolenic acid and heart disease. In L. U. Thompson, & S. C. Cunnane (Eds.), *Flaxseed in Human Nutrition*. AOCS Press: Champaign, IL. pp 245-259.
- Liu, S., Low, N. H., & Nickerson, M. T. (2009). Effect of pH, salt and biopolymer ratio on the formation of pea protein isolate-gum Arabic complexes. *Journal of Agricultural and Food Chemistry*, 57, 1521-1526.
- Madene, A., Jacquot, M., Scher, J., & Desobry, S. (2006). Flavour encapsulation and controlled release - a review. *International Journal of Food Science and Technology*, 41, 1- 21.
- Makri, E. A., & Doxastakis, G. I. (2007). Surface tension of *Phaseolus vulgaris* and *coccieus* proteins and effect of polysaccharides on their foaming properties. *Food Chemistry*, 101, 37-48.
- Mann, B., & Malik, R. C. (1996). Studies on some functional characteristics of whey protein-polysaccharide complex. *Journal of Food Science and Technology*, 33, 202-206.
- Martinez, K. D., Sanchez, C. C., Ruiz-Henestrosa, V. P., Rodriguez Patino, J. M., & Pilosof, A. M. R. (2007). Soy protein-polysaccharide interactions at the air-water interface. *Food Hydrocolloids*, 21, 804-812.
- Matsumura, Y., Egami, M., Satake, C., Maeda, Y., Takahashi, T., Nakamura, A., & Mori, T. (2003) Inhibitory effect of peptide-bound polysaccharides on lipid oxidation in emulsions. *Food Chemistry*, 83,107-119.

- Mattison, K. W., Brittain, I. J., & Dubin, P. L. (1995). Protein-polyelectrolyte phase boundaries. *Biotechnology Progress*, 11, 632-637.
- Mauguet, M. C., Legrand, J., Brujes, L., Carnelle, G., Larre, C., & Popineau, Y. (2002). Gliadin matrices for microencapsulation processes by simple coacervation method. *Journal of Microencapsulation*, 19, 377-384.
- Mekhloufi, G., Sanchez, C., Renard, D., Guillemin, S., & Hardy, J. (2005). pH-Induced structural transitions during complexation and coacervation of beta-lactoglobulin and acacia gum. *Langmuir*, 21, 386-394.
- Mohanty, B, & Bohidar, H. B. (2003). Systematic of alcohol induced simple coacervation in aqueous gelatin solution. *Biomacromolecules*, 4, 1080-1086.
- Mongenot, N., Charrier, S., & Chalier, P. (2000). Effect of ultrasound emulsification on cheese aroma encapsulation by carbohydrates. *Journal of Agricultural and Food Chemistry*, 48, 861-867.
- Morr, C. V., German, B., Kinsella, J. E., Regenstein, J. M., Buren, J. P. V., Kilara, A.; Lewis, B. A., & Mangino, M. E. (1985). A collaborative study to develop a standardized food protein solubility procedure. *Journal of Food Science*, 50, 1715-1718.
- Morris, D. H. (2007). Flax-a health and nutrition primer. Retrieved May 13, 2009, from <http://www.flaxcouncil.ca/english/index.jsp?p=primer&mp=nutrition>.
- Moure, A., Sineiro, J., Domínguez, H., & Parajó, J. C. (2006). Functionality of oilseed protein products: a review. *Food Research International*, 39, 945-963.
- Nickerson, M.T., Paulson, A.T., Wagar, E., Farnworth, R., Hodge, S.M., & Rousseau, D. (2006). Some physical properties of crosslinked gelatin-maltodextrin hydrogels. *Food Hydrocolloids*, 20, 1072-1079.
- Ortiz, M. S. E., Puppo, M. O., & Wagner, J. R. (2004). Relationship between structural changes and functional properties of soy protein isolates-carrageenan systems. *Food Hydrocolloids*, 18, 1045-1053.
- Overbeek, J. T. J., & Voorn, M. J. (1957). Phase separation in polyelectrolyte solutions. Theory of complex coacervation. *Journal of Cellular and Comparative Physiology*, 49, 7-26.

- Papalamprou, E. M., Makri, E. A., Kiosseoglou, V. D., & Doxastakis, G. (2005). Effect of medium molecular weight xanthan gum in rheology and stability of oil-in-water emulsion stabilized with legume proteins. *Journal of the Science of Food and Agriculture*, 85, 1967-1973.
- Park, E., Murakami, H., Mori, T., & Matsumura, Y. (2005). Effects of protein and peptide addition on lipid oxidation in powder model system. *Journal of Agricultural and Food Chemistry*, 53, 137-144.
- Pegg, R. (2005). Measurement of primary lipid oxidation products. In R. E. Wrolstad, T. E. Acree, & E. A. Decker (Eds.), *Handbook of Food Analytical Chemistry*. John Wiley & Sons, Inc.: Hoboken, NJ. pp 515-564.
- Pierucci, A. P. T. R., Andrade, L. R., Baptista, E. B., Volpato, N. M., & Rocha-Leão, M. H. M. (2006). New microencapsulation system for ascorbic acid using pea protein concentrate as coat protector. *Journal of Microencapsulation*, 23, 654-662.
- Plashchina, I. G., Mrachkovskaya, T. A., Danilenko, A. N., Kozhevnikov, G. O., Starodubrovskaya, N. Yu., Braudo, E. E., & Schwenke, K. D. (2001). Complex formation of faba bean legumin with chitosan: surface activity and emulsion properties complexes. In E. Dickinson, & R. Miller (Eds.), *Food Colloids-Fundamentals of Formulations*. The Royal Society of Chemistry: Cambridge, UK. pp 293-303.
- Prasad, K. (2003). Flaxseed and prevention of experimental hypercholesterolemic atherosclerosis. In L. U. Thompson, & S. C. Cunnane (Eds.), *Flaxseed in Human Nutrition*. AOCS Press: Champaign, IL. pp 260-273.
- Qi, W., Fong, C., & Lamport, D. T. A. (1991). Gum Arabic glycoprotein is a twisted hairy rope. *Plant Physiology*, 96, 848-855.
- Randall, R. C., Phillips, G. O., Williams P. A. (1989). Fractionation and characterization of gum from *Acacia senegal*. *Food Hydrocolloids*, 3, 66-75.
- Reichert, R. D., & MacKenzie, S. L. (1982). Composition of peas (*Pisum sativum*) varying widely in protein content. *Journal of Agricultural and Food Chemistry*, 30, 312-317.



- Samant, S. K., Singhal, R. S., Kulkarni, P. R., & Rege, D. V. (1993). Protein-polysaccharide interactions: a new approach in food formulations. *International Journal of Food Science and Technology*, 28, 547-562.
- Sanchez, C., Mekhloufi, G., & Renard, D. (2006). Complex coacervation between  $\beta$ -lactoglobulin and Acacia gum: A nucleation and growth mechanism. *Journal of Colloid and Interface Science*, 299, 867-873.
- Schmitt, C., Sanchez, C., Desobry-Banon, S., & Hardy, J. (1998). Structure and technofunctional properties of protein-polysaccharide complexes: a review. *Critical Reviews in Food Science and Nutrition*, 38, 689-753.
- Schmitt, C., Sanchez, C., Thomas, F., & Hardy, J. (1999). Complex coacervation between  $\beta$ -lactoglobulin and acacia gum in aqueous medium. *Food Hydrocolloids*, 13, 483-496.
- Schmitt, C., Sanchez, C., Despond, S., Renard, D., Thomas, F., & Hardy, J. (2000). Effect of protein aggregates on the complex coacervation between  $\beta$ -lactoglobulin and acacia gum at pH 4.2. *Food Hydrocolloids*, 14, 403-413.
- Schroeder, H. E. (1982). Quantitative studies on the cotyledonary proteins in the genus *Pisum*. *Journal of the Science of Food and Agriculture*, 33, 623-633.
- Shahidi, F. (2005). Extraction and measurement of total lipids. In R. E. Wrolstad, T. E. Acree, & E. A. Decker (Eds.), *Handbook of Food Analytical Chemistry*. John Wiley & Sons, Inc.: Hoboken, NJ. pp 425-435.
- Singh, S. S., Siddhanta, A. K., Meena, R., Prasad, K., Bandyopadhyay, S., & Bohidar, H. B. (2007). Intermolecular complexation and phase separation in aqueous solutions of oppositely charged biopolymers. *International Journal of Biological Macromolecules*, 41, 185-192.
- Soottitantawat, A., & Yoshii, H. (2003). Microencapsulation by spray drying: Influence of emulsion size on the retention of volatile compounds. *Journal of Food Science*, 68, 2256-2262.
- Soottitantawat, A., Takayama, K., Okamura, K., Muranaka, D., Yoshii, H., Furuta, T., Ohkawara, M., & Linko, P. (2005). Microencapsulation of l-menthol by spray drying and its release characteristics. *Innovative Food Science & Emerging Technologies*, 6, 163-170.

- Tainaka, K. (1979). Study of complex coacervation in low concentration by virial expansion method. I. Salt free systems. *Journal of the Physical Society of Japan*, 46, 1899-1906.
- Tainaka, K. (1980). Effect of counter ions on complex coacervation. *Biopolymers*, 19, 1289-1298.
- Thies, C. (2005). A survey of microencapsulation processes. In S. Benita (Ed.), *Microencapsulation - Methods and Industrial Application*. Marcel Dekker, Inc.: New York, NY. pp 1-20.
- Tolstoguzov, V. B. (1991). Functional properties of food proteins and role of protein-polysaccharide interaction. *Food Hydrocolloids*, 4, 429-468.
- Tuinier, R., Rolin, C., & de Kruif, C. G. (2002). Electrosorption of pectin onto casein micelles. *Biomacromolecules*, 3, 632-638.
- Turgeon, S. L., Beaulieu, M., Schmitt, C., & Sanchez, C. (2003). Protein-polysaccharide interactions: phase-ordering kinetics, thermodynamic and structural aspects. *Current Opinion in Colloid & Interface Science*, 8, 401-414.
- Turgeon, S. L., Schmitt, C., & Sanchez, C. (2007). Protein-polysaccharide complexes and coacervates. *Current Opinion in Colloid & Interface Science*, 12, 166-178.
- Uruakpa, F. O., & Arntfield, S. D. (2005). Emulsifying characteristics of commercial canola protein-hydrocolloid systems. *Food Research International*, 38, 659-672.
- Van de Weert, M., Anderson, M. B., & Frokjaer, S. (2004). Complex coacervation of lysozyme and heparin: complex characterization of protein stability. *Pharmaceutical Research*, 21, 2349-2354.
- Veis, A., & Aranyi, C. (1960). Phase separation in polyelectrolyte systems. I. Complex coacervates of gelatin. *Journal of Physical Chemistry*, 64, 1203-1210.
- Veis, A. (1961). Phase separation in polyelectrolyte solutions. II. Interaction effects. *Journal of Physical Chemistry*, 65, 1798-1803.
- Veis, A. (1963). Phase separation in polyelectrolyte systems. III. Effect of aggregation and molecular weight heterogeneity. *Journal of Physical Chemistry*, 67, 1960-1964.
- Veis, A., Bodor, E., & Mussell, S. (1967). Molecular weight fractionation and the self-suppression of complex coacervation. *Biopolymers*, 5, 37-59.

- Vikelouda, M., & Kiosseoglou, V. (2004). The use of carboxymethylcellulose to recover potato proteins and control their functional properties. *Food Hydrocolloids*, 18, 21-27.
- Wang, Y., Gao, J. Y., & Dubin, P. L. (1996). Protein separation via polyelectrolyte coacervation: selectivity and efficiency. *Biotechnology Progress*, 12, 356-362.
- Wang, X., Lee, J., Wang, Y., & Huang, Q. (2007). Composition and rheological properties of  $\beta$ -lactoglobulin/pectin coacervates: effects of salt concentration and initial protein/polysaccharide ratio. *Biomacromolecules*, 8, 992-997.
- Weinbreck, F., de Vries, R., Schrooyen, P. & de Kruif, C. G. (2003a). Complex coacervation of whey proteins and gum Arabic. *Biomacromolecules*, 4, 293-303.
- Weinbreck, F., Nieuwenhuijse, H., Robijn, G. W., & de Kruif, C. G. (2003b). Complex formation of whey proteins: exocellular polysaccharide EPS B40. *Langmuir*, 19, 9404-9410.
- Weinbreck, F. (2004). *Whey protein/polysaccharide coacervates: structure and dynamics*. PhD Thesis. Utrecht University.
- Weinbreck, F., Minor, M., & de Kruif, C. G. (2004a). Microencapsulation of oils using whey protein/gum Arabic coacervates. *Journal of Microencapsulation*, 21, 667-679.
- Weinbreck, F., Nieuwenhuijse, H., Robijn, G. W., & de Kruif, C. G. (2004b). Complexation of whey proteins with carrageenan. *Journal Agricultural and Food Chemistry*, 52, 3550-3555.
- Weinbreck, F., Rollema, H. S., Tromp, R. H., & de Kruif, C. G. (2004c). Diffusivity of whey protein and gum Arabic in their coacervates. *Langmuir*, 20, 6389-6395.
- Weinbreck, F., Tromp, R. H., & de Kruif, C. G. (2004d). Composition and structure of whey protein/gum Arabic coacervates. *Biomacromolecules*, 5, 1437-1445.
- Weinbreck, F., Wientjes, R. H. W, Nieuwenhuijse, H., Robijn, G. W., & de Kruif, C. G. (2004e). Rheological properties of whey protein/gum Arabic coacervates. *Journal of Rheology*, 48, 1215-1228.
- Wilde, P. J., & Clark, D. C. (1996). Foam formation and stability, In G. M. Hall (Ed.), *Methods of Testing Protein Functionality*. Chapman and Hall: New York, NY. pp 110-152.

- Xie, Y. R., & Hettiarachchy, N. S. (1997). Xanthan gum effects on solubility and emulsification properties of soy protein isolate. *Journal of Food Science*, 62, 1101-1104.
- Xie, Y. R., & Hettiarachchy, N. S. (1998). Effect of xanthan gum on enhancing the foaming properties of soy protein isolate. *Journal of the American Oil Chemists' Society*, 75, 729-732.
- Yadav, M. P., Manuel Igartuburu, J., Yan, Y., & Nothnagel, E. A. (2007). Chemical investigation of the structural basis of the emulsifying activity of gum Arabic. *Food Hydrocolloids*, 21, 297-308.
- Ye, A. (2008). Complexation between milk proteins and polysaccharides via electrostatic interaction: principles and applications – a review. *International Journal Food Science and Technology*, 43, 406-415.
- Yeo, Y., Bellas, E., Firestone, W., Langer, R., & Kohane, D. S. (2005). Complex coacervates for thermally sensitive controlled release of flavor compounds. *Journal of Agricultural and Food Chemistry*, 53, 7518-7525.